Stochastic dynamics for group field theories

Vincent Lahoche[1,*] and Dine Ousmane Samary [2,†]

[1]*Université Paris Saclay, CEA, LIST, Gif-sur-Yvette, F-91191, France*
[2]*Faculté des Sciences et Techniques (ICMPA-UNESCO Chair),*
Université d'Abomey-Calavi, 072 BP 50, Bénin

Phase transitions with spontaneous symmetry breaking are expected for group field theories as a basic feature of the geometogenesis scenario. The following paper aims to investigate the equilibrium phase for group field theory by using the ergodic hypothesis on which the Gibbs-Boltzmann distributions must break down. The breaking of the ergodicity can be considered dynamically by introducing a fictitious "time" inducing a stochastic process described through a Langevin equation, from which the randomness of the tensor field will be a consequence. This type of equation is considered particularly for complex just-renormalizable Abelian model of rank $d = 5$, and we study some of their properties by using a renormalization group considering a "coarse graining" both in time and space.

I. INTRODUCTION

For more than one decade, group field theories (GFTs) are considered as a promising way to address the quantum gravity conundrum. Mathematically, GFTs are fields theories defined on d copies of a group manifold G, called *group structure*, and distinguish themselves from standard quantum field theories (QFTs) by the specific nonlocality of their interactions [1–5]. In the point of view of quantization, the particles (quanta) associated to group fields are interpreted as elementary excitation of the gravitational field, which, instead of being characterized by concepts like energy, polarization, and so on, are characterized by topological and geometrical data. The quantized spacetime is of dimension d, and the elementary excitation is interpreted as $(d - 1)$ simplices with labeled faces. The interactions between these fields dictate the way the faces are "stuck" to each other according to these labels, to give effective d simplices. Thus, the nonlocal structure of the interaction tells us how dual $(d - 1)$ simplices are built and glued together. The structure group on the other hand has to reflect the local symmetry group of the dual spacetime. This interpretation can be motivated by the relation between GFTs and covariant approaches of loop quantum gravity (LQG) like *spin foams* [6]. Indeed, GFTs have been historically introduced in the context of the LQG [7–10] as a clever way to resume spin foam quantum amplitudes. Hence, on one hand, GFTs can be approached from the quantification of the classical general relativity (GR), which naturally leads to quantum states encoding discrete geometry as triangulation. It must be noticed that alternatively, GFT can be viewed as a second quantized version of LQG [11,12]. Finally, the choice of the group structure is imposed by this connection with LQG, as the local group of spacetime symmetries (SO(3,1) with the Lorentz signature, SO(4) for Euclidean quantum gravity, but other groups can be considered as toy models like SU(2) for Euclidean 3D gravity, U(1) or ℝ).

On the other hand, GFT can be approached directly through the prism of discrete random geometry, the continuum limit for quantum spacetime being recovered as a phase transition in the model. For 2D, the most popular approach in this direction is random matrix models (RMM). In RMM, Feynman amplitudes provide weights for discrete triangulation, the way the elementary "triangles" are glued together being imposed by the interactions between matrix fields. The main feature of RMM is the existence of a topological $1/N$ expansion, controlled by the genus $g(\Delta)$ of the dual triangulation Δ, and thus dominated by planar diagrams with $g = 0$. Critical properties and continuum limits of RMM are essentially consequences of this basic property [13–15]. Random tensors models (RTM) [16–18] are an attempt to extend the success of RMM to dimension higher than 2. The decisive step in this direction was the discovery by Gurau in 2009 of the existence of a power counting for colored random tensors, which admits an $1/N$ expansion analogous to RMM, controlled by a generalization (but unfortunately not topological) of the genus and called *Gurau degree* ϖ. It has been shown that the existence of such a power count is related to an internal structure group, typically U(N) (or O(N), see [19–22]), leaving the interactions invariant [18,23]. The leading-order

---

*vincent.lahoche@cea.fr
†dine.ousmanesamary@cipma.uac.bj

diagrams, having vanishing Gurau degree, are called melons, and critical properties of melonic sector, as well as double scaling limits, have been investigated for RTMs [24–26]. With this respect, GFTs can be viewed as generalized RTM, with group-valued rather than discrete indices. This leads to a restrictive class of RTM, called tensorial group field theories (TGFTs), which are GFT whose interactions have the same nonlocal structure as RTMs, said *tensorial interactions*. Note that some additional symmetries like *closure* (Gauss) constraint or *Plebanski* constraint have to be considered in the first point of view [27–30]. The closure constraint, for instance, is a specific kind of gauge symmetry, which requires that physical fields solutions are invariant under the global right translation of the group elements [31,32]. Imposing it at the quantum level, a Feynman amplitude looks like a partition function for a gauge theory on a random lattice fixed by the cellular complex defined by the Feynman graph, with flat discrete connections.

The main challenging issue for GFTs remains how a smooth spacetime structure corresponding to classical GR can be recovered by summing a very large number of quantum states having a very large number of quanta [33–36], and to this aim, the renormalization group (RG) is generally considered as the powerful tool to address this issue. RG is a general concept in physics to tackle the large-scale description of systems involving a very large number of (microscopic) interacting degrees of freedom [37,38]. There are many incarnations of this idea in physics, and all of them aim to extract the large-scale regularities of a system, replacing its full description with an approximate but effective theory, keeping only relevant features of the original quantum (or statistical) microscopic states. In the Wilsonian point of view, RG is constructed from a partial integration procedure, integrating out "rapid" modes to construct an effective physics for "slow" modes, keeping fixed the large distance physics. Two different strategies have been considered for constructing RG flow for GFTs. The first one is based on lattice renormalization, viewing spin foams as a direct space regularization of quantum gravity amplitudes [39]. The other approach is based on local field theories and renormalization techniques. Indeed, the existence of a power counting for TGFTs provides a novel notion of a locality called *traciality*, reflecting the way the divergences can be factorized out of some tensorial interaction. Renormalization "à la Wilson" requires identifying "slow" (infrared) and "rapid" (ultraviolet) modes. For TGFTs defined as enriched RTM with group valued indices, no such distinction exist between UV and IR modes. Indeed, usual GFT models or RTMs suggest that theories have to be ultralocal, with propagator equals to the identity matrix or suitable projectors, ensuring the global U(N) [or O(N)] invariance of RTMs. The triviality of the propagator is surely appropriate for simplicial quantum gravity perspectives but does not allow for the definition of

a proper notion of scale. However, this poses a difficulty, because, without such a suitable notion of scale, no distinction exists between fluctuating degrees of freedom. There are no "infrared" (IR) or "ultraviolet" (UV) degrees of freedom, and any partial integration procedure "à la Wilson" imposes to arbitrarily fix what are IR and UV. This point of view has been considered in a series of papers both using perturbative and nonperturbative RG technics [40–42,42–45], but to date, there is no consensus about the reliability of the resulting RG flow; see [46,47].

A solution considered in the literature consists in modifying the propagator by adding a "Laplacian" type term (defined on the considered structure group) to the Gaussian kernel, whose nontrivial spectrum then provides a nonambiguous notion of scale [48]. This Laplace type propagators may be viewed as a regulation that affects only UV degrees of freedom but disappears in the IR, leading to an effective, dynamically generated ultralocal theory for the RG flow. Moreover, the presence of such a Laplacian can be motivated by the computation of radiative corrections to GFTs, which require such a Laplacian as a counterterm to be well-defined as the cutoff in large momenta is removed [49]. There is vast literature and active research on this topic, exploring both the perturbative and nonperturbative aspects of the TGFTs [48,50–61]. These investigations generally seek to reveal fixed point solutions and phase transitions. Such solutions have been found for some models, although very dependent on the approximation scheme used to solve the flow equations in the nonperturbative regime. At first, it seemed that the existence of such fixed point solutions and second-order phase transitions was a quasiuniversal feature for TGFTs [55,56]. However, our recent works based on methods outperforming standard vertex expansion showed that it is not the case [62–65]. These methods consider both Ward identities and an effective vertex expansion (EVE) technique, which takes into account the full momenta dependence of the effective vertex and formally resumes branched sectors as the melonic one [46,62–67]. The existence of second-order phase transitions in the phase space of TGFTs is expected to be a basic requirement for geometrogenesis-type scenarios, where the semiclassical spacetime is assumed to emerge as an "intertheoretical process" from a Bose-Einstein condensation. It is worth mentioning that the hypothesis of the existence of such condensates has allowed the rapid development of a whole literature exploring models of quantum cosmology [27,68–80].

In this paper, we address the problem of quantization of GFTs through a first-order stochastic Langevin-type equation, such that equilibrium configurations match with standard path integral quantization for pure gravity models. The introduction of this equation can be considered a purely mathematical exercise, but it can also have real physical meaning. It can be seen as a way to dynamically (i.e., out of equilibrium) address the phase transitions

revealed by the RG for equilibrium theory. Indeed, in general, although the phase transitions are discussed in equilibrium, assuming the existence of an observer outside the system and adjusting adiabatically the parameters of the theory, a realistic description of the transition requires a nonequilibrium approach to this phenomenon. However, such a nonequilibrium treatment is generally a difficult task [34,81]. In the quantum gravity context, an additional question that one is entitled to ask concerns the choice of the variable identified as a "time." This question is closely related to the issue of time in classical and quantum gravity. Indeed, already at the classical level, general relativity does not allow in general to isolate a physical variable as a preferred time in the infinity of possible choices of "coordinated time," and experimentally, this is always the evolution of a physical variable, for a given problem, which defines a particular notion of the clock. Notice that this point of view is in agreement with the standard relational interpretation, where space and time are understood as relative special configurations of some fields, used as a "clock" and "rulers" [34]. An intriguing relation between the choice of a physical time and the definition of equilibrium states has been proposed in the series of works [8,82–86]. For instance, it is shown that the statistical properties of the cosmic radiation background reveal a preferred time, which happens to be the "cosmic time" considered in the literature. A discussion for quantum theories is given in [87], where authors consider the one-parameter group of automorphism underlying by von Neumann algebra of quantum systems through Tomita-Takesaki theorem, as a single-out time flow. Thermal equilibrium states have been already considered for GFTs, especially in the context of cosmology; see [88] and references therein for an extended discussion about relational functional dynamics. However, except for these special configurations, no preferred time is expected at the fundamental level for a background-independent quantum theory of gravitation. Indeed, the structured spacetime manifold is assumed to be entirely dissolved at the phase transition points where collective states of gravity quantum modes are not suitably described by Bose-Einstein condensates, and the concept of "direction" disappears as the concept of a smooth manifold. Phase transition in the GFTs is for this reason generally understood as a change of the theoretical paradigm—i.e., as the identification of some regions of the phase space where the collective behavior of quantum gravity atoms can be approached with an effective, semiclassical theory, as a quantum gravity condensate for current cosmological solutions discussed previously. A way to recover a notion of temporality even approximates is through the notion of relational (space)time, which is already found in classical GR. The contiguity relations between fields allow us to define spacetime properties, and, in particular, the coupling with gravitation defines the metric field. In that point of view, matter fields can be used to construct material frames locally, one of them playing the role of physical time. Let us recall how that works in the classical setting. Consider a theory involving N fields $\phi_i(x_0, \vec{x})$, for $i = 1, \ldots, N$, and $(x_0, \vec{x})$ are arbitrary coordinates for spacetime evens. In concrete experiments, clocks and other reference frames are defined as specific configurations of four of these fields, which are assumed to behave as classically as to define such a reference frame, and we denote them as $\phi_0, \ldots, \phi_3$. To be a good reference frame, we assume that locally spacetime coordinates x^μ can be expressed uniquely in terms of the four numbers ϕ_μ. In particular, $x^0 = F_0(\phi_0, \phi_1, \phi_2, \phi_3)$, and, we can express the equations of motions for the remaining fields in terms of the physical coordinates $(\phi_0, \vec{\phi})$ [8,87]. This relational viewpoint can be expected to survive when the gravitational field is described in a quantum manner, at least in a certain regime. An auxiliary (discretized) matter field could play the role of a clock, as long as one can neglect the quantum character of this field. One can expect that such a regime would allow describing the (relational) dynamics of spacetime toward or from the emergence of classical spacetime, but the transition point (geometrogenesis), where the quantum nature of all fields cannot be neglected, breaks the dynamical description. For more details on the concept of emergence of time in quantum gravity, the reader may consult for instance [34,35]. Recent application of relational time for TGFTs in the context of quantum cosmology can be found in [36,77,89–91].

In the mathematical formalism presented in this paper, the GFT is quantized by a stochastic equation. This dynamics can be rewritten as a functional integral by the method detailed in the Sec. II B, where time appears formally as a scalar variable, and the corresponding field theory is identified with a GFTs on the structure group $G^{\times d} \times \mathbb{R}$, considered, for instance, in [89,91] as describing a scalar field coupled to gravity. In this paper, intended to be the first of a series, we provide the foundations of the formalism. We consider an Abelian TGFT without closure constraint, whose structure group will be U(1) and whose equilibrium states will correspond to a GFT without matter degree of freedom, just renormalizable in rank $d = 5$. This choice may seem a bit artificial since the GFTs selected as physically realistic candidates for quantum gravity are based on non-Abelian groups and incorporate a certain number of constraints such as the closure constraint or Plebanski's constraint [29]. However, our goal in this paper is essential to show how the RG methods we have developed can be adapted to a new situation, such as a stochastic GFT, and to understand what this new approach can bring compared to the traditional point of view for a model where these techniques can be more easily handled. Thus, this paper should be seen as the first of a series of explorations, and we will focus essentially on aspects related to the combinatorics of interactions in the construction of

the RG.[1] Our approach in this paper is essentially based on the nonperturbative RG (NPRG) formalism [92–96] and construct approximate solutions of the exact Wetterich equation using both effective vertex expansion (EVE) recently introduced in the GFTs context [62–65,67,97,98] and Ward's identities to determine the derivative of the effective vertices with respect to the external momentum, involved in the computation of the anomalous dimension. The resulting equations are then analyzed numerically. The most relevant feature of this formalism is the existence of an intrinsic scaling provided by time evolution, which allows for coarse-grain random degrees of freedom in the frequency space. Besides, we focus on TGFTs, and we expect the same formalism should be used to investigate analogue regimes for theories with trivial propagators (i.e., without intrinsic scaling), as RMMs and RTMs, which will be the topic of forthcoming work.

In the Sec. II, we define the model and provide the path integral approach, allowing us to well define the functional renormalization group applicable with the so-called Wetterich equation. In Sec. III, we introduce the FRG formalism and the time reflection symmetry and causality that allows for coarse grain by modifying the original Langevin equation. This also helps to add in the Langevin equation a driving force that depends nonlocally on the standard time on the classical trajectory and preserves causality. We also provide the scaling dimension of the model. In Sec. IV, we use standard local potential approximation to construct solutions of the exact RG equation. We consider two approximations: The first is the crude truncation, and the second comes from the effective vertex expansion in the leading-order melonic approximation. In Sec. V, we study the symmetry of our model given by the Ward identities and provide the rigorous analysis of compatibility with the flow equation and the optimal choices of the regulators. Section VI is deserving of the numerical analysis. We conclude our work in Sec. VII.

II. STOCHASTIC GROUP FIELD THEORIES

In this section, we define the models and conventions used in the rest of the paper. We also derive a path integral representation and a few formal properties, which we will exploit in the next section devoted to the renormalization group. The reader may consult [37,38,81] for more details about formal computations of the Langevin equation.

A. The model

A group field φ is a field defined on d copies of a group manifold **G**:

$$\varphi:(g_1,...,g_d)\in(\mathbf{G})^{\times d}\to\varphi(g_1,...,g_d)\in\mathbb{K}. \quad (2.1)$$

Usually, $\mathbb{K}=\mathbb{C},\mathbb{R}$. In this paper, we focus on complex group fields, $\mathbb{K}\equiv\mathbb{C}$. To shorten the notations, we will denote by $\boldsymbol{g}:=(g_1,...,g_d)$ the elements of $(\mathbf{G})^{\times d}$ and by $\varphi(\boldsymbol{g})$ the value taken by the field at the point $\boldsymbol{g}$. We generally assume φ to be a square-integrable function, and the standard $L^2((\mathbf{G})^{\times d})$ inner product

$$(\varphi,\varphi'):=\int d\boldsymbol{g}\,\bar{\varphi}(\boldsymbol{g})\varphi'(\boldsymbol{g}) \quad (2.2)$$

is assumed to be bounded: $\|\varphi\|:=(\varphi,\varphi)<\infty$. In these notations, $\bar{\varphi}$ designates the standard complex conjugation of φ, and

$$d\boldsymbol{g}:=dg_1dg_2\cdots dg_d, \quad (2.3)$$

where dg_ℓ is the Haar measure over **G**. We will suppose that this field is moreover a dynamic variable, depending on a parameter $t\in\mathbb{R}$ called the "time." The evolution of the field is postulate to satisfy the dissipative Langevin equation, which is given by the following:

$$\boxed{\dot{\varphi}(\boldsymbol{g},t)=-\Omega\frac{\partial}{\partial\bar{\varphi}(\boldsymbol{g},t)}\mathcal{H}[\varphi,\bar{\varphi}]+\eta(\boldsymbol{g},t),} \quad (2.4)$$

where $\eta(\boldsymbol{g},t)$ is a random group field, playing the role of white noise, $\Omega>0$ is a timescale, the notation "dot" means d/dt, and $\mathcal{H}$, the Hamiltonian, defines the deterministic parts of the equation.

Remark 1. Before continuing with the definition of the model, let us make a small general remark about our point of view in this paper. The so-called time here is not standard as it is in the literature for GFTs, where relational time is usually implemented via clock fields implying second derivatives with respect to this time [91]. In this respect, time evolution could be viewed as "nonrelativistic" at this stage. However, we expect that such a point of view is meaningless here. Indeed, general covariance is not scheduled in our construction and would probably require additional degrees of freedom to be discussed, as is the case in more complete and physical GFT models. One could imagine that the Langevin equation derives from a kind of "slow rolling" approximation, a bit like for stochastic inflation, for an equation preserving a sort of general covariance. However, such an approximation might be a bit too hasty in the absence of more serious investigations, and we believe that talking about covariance or a "nonrelativistic" regime does not (yet) make sense in the present framework. We will thus simply say that our model

---

[1]However, let us also note that an Abelian GFT with trivial propagator and Λ cutoff in moment is nothing more than a rank 5 random tensor model in disguise. In this respect, we can abusively speak about "pure gravity model" for equilibrium states, in reference to the fact that no degree of freedom for matter field are included.

is a simple model allowing us to study the fluctuations around some equilibrium state with respect to which a preferred time is defined [see equation (2.4)].

Without additional constraint on the random field φ, we assume that the probability measure for $\eta(\boldsymbol{g}, t)$ is

$$d\rho(\eta) := \frac{1}{z_0} \exp\left(-\frac{1}{\Omega} \int dt d\boldsymbol{g} \bar{\eta}(\boldsymbol{g}, t) \eta(\boldsymbol{g}, t)\right) d[\eta], \quad (2.5)$$

where $d[\eta] := \prod_{\boldsymbol{g}, t} d\eta(\boldsymbol{g}, t) d\bar{\eta}(\boldsymbol{g}, t)$ is the formal functional measure defining path integral, and the normalization z_0 being such that

$$\langle \eta(\boldsymbol{g}, t) \bar{\eta}(\boldsymbol{g}', t') \rangle_\eta = \Omega \delta(\boldsymbol{g}'(\boldsymbol{g})^{-1}) \delta(t - t'), \quad (2.6)$$

the notation $\langle X \rangle_\eta$ meaning average over η with probability density $d\rho(\eta)/d[\eta]$, and

$$\delta(\boldsymbol{g}'(\boldsymbol{g})^{-1}) := \prod_{\ell=1}^{d} \delta(g'_\ell g_\ell^{-1}), \quad (2.7)$$

where $\delta(g_\ell g_\ell^{-1})$ denotes the standard Dirac delta over $\mathbf{G}$,

$$\int dg \delta(g'(g)^{-1}) f(g) = f(g'), \quad (2.8)$$

for some function f. The Hamiltonian $\mathcal{H}$ will be designed such that equilibrium configurations (see Sec. II B) reproduce the generalized Gibbs states used in standard definitions of GFTs. With the previous definition, longtime equilibrium states (i.e., the probability density for a field configuration) must behave like $P[\varphi, \bar{\varphi}] \sim e^{-\mathcal{H}[\varphi, \bar{\varphi}]}$, according to the usual definition provided that $\mathcal{H}$ is nothing but the microscopic action for group field. Because we focus on the TGFT formalism, we expect $\mathcal{H}$ is the sum of two contributions:

(1) A kinetic part $\mathcal{H}_{\text{kin}}$, involving a nontrivial kernel depending on the Laplace-Beltrami operator $\Delta_{\boldsymbol{g}}$ over the manifold $(\mathbf{G})^{\times d}$:

$$\mathcal{H}_{\text{kin}}[\varphi, \bar{\varphi}] := \int d\boldsymbol{g} \bar{\varphi}(\boldsymbol{g})(-\Delta_{\boldsymbol{g}} + m^2)\varphi(\boldsymbol{g}), \quad (2.9)$$

for some coupling constant m^2 defining a *mass scale*.

(2) An interaction $\mathcal{H}_{\text{int}}$, which expands in power of fields. The terms involved in that expansion, as the interaction Hamiltonian itself, are furthermore assumed to be invariants under unitary transformations $U \colon L^2(\mathbf{G}) \to L^2(\mathbf{G})$ defined as:

$$\varphi(\boldsymbol{g}) \to \varphi'(\boldsymbol{g}) := \int d\boldsymbol{g}' \left[\prod_{\ell=1}^{d} U_\ell(g_\ell, g'_\ell)\right] \varphi(\boldsymbol{g}').$$

$$(2.10)$$

This defines a particular nonlocality for interactions, called "tensoriality," and terms involved in the expansion of $\mathcal{H}$ are *tensorial invariants*.

These invariants admit an elegant representation in terms of d-colored bipartite regular graphs. The receipt is the following:

(1) To each field φ and $\bar{\varphi}$, we assign a black and white dot, respectively, with d half-colored edges hooked to them, materializing the d group variables $g_1, \ldots, g_d$:
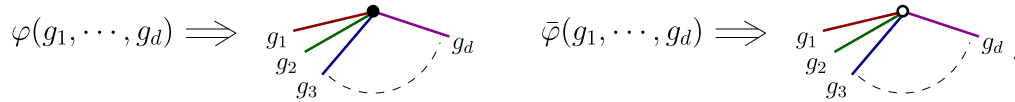
(2) Colored edges are then hooked together accordingly, with their respective colors, between black and white dots only. In Fig. 1, we show some examples for $d = 3$. To provide an explicit example, the first diagram reads explicitly as

$$\equiv \int \prod_{i=1}^{3} dg_i dg'_i \varphi(g_1, g_2, g_3) \bar{\varphi}(g_1, g'_2, g'_3) \varphi(g'_1, g'_2, g'_3) \bar{\varphi}(g'_1, g_2, g_3), \quad (2.11)$$

assuming that the red edge corresponds to color 1. As illustrated by the last example in Fig. 1, graphs can be connected or not, and in this case, they are the product of connected graphs. We call *a bubble* such a connected graph, made of a single piece. We moreover assume that $\mathcal{H}_{\text{int}}$ expands as
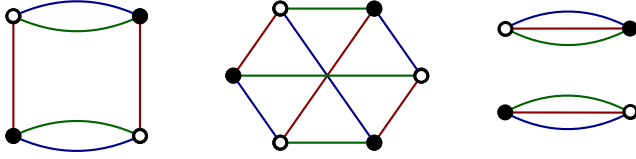
FIG. 1. Example of tensorial invariants for $d = 3$.

$$\mathcal{H}_{\text{int}}[\varphi, \bar{\varphi}] = \int dt \sum_b \lambda_b \text{Tr}_b[\varphi(t), \bar{\varphi}(t)], \quad (2.12)$$

the sum running over bubbles b involving more than two fields, and $\text{Tr}_b[\varphi, \bar{\varphi}]$ denotes the corresponding tensorial invariant. Longtime equilibrium states (i.e., the probability density that a group field φ has a given value in the "volume"[2] $D[\varphi] := \prod_g d\varphi(g) d\bar{\varphi}(g)$, if it exists, must behave like (see Sec. II B):

$$\rho[\varphi, \bar{\varphi}] = \frac{1}{Z[\{\lambda_b\}]} e^{-2\mathcal{H}[\varphi, \bar{\varphi}]}, \quad (2.13)$$

and the partition function $Z[\{\lambda_b\}]$ that normalizes the state is given by the formal path integral over field configurations:

$$Z[\{\lambda_b\}] := \int D[\varphi] e^{-2\mathcal{H}[\varphi, \bar{\varphi}]}. \quad (2.14)$$

Hence, the time variable is related to the definition of equilibrium states given by (2.13), accordingly with the point of view of [82,83], and we are aiming to study small perturbations with respect to it, described by the Langevin equation (2.4). The perturbative expansion of the partition function organizes as a sum over quantum amplitudes that we denote as $A(G)$, labeled with vacuum Feynman graphs G. An example of such a Feynman graph is provided by Fig. 2, the dotted edges materializing Wick contractions with free propagator $C(\boldsymbol{g}, \boldsymbol{g}')$,

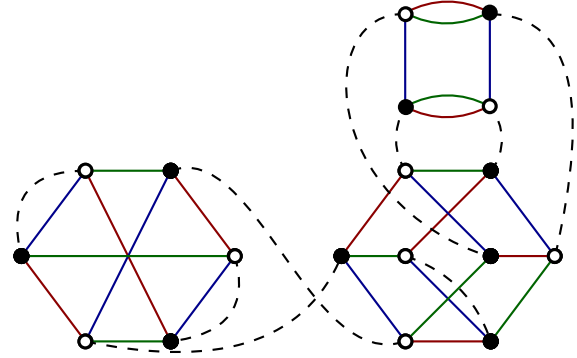$$C(\boldsymbol{g}, \boldsymbol{g}') := \frac{1}{2} \int_{1/\Lambda^2}^{+\infty} d\alpha e^{-\alpha m^2} \prod_{\ell=1}^d K_\alpha(g'_\ell(g_\ell)^{-1}), \quad (2.15)$$

for some UV cutoff Λ, and $K_\alpha(g'(g)^{-1})$ denotes the heat kernel, solution of the equation:

$$\frac{\partial}{\partial \alpha} K_\alpha(g) = \Delta_g K_\alpha(g), \quad (2.16)$$

with boundary conditions $K_{\alpha \to 0}(g'(g)^{-1}) = \delta(g'(g)^{-1})$. Feynman graphs like the one pictured in Fig. 2 look like bipartite regular $(d + 1)$-colored graphs, attributing the

---

FIG. 2. A typical Feynman graph for $d = 3$, with three vertices and nine propagator edges.

color "0" to the dotted edges. A very important notion for such a graph is the faces, and we recall the definition here:

Definition 1. A face f is a bicolored cycle (including color 0), indexed by a couple $(\ell, \ell'), \ell \neq \ell'$. Such a cycle may be open (open face) or closed (closed face). The boundary of a face, ∂f is the set of colored edges along the cycle.

In the rest of this article, we will focus on the compact Abelian group $\boldsymbol{G} = U(1)$, and we normalize the Haar measure as

$$\int d\boldsymbol{g} = 1. \quad (2.17)$$

The group is isomorphic to the unit circle, and each element of the group can be represented by $g \in U(1) \equiv e^{i\theta} \in S_1$, where $\theta \in [0, 2\pi]$. Irreducible representations of the group are therefore $e^{ip\theta}$ for $p \in \mathbb{Z}$, and the standard Peter-Weyl theorem allows decomposing functions over the group manifold $U(1)$ along this basis. For the heat kernel, for instance, we have

$$K_\alpha(g)|_{g \equiv e^{i\theta}} = \sum_{p \in \mathbb{Z}} e^{-\alpha p^2} e^{ip\theta}, \quad (2.18)$$

and the propagator in the Fourier representation reads,

$$C(\boldsymbol{p}, \boldsymbol{p}') = \frac{1}{2} \frac{\delta_{\boldsymbol{p}\boldsymbol{p}'}}{\boldsymbol{p}^2 + m^2}, \quad (2.19)$$

where $\boldsymbol{p} \in \mathbb{Z}^d$, $\boldsymbol{p}^2 := \sum_{\ell=1}^d p_\ell^2$, and $\delta_{\boldsymbol{p}\boldsymbol{p}'} := \prod_{\ell=1}^d \delta_{p_\ell p'_\ell}$. This theory has the property to be power countable, and we have the following statement [31,32,99,100]:

Proposition 1. Let $A(G)$ the regularized Feynman amplitude associated with a Feynman diagram G, with $L(G)$ dotted edges and $F(G)$ closed faces of type (0ℓ), $\ell \in [\![1, d]\!]$. Its dependence on the UV cutoff Λ is given by

$$|A(G)| \sim \Lambda^{\omega(G)}, \quad (2.20)$$

where:

$$\omega(G) = -2L(G) + F(G). \qquad (2.21)$$

Leading-order graphs are those for which ω is optimal. The diagrams that make this counting optimal are called melons and can be defined by a simple recursion; see [32,97] and Sec. IV B. Melonic graphs are those for which the number of faces is maximal as $L(G)$ fixed. We can show that for these diagrams the number $V(G)$ of vertices is related to the numbers $F(G)$ and $L(G)$ by [32,97]:

$$F(G) = (d-1)(L(G) - V(G) + 1). \qquad (2.22)$$

Hence, defining $\rho := (d-1)(L(G) - V(G) + 1) - F$, it can be established that the power counting can be read as:

$$\omega(G) = \sum_k ((d-3)k - (d-1))v_k(G) + (d-1)$$
$$- \frac{N(G)}{2}(d-3) - \rho(G). \qquad (2.23)$$

In that equation, $v_k(G)$ denotes the number of bubbles with valence $2k$ (with k white nodes), and $N(G)$ is the number of external edges.

Definition 2. For melonic diagrams $\rho(G) = 0$, and it can be proved that $\rho(G) > 0$ otherwise.
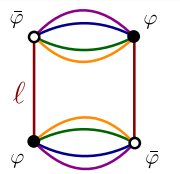
The theory will be *power counting just renormalizable* if and only if $(d-3)k - (d-1) = 0$. In particular, the sixtic model is just renormalizable for $d = 4$. In this paper, we will focus on the melonic quartic model, which is just renormalizable for $d = 5$, where power counting reads as:

$$\boxed{\omega_{\mathrm{melon}} = 4 - N(G)}. \qquad (2.24)$$

In particular, only two- and four-point diagrams are power counting divergent and required to be renormalized. The melonic diagrams have the property to be *contractible*. This property invites the definition of a locality principle, and tensorial invariants that are connected and contractible are said to be local in that point of view. We will speak of *traciality* to designate this specific notion of locality. This principle of locality allows us to define counterterms, and we can show the following theorem [99,100]:

Theorem 1. The quartic melonic model in $d = 5$ is just renormalizable, and divergences can be removed with counterterms for mass, quartic couplings, and field strength normalization.

Explicitly, the renormalizable Hamiltonian reads as

$$\mathcal{H}[\varphi, \bar{\varphi}] := \int d\boldsymbol{g}\, \bar{\varphi}(\boldsymbol{g})(-\Delta_{\boldsymbol{g}} + m^2)\varphi(\boldsymbol{g}) + \lambda \sum_{\ell=1}^{5} \ell \quad \overset{\bar{\varphi} \qquad \varphi}{\underset{\varphi \qquad \bar{\varphi}}{\bigcirc}}, \qquad (2.25)$$

where we attributed the same coupling constant for all the quartic interactions.

Traciality allows us to think of locality in that context, as related to tensorial invariance, and we adopt the following definition in this paper:

Definition 3. Any tensorial invariant whose graph is a bubble is said to be local. In the same way, any function that expands as a sum of terms labeled with bubbles only will say to be local.

B. Dynamic action and path integral

We denote as $\boldsymbol{q}(t) := \{\varphi(\boldsymbol{g}, t), \bar{\varphi}(\boldsymbol{g}, t)\}$ a given position for the random complex field in the functional space. Due to the randomness of the white noise $\eta(\boldsymbol{g}, t)$, trajectories can be suitably described through a probability distribution:

$$P(\boldsymbol{q}, t; \boldsymbol{q}', t') = \langle \delta(\boldsymbol{q}(t) - \boldsymbol{q}) \rangle_\eta, \qquad (2.26)$$

for $t > t'$, assuming the initial condition $\boldsymbol{q}(t') = \boldsymbol{q}'$. In the rest of the paper, we will use the shortest notation $P(\boldsymbol{q}, t)$

for $P(\boldsymbol{q}, t; \boldsymbol{q}', t')$, disregarding the initial state. The Langevin equation (2.4) being local in time, Eq. (2.26) defines a Markov process whose evolution follows a Fokker-Planck equation [37]:

$$\frac{\partial}{\partial t}P(\boldsymbol{q}, t) = 2\Omega \hat{H} P(\boldsymbol{q}, t), \qquad (2.27)$$

with:

$$\hat{H} := \int d\boldsymbol{g}\left(\frac{\delta^2}{\delta\varphi(\boldsymbol{g})\partial\bar{\varphi}(\boldsymbol{g})} + 4\frac{\delta^2\mathcal{H}}{\delta\varphi(\boldsymbol{g})\partial\bar{\varphi}(\boldsymbol{g})} + 2\frac{\delta\mathcal{H}}{\delta\varphi(\boldsymbol{g})}\frac{\delta}{\delta\bar{\varphi}(\boldsymbol{g})}\right.$$
$$\left. + 2\frac{\delta\mathcal{H}}{\delta\bar{\varphi}(\boldsymbol{g})}\frac{\delta}{\delta\varphi(\boldsymbol{g})}\right). \qquad (2.28)$$

This equation admits a longtime equilibrium solution; if it exists, this solution is given by:

$$\rho(\boldsymbol{q}) := \lim_{t \to +\infty} P(\boldsymbol{q}, t; \boldsymbol{q}', t'), \qquad (2.29)$$

which corresponds to stationary solutions of the Fokker-Planck equation, and it is easy to check that $\rho(\boldsymbol{q}) \sim e^{-2\mathcal{H}}$, accordingly with Eq. (2.13). This equilibrium solution exists provided that it is normalizable, i.e., that the integral (2.14) exists. The transition probability $P(\boldsymbol{q}, t; \boldsymbol{q}', t')$ can be represented as a path integral. We introduce it here with some details—see [37,81] for a complement. The basic ingredient is the following formal relation[3]:

$$1 \equiv \int d\boldsymbol{q}\, \delta(\dot{\varphi} + \delta_{\bar{\varphi}}\mathcal{H}' - \eta)\delta(\dot{\bar{\varphi}} + \delta_{\varphi}\mathcal{H}' - \bar{\eta})(\det \mathcal{M})^2, \tag{2.30}$$

where $\mathcal{H}' := \Omega\mathcal{H}$, $\mathcal{M}$ is the operator matrix with entries

$$\mathcal{M}(\boldsymbol{g}', t'; \boldsymbol{g}, t) := \delta(\boldsymbol{g}'(\boldsymbol{g})^{-1})\frac{d}{dt}\delta(t - t') + \frac{\delta^2\mathcal{H}'}{\delta\bar{\varphi}(\boldsymbol{g}, t)\delta\varphi(\boldsymbol{g}', t')}. \tag{2.31}$$

We can then use this representation of the identity to determine the classical action associated with the Markov process by rewriting the generating function:

$$Z[J, \bar{J}] := \left\langle \exp\left(\int dt d\boldsymbol{g} J(\boldsymbol{g}, t)\bar{\varphi}(\boldsymbol{g}, t) + \int dt d\boldsymbol{g} \bar{J}(\boldsymbol{g}, t)\varphi(\boldsymbol{g}, t)\right)\right\rangle_\eta. \tag{2.32}$$

Note that, because of the normalization for the averaging over η, we must have $Z[J = 0, \bar{J} = 0] = 1$, fixing the normalization; moreover, $\boldsymbol{q}(t)$ is assumed to be a solution of the motion equation for some initial conditions. It can be suitable to take the initial condition for $t' = -\infty$ to ensure that the distribution is in equilibrium (if it exists). We introduce the shortest notation $\boldsymbol{J}(t) = \{\bar{J}(\boldsymbol{g}, t), J(\boldsymbol{g}, t)\}$, and we define the dot product:

$$\boldsymbol{J} \cdot \boldsymbol{q} := \int dt d\boldsymbol{g} \bar{\varphi}(\boldsymbol{g}, t)J(\boldsymbol{g}, t) + \int dt d\boldsymbol{g} \bar{J}(\boldsymbol{g}, t)\varphi(\boldsymbol{g}, t). \tag{2.33}$$

Introducing the identity (2.30) in the previous equation, it becomes:

$$Z[J, \bar{J}] = \int d\boldsymbol{q} d\rho(\boldsymbol{\eta})e^{\boldsymbol{J}\cdot\boldsymbol{q}}\delta(\dot{\varphi} + \delta_{\bar{\varphi}}\mathcal{H}' - \eta)\delta(\dot{\bar{\varphi}} + \delta_{\varphi}\mathcal{H}' - \bar{\eta})$$
$$(\det \mathcal{M})^2. \tag{2.34}$$

---

[3]Note that the Langevin equation that we consider is a first-order differential equation, admitting a single causal solution; see [37]. This uniqueness can be challenged for some nonequilibrium configurations, whose classical action admits a large number of minima.

The delta functions can be easily integrated out, and to compute the determinant, we can use the well-known formula $\det \mathcal{M} = \exp(\operatorname{Tr}\ln(\mathcal{M}))$. One can easily check that:

$$\det \mathcal{M} \sim \exp\left(\theta(0)\int dt d\boldsymbol{g}\frac{\partial^2\mathcal{H}'}{\partial\bar{\varphi}(\boldsymbol{g}, t)\partial\varphi(\boldsymbol{g}, t)}\right). \tag{2.35}$$

In this equation, the choice of this function as the inverse of $\partial/\partial t$ is required by causality (which is expected from the Langevin equation). However, a problem arises because $\theta(0)$ is undefined. There are two allowed solutions, depending on if we use Îto or Stratonovich prescription for computing the time discretized version of path integrals [37,101,102]:

(1) In the Îto sense, we evaluate the integrand at the left end point.
(2) In the Stratonovich sense, we evaluate the integrand at the "middle" point.

Each of these choices corresponds to a different convention for $\theta(0)$. Thus, $\theta(0) = 0$ for Îto and $\theta(0) = 1/2$ for Stratonovich. In this paper, we will work within Îto convention, and we set $(\det \mathcal{M})^2 = 1$ in the calculations, leading to

$$Z[J, \bar{J}] = \int d\boldsymbol{q}\, e^{-\frac{1}{\Omega}\int dt d\boldsymbol{g}(\dot{\varphi} + \delta_{\bar{\varphi}}\mathcal{H}')(\dot{\bar{\varphi}} + \delta_{\varphi}\mathcal{H}') + \boldsymbol{J}\cdot\boldsymbol{q}}. \tag{2.36}$$

As a final step, we introduce a complex intermediate group field, χ, called *response field*, such that $Z[J, \bar{J}]$ can be rewritten as, using basic properties of Gaussian integration,

$$Z[J, \bar{J}, \jmath, \bar{\jmath}] = \int d\boldsymbol{q} d\chi e^{-\Omega^2 S[\boldsymbol{q}\chi] + \boldsymbol{J}\cdot\boldsymbol{q} + \jmath\cdot\chi}, \tag{2.37}$$

where we introduced a source $\jmath = (\jmath, \bar{\jmath})$ for the response field, and where the complex classical action $S[\boldsymbol{q}, \chi]$ is given by

$$\Omega^2 S[\boldsymbol{q}, \chi] := \int dt d\boldsymbol{g}[\Omega\bar{\chi}(\boldsymbol{g}, t)\chi(\boldsymbol{g}, t) + i\bar{\chi}(\boldsymbol{g}, t)(\dot{\varphi} + \Omega\delta_{\bar{\varphi}}\mathcal{H})(\boldsymbol{g}, t) + i(\dot{\bar{\varphi}} + \Omega\delta_{\varphi}\mathcal{H})(\boldsymbol{g}, t)\chi(\boldsymbol{g}, t)]. \tag{2.38}$$

It will be useful in the following to work in the Fourier representation. We will note $T_{\boldsymbol{p}}(\omega)$ [resp. $\bar{T}_{\boldsymbol{p}}(\omega)$] the Fourier components of $\varphi(\boldsymbol{g}, t)$ [resp. $\bar{\varphi}(\boldsymbol{g}, t)$], where $\boldsymbol{p} \in \mathbb{Z}^d$, such that:

$$\varphi(\boldsymbol{g}, t) = \int_{-\infty}^{+\infty}\frac{d\omega}{\sqrt{2\pi}}e^{-i\omega t}\sum_{\boldsymbol{p}\in\mathbb{Z}^d}T_{\boldsymbol{p}}(\omega)\prod_{\ell=1}^d e^{ip_\ell\theta_\ell}, \tag{2.39}$$

where $e^{i\theta_\ell} := g_\ell$. In that way, the Hamiltonian reads,

$$\mathcal{H}[T,\bar{T}] := \sum_{\boldsymbol{p} \in \mathbb{Z}^5} \int_{-\infty}^{+\infty} d\omega \bar{T}_{\boldsymbol{p}}(\omega)(\boldsymbol{p}^2 + m^2)T_{\boldsymbol{p}}(\omega)$$

$$+ \frac{\lambda}{2\pi} \sum_{\ell=1}^{5} \sum_{\{\boldsymbol{p}_i\}} \int \prod_{i=1}^{4} d\omega_i \delta(\omega_1 + \omega_3 - \omega_2 - \omega_4)$$

$$\times \mathcal{W}^{(\ell)}_{\boldsymbol{p}_1,\boldsymbol{p}_2,\boldsymbol{p}_3,\boldsymbol{p}_4} T_{\boldsymbol{p}_1}(\omega_1) \bar{T}_{\boldsymbol{p}_2}(\omega_2) T_{\boldsymbol{p}_3}(\omega_3) \bar{T}_{\boldsymbol{p}_4}(\omega_4), \tag{2.40}$$

where we introduced the symbols $\mathcal{W}^{(\ell)}_{\boldsymbol{p}_1,\boldsymbol{p}_2,\boldsymbol{p}_3,\boldsymbol{p}_4}$ defined as

$$\mathcal{W}^{(\ell)}_{\boldsymbol{p}_1,\boldsymbol{p}_2,\boldsymbol{p}_3,\boldsymbol{p}_4} := \delta_{p_{1\ell}p_{4\ell}} \delta_{p_{2\ell}p_{3\ell}} \prod_{j \neq i} \delta_{p_{1j}p_{2j}} \delta_{p_{3j}p_{4j}}. \tag{2.41}$$

Hence, $S[\boldsymbol{q},\boldsymbol{\chi}]$ splits as

$$S =: S_{\text{kin}} + S_{\text{int}}, \tag{2.42}$$

where

$$S_{\text{kin}} = \sum_{\boldsymbol{p} \in \mathbb{Z}^5} \int_{-\infty}^{+\infty} d\hat{\omega} \Big(\bar{\chi}_{\boldsymbol{p}}(\hat{\omega}) \chi_{\boldsymbol{p}}(\hat{\omega}) + i\bar{\chi}_{\boldsymbol{p}}(\hat{\omega})$$

$$\times (-i\hat{\omega} + \boldsymbol{p}^2 + m^2) T_{\boldsymbol{p}}(\hat{\omega})$$

$$+ i\bar{T}_{\boldsymbol{p}}(\hat{\omega})(i\hat{\omega} + \boldsymbol{p}^2 + m^2) \chi_{\boldsymbol{p}}(\hat{\omega}) \Big), \tag{2.43}$$

and

$$S_{\text{int}} = \frac{i\lambda}{4\pi} \sum_{\ell=1}^{d} \left(\vcenter{\hbox{}} + \vcenter{\hbox{}} \right), \tag{2.44}$$

where, in the previous equation, we introduced the graphical rule according to which response fields χ and $\bar{\chi}$ will be materialized by black and white square nodes, respectively, and where we introduced the dimensionless frequency $\omega \equiv \Omega\hat{\omega}$.

The free propagator C takes the form of a 2×2 matrix, with components $C_{\chi\bar{\chi}}$, $C_{T\bar{\chi}}$, $C_{\chi\bar{T}}$, and $C_{T\bar{T}}$. It is easy to check that the response field does not propagate; i.e.,

$$C_{\chi\bar{\chi}}(\hat{\omega},\boldsymbol{p}^2) = 0. \tag{2.45}$$

Other components are given by

$$C_{\bar{\chi}T}(\hat{\omega},\boldsymbol{p}^2) = \frac{1}{\Omega^2} \frac{\hat{\omega} - i(\boldsymbol{p}^2 + m^2)}{\hat{\omega}^2 + (\boldsymbol{p}^2 + m^2)^2},$$

$$C_{\bar{T}\chi}(\hat{\omega},\boldsymbol{p}^2) = -\frac{1}{\Omega^2} \frac{\hat{\omega} + i(\boldsymbol{p}^2 + m^2)}{\hat{\omega}^2 + (\boldsymbol{p}^2 + m^2)^2}, \tag{2.46}$$

and

$$C_{T\bar{T}}(\hat{\omega},\boldsymbol{p}^2) = \frac{1}{\Omega^2} \frac{1}{\hat{\omega}^2 + (\boldsymbol{p}^2 + m^2)^2}. \tag{2.47}$$

The result (2.45) valid at order zero in the perturbative expansion survives to all orders, and is in fact an exact, nonperturbative relation [103], meaning that component $\chi\bar{\chi}$ of the exact propagator G (or equivalently the component $\bar{T}T$ of the mass matrix $\Gamma^{(2)}$) vanishes:

$$\boxed{G_{\chi\bar{\chi}}(\hat{\omega},\boldsymbol{p}^2) = 0}. \tag{2.48}$$

The origin of this relation can be traced as follows. Let us consider $Z[J,\bar{J},\jmath,\bar{\jmath}]$, the generating functional (2.37). Let us add *a linear* driving force $\frac{1}{\Omega} \int dt \sum_{\boldsymbol{p}} \bar{k}_{\boldsymbol{p}}(t) T_{\boldsymbol{p}}(t) + \text{c.c}$ to the Hamiltonian $\mathcal{H}$. This is equivalent to translating sources $\jmath$ and $\bar{\jmath}$ as

$$J_{\boldsymbol{p}} \to J_{\boldsymbol{p}} - ik_{\boldsymbol{p}}, \qquad \bar{J}_{\boldsymbol{p}} \to \bar{J}_{\boldsymbol{p}} + i\bar{k}_{\boldsymbol{p}}. \tag{2.49}$$

Hence, from the normalization conditions of the partition function, we must have $Z[0,0,-ik,i\bar{k}] = 1$, and therefore,

$$G_{\chi\bar{\chi}} = -\frac{\delta^2}{\delta k_{\boldsymbol{p}} \delta \bar{k}_{\boldsymbol{p}'}} Z[0,0,-ik,i\bar{k}] \equiv -\frac{\delta^2 1}{\delta k_{\boldsymbol{p}} \delta \bar{k}_{\boldsymbol{p}'}} = 0. \tag{2.50}$$

In the rest of this paper, we fix the original timescale such that $\Omega = 1$, keeping the dependency over Ω explicit only for technical points. Such a choice simplifies all the expressions before.

III. FUNCTIONAL RENORMALIZATION GROUP

In this section, we introduce the formalism of the nonperturbative renormalization group as originally formulated by Wetterich and Morris [92–94,96]. This formalism is particularly well suited to deal with discrete models of quantum gravity, such as GFTs or random tensors. We will introduce this formalism for the dynamic GFT model introduced above. In this study, we limit ourselves to the equilibrium dynamics.

A. Regularization and flow equation

The RG as conceived by Wilson and Kadanoff aims to interpolate between a microscopic model and a macroscopic, effective description. The effective description is constructed by integrating out quantum or thermodynamic fluctuation scale by scale, integrating out firstly the modes

having a small wavelength and ending with the ones having a large wavelength. This paradigm generally focuses on equilibrium physics. For nonequilibrium systems, temporal fluctuations can no longer be ignored. There are then two possible attitudes:

(i) Consider a coarse graining only on the group variables (i.e., on the spectrum of the Laplacian Δ_g).

(ii) Or include the time to the notion of scale and integrate partially on both the spectrum of the operators $-i\partial/\partial t$ and Δ_g.

We can still imagine partially integrating only on the ω frequencies by integrating on the whole spectrum of Δ_g, but we will not consider this possibility in the following. The possibility of a coarse graining in frequency has been considered in [104] through the Wetterich framework, about nonequilibrium systems, and in [105] about a disordered Langevin type equation. Other approaches considering a frequency coarse graining have been considered, notably for quantum mechanical problems [106,107], inflation theory [108], Brownian motion [109,110], dissipative (open) quantum system [111–113], and references therein. The reader can also consult the recent review [96]. In this paper, we follow the same strategy, and we focus on a coarse graining both in frequency ω and momenta $\boldsymbol{p}$ that interpolates between two regimes:

(1) The UV regime, where fluctuations are frozen and fields configurations are determined by stationary points of the classical action S.

(2) The IR regime, where fluctuations are all integrated out, and field configurations are described through the effective action Γ, the Legendre transform of the Gibbs free energy.

The standard procedure is to add a regulator to the classical action S, which has generally the form:

$$\Delta S_k = \sum_{\boldsymbol{p}\in\mathbb{Z}^d}\sum_{a,b}\int_{-\infty}^{+\infty}d\omega\,\bar{\Xi}_a(\boldsymbol{p},\omega)R_{ab,k}(\boldsymbol{p},\omega)\Xi_b(\boldsymbol{p},\omega),$$

$$(3.1)$$

where $\Xi(\boldsymbol{p},\omega) = (\chi_{\boldsymbol{p}}(\omega), T_{\boldsymbol{p}}(\omega))$. The *regulator* $R_{ab,k}(\boldsymbol{p},\omega)$ is assumed to be a differentiable function of k, $\boldsymbol{p}$, and ω. It behaves as a scale-dependent mass and is designed such that high energy modes concerning the scale k (i.e., such that $\hat{\omega}/k^2, \boldsymbol{p}^2/k^2 \ll 1$) receive a small mass, whereas low energy modes are essentially frozen, decoupling them from long range physics. In such a way, we are expecting to construct a smooth interpolation Γ_k between microscopic physics described by classical action $\Omega^2 S$ for $k = \Lambda$ and macroscopic physics described by effective action Γ—the Legendre transform of the Gibbs free energy–for $k = 0$. We introduce the mathematical definition of the effective average action Γ_k:

$$\Gamma_k[\boldsymbol{M},\boldsymbol{\sigma}] + \Delta S_k[\boldsymbol{M},\boldsymbol{\sigma}] = \boldsymbol{M}\cdot\boldsymbol{J} + \boldsymbol{\sigma}\cdot j - W_k[\boldsymbol{J},j],\quad(3.2)$$

where $\boldsymbol{M}:=(\bar{M},M)$ and $\boldsymbol{\sigma}:=(\bar{\sigma},\sigma)$ denote the classical fields; i.e.,

$$M:=\frac{\delta W_k}{\delta\bar{J}},\qquad \sigma:=\frac{\delta W_k}{\delta\bar{j}}.\qquad(3.3)$$

The microscopic scale Λ is assumed to be large enough, and we will take the *continuum limit* $\Lambda\to\infty$ in the computation of the β function. For the equilibrium distributions, this limit makes sense because the model that we consider is just renormalizable and asymptotically free [100,114]. In the deep IR regime, for $k\sim 0$, one expects that regulator $R_{ab,k}$ almost vanishes, ensuring that symmetries, in particular, should be ultimately restored, at least formally, for the exact RG equation [95]:

$$\frac{\partial}{\partial k}\Gamma_k = \mathrm{Tr}\frac{\partial\boldsymbol{R}_k}{\partial k}(\boldsymbol{\Gamma}_{\boldsymbol{k}}^{(2)} + \boldsymbol{R}_k)^{-1},\qquad(3.4)$$

where capital bold letters designate 2×2 matrix-valued functions, and the trace runs over all the fields indices. Note that the expression assumes implicitly that $\Omega = 1$, and we define the effective propagator $\boldsymbol{G}_k$ as

$$\boldsymbol{G}_k := (\boldsymbol{\Gamma}_{\boldsymbol{k}}^{(2)} + \boldsymbol{R}_k)^{-1}.\qquad(3.5)$$

The situation is, however, not so easy, because Eq. (3.4) cannot be solved exactly, even for very simple models, and approximations currently considered solving it introduce a spurious dependency on the regulator for IR quantities [115,116]. In this paper, we will consider the *minimal sensitivity prescription* (MSP) as a reliability criterion to quantify the dependency on the regulator; see [104,117,118]. Methods usually considered for solving flow equations are called truncation and project them along a finite-dimensional subspace. The choice of this finite-dimensional subspace depends on physical constraints and symmetries expected to be unbroken along the flow, up to IR scales. This can be achieved by demanding that the regulator preserve the original symmetries of the classical action, i.e., that Ward-Takahashi (WT) identities remain unchanged along the flow [119]. This condition, however, is usually too restrictive, and in many situations, symmetries are only restored in the deep IR, making the dependency on the regulator difficult to avoid. This is especially the case for gauge theories [120], another unconventional example being provided by RMMs and RTMs [46,47]. In that paper, we only consider regulator compatibles with time-reversal symmetry preserved along the flow, but not only asymptotically. Time-reversal symmetry is expected because we assume to consider only *equilibrium dynamics*, starting with a generalized Gibbs state $\rho(\boldsymbol{q})$ and relaxing toward equilibrium [37].

B. Time reflection symmetry and causality

A way to construct coarse graining is to modify the original Langevin equation (2.4), adding to it a nonlocal driving force (see [104] for more detail):

$$\dot{T}_p(t) = -\Omega \frac{\partial \mathcal{H}}{\partial \bar{T}_p(t)} - f_p(t, [\mathbf{q}(t)]) + \eta_p(t), \quad (3.6)$$

where the driving force f is nonlocal in time and takes the form,

$$f_p(t, [\mathbf{q}(t)]) := \int dt' R_k^{(1)}(\mathbf{p}, t - t') T_p(t'), \quad (3.7)$$

where $R_k^{(1)}$ is assumed to be a real kernel. The effect of this force is to "freeze" IR contributions. In addition, we modify the noise correlation function, adding to it a nonlocal contribution introducing a *short memory* in the system:

$$\langle \eta(\mathbf{g}, t) \bar{\eta}(\mathbf{g}', t') \rangle = \Omega \delta(\mathbf{g}'(\mathbf{g})^{-1}) \left[\delta(t - t') + \frac{1}{\Omega} R_k^{(2)}(t - t') \right]. \quad (3.8)$$

Following the same steps as for the deduction of the generating functional (2.37), we find

$$Z_k[J, \bar{J}, j, \bar{j}] := \int d\mathbf{q} d\chi e^{-\Omega^2 S[\mathbf{q}, \chi] - \Delta S_k[\mathbf{q}, \chi] + J \cdot \mathbf{q} + j \cdot \chi}, \quad (3.9)$$

where

$$\Delta S_k[\mathbf{q}, \chi] = \sum_{p \in \mathbb{Z}^d} \int d\omega \left(\bar{\chi}_p(\omega) R_k^{(2)}(\mathbf{p}, \omega) \chi_p(\omega) \right.$$
$$+ i R_k^{(1)}(\mathbf{p}, \omega) \bar{\chi}_p(\omega) T_p(\omega)$$
$$\left. + i R_k^{(1)}(\mathbf{p}, -\omega) \bar{T}_p(\omega) \chi_p(\omega) \right), \quad (3.10)$$

which define the components of the bold matrix $\mathbf{R}_k$:

$$\mathbf{R}_k(\mathbf{p}, \omega) := \begin{pmatrix} R_k^{(2)}(\mathbf{p}, \omega) & +i R_k^{(1)}(\mathbf{p}, \omega) \\ i R_k^{(1)}(\mathbf{p}, -\omega) & 0 \end{pmatrix}, \quad (3.11)$$

and where Fourier components of $R_k(\mathbf{p}, \omega)$ are defined as

$$R_k(\mathbf{p}, t) := \frac{1}{2\pi} \int d\omega e^{-i\omega t} R_k(\mathbf{p}, \omega). \quad (3.12)$$

The partition function has the expected form. There are, however, two physical constraints to take into account. Causality and time-reversal symmetry, are closely related to the fluctuation-dissipation theorem (FDT) [103,121,122]. Note that the Langevin equation (2.4), being of the first

order, admits only one causal solution. We will describe the constraints on the regulator so that these physical conditions are preserved by the regularized theory, i.e. so that the effective models along the RG flow still describe an equilibrium dynamics compatible with causality. Note that this construction ensures that the component $\bar{\chi}\chi$ of propagator (3.5) vanishes, $G_{k,\bar{\chi}\chi} = 0$.

Time-reversal symmetry and FDT. The time-reflection symmetry is a direct consequence of this equilibrium dynamics, to which we will limit ourselves in this paper. It is realized by the following transformations on the fields $\Xi \to \Xi'$ for the nonregularized theory ($\mathbf{R}_k = 0$) as

$$T'_p(t) = T_p(-t), \qquad \chi'_p(t) = \chi_p(-t) - \frac{2i}{\Omega} \dot{T}_p(-t), \quad (3.13)$$

and for complex conjugates:

$$\bar{T}'_p(t) = \bar{T}_p(-t), \qquad \bar{\chi}'_p(t) = \bar{\chi}_p(-t) + \frac{2i}{\Omega} \dot{\bar{T}}_p(-t). \quad (3.14)$$

It is easy to see that these transformations leave the nonregularized classical action $S[\mathbf{q}, \chi]$ invariant, within total derivatives. Moreover, the Jacobian of the transformation being equaled to 1, the path integral defining the partition function is invariant as well for zero external sources. The transformations of the source terms into counterparts give a certain number of relations between observable, from which the classical FDT follows. Let us derive it from the expected invariance of the functional integral. The source term—$J \cdot \mathbf{q} + j \cdot \chi$—in (2.37) transforms as

$$J \cdot \mathbf{q} + j \cdot \chi \to \tilde{J} \cdot \mathbf{q} + \tilde{j} \cdot \chi$$
$$- \frac{2i}{\Omega} \sum_p \int dt \left(\bar{\tilde{j}}_p(t) \dot{T}_p(t) - \tilde{j}_p(t) \dot{\bar{T}}_p(t) \right), \quad (3.15)$$
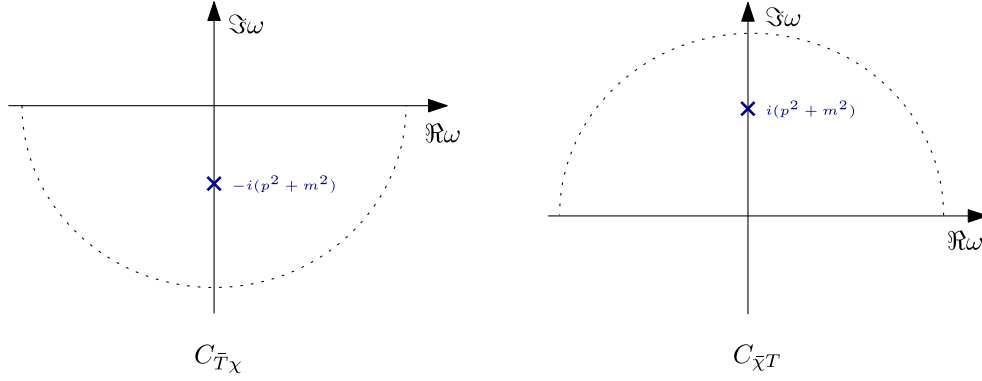
up to total derivative contributions. We moreover introduced the notation $\tilde{X}(t) := X(-t)$. We introduce the following definitions:

$$R_p(t, t') := \langle \bar{\chi}_p(t) T_p(t') \rangle, \qquad D_p(t, t') := \langle \bar{T}_p(t) T_p(t') \rangle, \quad (3.16)$$

and the transformation (3.15) leads to the FDT:

$$\boxed{R_p(t, t') - R_p(-t, -t') = \frac{2i}{\Omega} \frac{d}{dt} D_p(t, t').} \quad (3.17)$$

Since $D_p(t, t')$ is symmetric, and assuming translation invariance, i.e. $R_p(t, t') \equiv R_p(t - t')$, this relation be rewritten as

FIG. 3. Poles of the components $C_{\bar{T}\chi}$ and $C_{\bar{\chi}T}$ of the free propagator.

$$R_p(t) = \frac{2i}{\Omega}\theta(t)\frac{d}{dt}D_p(t). \qquad (3.18)$$

These relations can be converted to the Fourier representation as

$$\boxed{G_{\bar{\chi}T}(\hat{\omega},p^2) - G_{\bar{\chi}T}(-\hat{\omega},p^2) = 2\hat{\omega}G_{\bar{T}T}(\hat{\omega},p^2)}. \qquad (3.19)$$

It is easy to check that this relation is satisfied, at zero order, by free propagators (2.46) and (2.47). Let us show how the regulator can be compatible with these physical constraints. We would like to construct a regulator ΔS_k that is compatible with the time reversal, i.e., which is invariant under the transformations (3.13) and (3.14). A calculation detailed in Appendix B shows the we must have

$$\boxed{R_k^{(1)}(p, t' - t) - R_k^{(1)}(p, t - t') - \frac{2}{\Omega}\dot{R}_k^{(2)}(p, t' - t) = 0}. \qquad (3.20)$$

In terms of Fourier components, this relation reads,

$$R_k^{(1)}(p, \omega) - R_k^{(1)}(p, -\omega) = -2i\hat{\omega}R_k^{(2)}(p, \omega). \qquad (3.21)$$

For such a time-reversal symmetric regulator, FDT (3.19) holds for all k.

Causality. The driving force $f_p(t, [q(t)])$ added to the Langevin equation depending nonlocally (in time) on the trajectory $q(t)$, we must have to preserve causality:

$$\boxed{R_k^{(1)}(p, t - t') \propto \theta(t - t')}. \qquad (3.22)$$

For the theory without a regulator, the free propagators satisfy nontrivial causality conditions, which can be investigated from the explicit expressions (2.46) and (2.47). For instance, the component $C_{\bar{\chi}T}$ reads as

$$C_{\bar{\chi}T}(\omega, p^2) = \frac{1}{\omega + i(p^2 + m^2)}, \qquad (3.23)$$

which has a single pole $\omega = -i(p^2 + m^2)$, in the lower half part of the complex part (see Fig. 3). Hence, the free two-point function,

$$\langle \bar{\chi}_p(t)T_p(t') \rangle = \int \frac{d\omega}{\sqrt{2\pi}} \frac{e^{i\omega(t-t')}}{\omega + i(p^2 + m^2)}, \qquad (3.24)$$

which vanishes for $t - t' > 0$ from residue theorem. Hence,

$$\langle \bar{\chi}_p(t)T_p(t') \rangle \propto \theta(t' - t). \qquad (3.25)$$

Note also that at zero moments, it is the mass that removes the ambiguity on the position of the poles.[4] This causality will be an important condition to respect in the construction of the nonperturbative RG, and we will impose the effective two-point functions to satisfy them, asking that the poles of the functions $G_{k,\bar{T}\chi}$ and $G_{k,\bar{\chi}T}$ are, respectively, located in the half lower part and the half upper part of the complex plane, as in Fig. 3. This condition allows us to understand an important point. In the following sections, we will construct an approximation for the Γ_k functional through a truncation. Causality allows us to understand that this functional cannot contain independent contributions from the response fields χ and $\bar{\chi}$. In other words, it must necessarily have

$$\Gamma_k|_{\chi=\bar{\chi}=0} = 0, \quad \forall\, k, \qquad (3.26)$$

a property that we call *heteroclicity*. We already know that this condition is realized initially for the action S; see (2.38). To show that this contribution is zero, it is therefore sufficient to show that its flow is zero, in other words, that:

---

[4]For a zero mass, we should have to regularize with a parameter $\epsilon \to 0^+$ to guarantee causality.

$$\frac{d}{dk}\Gamma_k|_{\chi=\bar{\chi}=0} = 0, \quad \forall \, k. \tag{3.27}$$

This is easy from (3.4). The flow equation involves three contributions. The first one involves the product

$$\frac{d}{dk}R_k^{(2)}(\boldsymbol{p}, t-t')\langle\bar{\chi}_{\boldsymbol{p}}(t)\chi_{\boldsymbol{p}}(t')\rangle,$$

which vanishes due to the condition (2.48). The second contribution has the form

$$\frac{d}{dk}R_k^{(1)}(\boldsymbol{p}, t-t')\langle\bar{\chi}_{\boldsymbol{p}}(t)T_{\boldsymbol{p}}(t')\rangle,$$

and vanishes because $R_k^{(1)}(t-t') \propto \theta(t-t')$ and $\langle\bar{\chi}(t)T(t')\rangle \propto \theta(t'-t)$. The third contribution vanishes for the same reason.

Remark 2. It is important to note that the condition (3.27) is easy to check in the case of coarse graining in time, as is the case in this paper. It is more subtle in the case where we practice coarse graining only on moments and not on frequencies. In this case, one must return to the discrete version of the equations in the Îto prescription; see, for instance, [101]. In this case, we show that the coincident time correlations must be replaced by regularized versions:

$$\langle\bar{\chi}_{\boldsymbol{p}}(t)T_{\boldsymbol{p}'}(t')\rangle_\epsilon \equiv \langle\bar{\chi}_{\boldsymbol{p}}(t+\epsilon)T_{\boldsymbol{p}'}(t')\rangle, \tag{3.28}$$

which introduces a factor $e^{i\omega\epsilon}$ in the Fourier integrals. This factor ensures convergence of integrals in the upper or lower part of the complex integrals, and the previous condition (3.27) follows from the expected position of poles in the integrals, once again as a consequence of causality. Note moreover that the last condition is obvious in the supersymmetric formalism, quite natural in the Stratonovich sense. Supersymmetry, which is ensured by Ward-Takahashi identities for the quantum theory, implies that the constant term flows vanish due to the cancellation of bosonic and fermionic loops [105].

Remark 3. The condition (3.27) can be checked from perturbation theory as follows. Let us focus on the quartic melonic model. Figure 4 lists the expected boundaries for effective vertex functions, which can be generated in
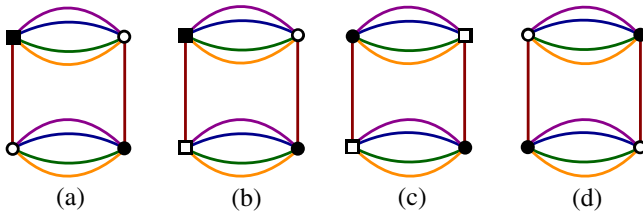
FIG. 4. List of boundaries which can be generated from initial conditions by Feynman diagrams.
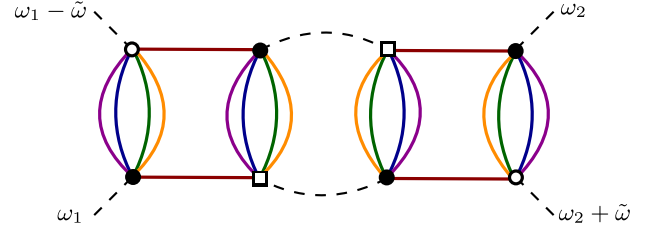
FIG. 5. The one-loop Feynman graph contributing to the 1PI effective vertex function corresponding to boundary (d).

leading order from melonic diagrams. Note that all the allowed configurations are not pictured in the figure. For instance, there exist the same configuration as (a), obtained by reversing the black and white colors of the nodes. We will denote as $(\bar{a})$ this configuration. Note that some edges are their own deputy. Thus, $d = \bar{d}$. Note, moreover, that only boundaries of type a and $\bar{a}$ are involved in the classical action. At one loop, the boundary diagram d, which does not contain the response field, comes from the diagram pictured in Fig. 5. For zero external momenta $\boldsymbol{p}$, the corresponding Feynman amplitude reads as

$$\mathcal{A} \sim -\sum_{\boldsymbol{q}\in\mathbb{Z}^4}\int\frac{d\omega}{\sqrt{2\pi}}\frac{e^{i\omega\epsilon}}{\omega+i(\boldsymbol{q}^2+m^2)}\frac{e^{i(\omega-\tilde{\omega})\epsilon}}{(\omega-\tilde{\omega})+i(\boldsymbol{q}^2+m^2)},$$

$$\tag{3.29}$$

where, according to the remark (2), we introduced a factor $e^{i\omega\epsilon}$, $\epsilon \to 0^+$ [equation (3.28) of remark (2)] and where $\tilde{\omega}$ denote the total external frequency. Introducing Feynman parameters [123], the integrand reads

$$\frac{e^{i\omega\epsilon}}{\omega+i(\boldsymbol{q}^2+m^2)}\frac{e^{i(\omega-\tilde{\omega})\epsilon}}{(\omega-\tilde{\omega})+i(\boldsymbol{q}^2+m^2)}$$

$$= \int_0^1 dx\frac{e^{i(2\omega-\tilde{\omega})\epsilon}}{[\omega+i(\boldsymbol{q}^2+m^2)-x\tilde{\omega}]^2}$$

$$= e^{i\tilde{\omega}\epsilon}\int_0^1 dx\frac{e^{2i\omega\epsilon}}{[\omega+i(\boldsymbol{q}^2+m^2)-x\tilde{\omega}]^2}$$

$$= e^{i\tilde{\omega}\epsilon}\frac{d}{d\tilde{\omega}}\int_0^1\frac{dx}{x}\frac{e^{2i\omega\epsilon}}{\omega+i(\boldsymbol{q}^2+m^2)-x\tilde{\omega}}.$$

The unique pole is in the half lower part of the complex plane, and the integral over ω vanishes identically, in agreement with (3.27).

C. Renormalization and scaling dimension

1. Renormalized theory

According to the theorem 2.1, the equilibrium distribution of the quartic melonic model is just renormalizable for $d = 5$. Thus, it must be possible to make the perturbation

theory for the equilibrium distribution $\rho(\boldsymbol{q}) \sim e^{-\mathcal{H}[q]}$ finite at any order,[5] using a finite number of counterterms. There are three of such a counterterms Z_m, Z_λ, and Z_∞, and we renormalize, respectively, the mass $m^2 \to Z_m m_r^2$, the coupling $\lambda \to Z_\lambda \lambda$, and the field $\varphi \to Z_\infty^{1/2} \varphi$ [37]. We will assume that these counterterms are adjusted so that the continuous limit exists (the theory being asymptotically free, [114]). To simplify the notations, we will simply call λ and m^2 the coupling and mass parameters, including counterterms, and we will note λ_r and m_r^2 the renormalized

(finite) versions of these parameters. Moreover, we will fix the finite part of Z_∞ so that the effective propagator of the equilibrium theory behaves as[6]

$$G_{\text{eq}}(\boldsymbol{p}^2) \sim \frac{1}{\boldsymbol{p}^2 + m_r^2}, \qquad (3.30)$$

as $k \to 0$ and for $\boldsymbol{p}$ small enough. The regularized kinetic Lagrangian then reads as

$$S_{\text{kin}} = \sum_{\boldsymbol{p} \in \mathbb{Z}^5} \int_{-\infty}^{+\infty} d\hat{\omega} \left(\bar{\chi}_{\boldsymbol{p}}(\hat{\omega})\chi_{\boldsymbol{p}}(\hat{\omega}) + i\bar{\chi}_{\boldsymbol{p}}(\hat{\omega})(-i\hat{\omega} + Z_\infty \boldsymbol{p}^2 + m^2)T_{\boldsymbol{p}}(\hat{\omega}) - i\bar{T}_{\boldsymbol{p}}(\hat{\omega})(i\hat{\omega} + Z_\infty \boldsymbol{p}^2 + m^2)\chi_{\boldsymbol{p}}(\hat{\omega}) \right), \quad (3.31)$$

disregarding the renormalization of the response field that we will consider later. The quartic interaction receives counterterms as well, and in (2.44), we must replace $\lambda \to Z_\infty^2 Z_\lambda \lambda_r$. For this model, the counterterms Z_∞ and Z_λ can be formally computed, as the authors in [65] showed. We recall their conclusions here for self-consistency:

Proposition 2. With the normalization condition (3.30) and the renormalized coupling, λ_r providing the correct four-point function at zero momenta, the countersterms Z_∞ and Z_λ are equal to all orders of the perturbation theory. Moreover,

$$Z_\infty^{-1} := 1 - 2\lambda_r A_\infty, \qquad (3.32)$$

with A_∞ given by

$$A_\infty := \sum_{\boldsymbol{p} \in S_\Lambda \subset \mathbb{Z}^4} \left(\frac{1}{Z_\infty \boldsymbol{p}^2 + Z_m m_r^2 - \Sigma_\infty(\boldsymbol{p})} \right)^2, \qquad (3.33)$$

where the sum is assumed to have some UV cutoff Λ ($\lim_{\Lambda \to \infty} S_\Lambda = \mathbb{Z}^4$) and $\Sigma_\infty(\boldsymbol{p})$ has quartic and logarithmic divergences with respect to Λ.

The counterterms in (3.33) cancels all the divergences in $\Sigma_\infty(\boldsymbol{p})$, except the global one of the sum, which corresponds to the last subtraction in the Zimmerman forest. Hence, A_∞ behaves as $\ln(\Lambda)$. More details can be found in Appendix A 1.

2. Scaling dimension

In quantum theory in ordinary fields, the scaling dimension is closely related to renormalizability. An analogous notion can be defined for TGFTs (see the

references [59,97], or [61]), which accommodates the nonlocal nature of the interactions and the background independent definition of the theory. We have the following definition:

Definition 4. Let b a bubble having $n(b)$ white vertices and $\mathbb{G}$ the set of two-point diagrams made of a single vertex of type b. The scaling dimension $\dim(b)$ is defined as

$$\dim(b) = 2 - \max_{r \in \mathbb{G}} \omega(r). \qquad (3.34)$$

This definition in particular implies that two-point bubbles have dimension 2, and in particular, the mass must have dimension 2: $[m^2] = 2$. In the same way, from (2.23), the leading-order two-point functions built with a single quartic melonic vertex are such that $\omega(r) = 2$, and the canonical dimension vanish $[\lambda] = 0$, in agreement with the just renormalizability of the quartic model.

IV. MELONIC APPROXOMIATION

A. Truncation and regulation

Solving the exact RG equation (3.4) is a difficult task, even for simple problems, and requires approximations. Usually, these approximations take the form of truncation in the full theory space, which is the functional space of infinite dimension spanned by all allowed classical actions defined by the condition that the classical Hamiltonian $\mathcal{H}[\varphi, \bar{\varphi}]$ is a sum of connected invariants. The truncation will allow for the restriction of the phase space to a smaller domain where the equations will be easily solvable. The method that we propose, the EVE, nevertheless allows capturing entire sectors, containing an infinite number of interactions, as well as the dependence of the effective vertices on the external momenta.

---

[5]Note that to agree with the convention in the literature and in Appendix A 1, we canceled the global factor 2 by a suitable redefinition of fields and couplings in this section.

[6]Avoiding IR fixed points; see [97] for more details.

We will choose the following ansatz for the effective average action Γ_k:

$$\Gamma_k[M, \bar{M}, \sigma, \bar{\sigma}] = \Omega^2 \sum_{\boldsymbol{p} \in \mathbb{Z}^5} \int_{-\infty}^{+\infty} d\hat{\omega} \left(Y(k)\bar{\sigma}_{\boldsymbol{p}}(\hat{\omega})\sigma_{\boldsymbol{p}}(\hat{\omega}) + i\bar{\sigma}_{\boldsymbol{p}}(\hat{\omega})(-iY(k)\hat{\omega} + Z(k)\boldsymbol{p}^2 + m^2(k))M_{\boldsymbol{p}}(\hat{\omega}) \right.$$

$$\left. + i\bar{M}_{\boldsymbol{p}}(\hat{\omega})(iY(k)\hat{\omega} + Z(k)\boldsymbol{p}^2 + m^2(k))\sigma_{\boldsymbol{p}}(\hat{\omega}) + i\left(\bar{\sigma}_{\boldsymbol{p}}(\hat{\omega})\frac{\delta\hat{\mathcal{H}}_{\text{int},k}}{\delta\bar{M}_{\boldsymbol{p}}(\hat{\omega})} + \sigma_{\boldsymbol{p}}(\hat{\omega})\frac{\delta\hat{\mathcal{H}}_{\text{int},k}}{\delta M_{\boldsymbol{p}}(\hat{\omega})} \right) \right), \quad (4.1)$$

where $Y(k)$ as $Z(k)$ and $m(k)$ look like a kinetic coupling, and this parameter ensures the time reversal symmetry with respect to the transformation (3.13) and (3.14), and

$$\hat{\mathcal{H}}_{\text{int},k}[M, \bar{M}] = \int d\hat{t} \sum_b k^{\dim(b)} Z^{n(b)}(k)\bar{\lambda}_b \text{Tr}_b[\varphi(\hat{t}), \bar{\varphi}(\hat{t})], \tag{4.2}$$

provided that $\mathcal{H}_{\text{int}}$ is given by (2.12), and the dimensionless time $\hat{t}$ is $\hat{t} := \Omega t$. The sum runs over connected tensorial invariants, $\dim(b)$ is the scaling dimension of the bubble b [see (3.34)], and $n(b)$ the number of fields $\varphi(\boldsymbol{g}, t)$ involved in the interaction b. One can justify the truncation (4.1) as follows. First, the time-reversal symmetry (3.13) implies that the quadratic term in $\bar{\sigma}_{\boldsymbol{p}}(\hat{\omega})\sigma_{\boldsymbol{p}}(\hat{\omega})$ renormalizes as the linear terms $i\hat{\omega}\bar{\sigma}_{\boldsymbol{p}}(\hat{\omega})M_{\boldsymbol{p}}(\hat{\omega})$ and $-i\hat{\omega}\bar{M}_{\boldsymbol{p}}(\hat{\omega})\sigma_{\boldsymbol{p}}(\hat{\omega})$.

Remark 4. The truncation (4.1) is compatible with a symmetric phase approximation, i.e., with an expansion around zero vacuum field. In the symmetric phase, it is easy to check that two-point functions are diagonals in their momenta indices. Moreover, odd vertex function vanishes identically—see [97] for an extended discussion.

Let us move on to the choice of the regulator. For all our investigations, we chose regulators $R_k^{(1)}$ and $R_k^{(2)}$ as a product of a pure frequency regulator with a momentum regulator. For the frequency regulator, we choose[7]

$$R_k^{(1)}(\boldsymbol{p}, \omega) = \Omega k^2 Z(k)\rho_k(\omega) r_k(\boldsymbol{p}^2), \tag{4.3}$$

and for the momentum regulator $r_k(\boldsymbol{p}^2)$, we choose the usual Litim regulator:

$$r_k(\boldsymbol{p}^2) := \alpha\left(1 - \frac{\boldsymbol{p}^2}{k^2}\right)\theta(k^2 - \boldsymbol{p}^2). \tag{4.4}$$

For the frequency regulator, we chose

$$\rho_k(\omega) := \frac{k^2}{k^2 - i\beta\omega/\Omega}. \tag{4.5}$$

This choice has been considered in [104,105]. It is causal (with a single pole in the lower part of the complex plane),

and its Fourier transform behaves like $\sim e^{-k^2\Omega t/\beta}\theta(t)$. Numerical coefficients α, β should be numerically tuned from the MSP, which assumes that an optimized flow induces a minimal dependence on the choice of the regulator [101,104,124]. Thus, by numerically computing the critical exponents and varying the parameters α and β, the MSP will fix their values at the points where the derivatives of the exponents concerning these parameters will vanish. In particular, for $\beta = 0$, the coarse graining is about momenta only, and we recover the standard RG without time regularization. In the rest of this paper, we will introduce dimensionless momenta x and frequencies y, defined as

$$\boldsymbol{p}^2 = k^2 x, \qquad \omega = \Omega Z(k)k^2 Y^{-1}(k)y. \tag{4.6}$$

We furthermore define the renormalized β as

$$\beta = Z^{-1}(k)Y(k)\hat{\beta}, \tag{4.7}$$

such that $\rho_k(\omega)$ transforms as

$$\rho_k(\omega) \to \hat{\rho}(y) = \frac{1}{1 - i\hat{\beta}y}, \tag{4.8}$$

and

$$R_k^{(1)}(\boldsymbol{p}, \omega) \to \hat{R}^{(1)}(x, y) := Z(k)\hat{\rho}(y)r(x), \tag{4.9}$$

where $r(x) := \alpha(1 - x)\theta(1 - x)$. The equation for $R_k^{(2)}$ can be derived from (3.21), and we have

$$R_k^{(2)}(\boldsymbol{p}, \omega) = \frac{\Omega^2 k^2}{2i\omega}Z(k)(\rho_k(-\omega) - \rho_k(\omega))r_k(\boldsymbol{p}^2), \tag{4.10}$$

and we get

$$R_k^{(2)}(\boldsymbol{p}, \omega) =: \Omega Y(k)\hat{\tau}(y)r_k(\boldsymbol{p}^2), \tag{4.11}$$

where

$$\hat{\tau}(y) = -\frac{\hat{\beta}}{1 + \hat{\beta}^2 y^2}, \tag{4.12}$$

which defines a dimensionless function $\hat{R}^{(2)}(x, y)$ as:

---

[7]Although we chose $\Omega = 1$ above, we reintroduce Ω here to clarify the conventions.

$$\hat{R}^{(2)}(x, y) := Y(k)\hat{\tau}(y)r(x). \tag{4.13}$$

Derivatives with respect to k can be easily computed, and we get for $R_k^{(1)}(\boldsymbol{p}, \omega)$:

$$k\frac{d}{dk}R_k^{(1)}(\boldsymbol{p}, \omega) = (2 + \eta)R_k^{(1)}(\boldsymbol{p}, \omega)$$

$$- Z(k)\Omega k^2 \frac{2 - i\hat{\beta}y(\eta_Y - \eta)}{(1 - i\hat{\beta}y)^2} r(x)$$

$$+ 2\alpha\Omega k^2 Z(k)\frac{1}{1 - i\hat{\beta}y}\theta(1 - x), \tag{4.14}$$

and for $R_k^{(2)}(\boldsymbol{p}, \omega)$:

$$k\frac{d}{dk}R_k^{(2)}(\boldsymbol{p}, \omega) = (2 + \eta_Y)R_k^{(2)}(\boldsymbol{p}, \omega)$$

$$+ 2\Omega Y(k)\hat{\beta}\frac{2 + \hat{\beta}^2 y^2(\eta_Y - \eta)}{(1 + \hat{\beta}^2 y^2)^2} r(x)$$

$$- 2\alpha\Omega Y(k)\frac{\hat{\beta}x^2}{1 + \hat{\beta}^2 y^2}\theta(1 - x). \tag{4.15}$$

For future calculations, we will define two dimensionless quantities:

$$\mu_1(x, y) := (2 + \eta)\rho(y)r(x) - \frac{2 - i\hat{\beta}y(\eta_Y - \eta)}{(1 - i\hat{\beta}y)^2} r(x)$$

$$+ 2\alpha\frac{1}{1 - i\hat{\beta}y}\theta(1 - x), \tag{4.16}$$

and

$$\mu_2(x, y) := \eta_Y\hat{\tau}(y)r(x) + 2\hat{\beta}\frac{2 + \hat{\beta}^2 y^2(\eta_Y - \eta)}{(1 + \hat{\beta}^2 y^2)^2} r(x)$$

$$- \frac{2\alpha\hat{\beta}x^2}{1 + \hat{\beta}^2 y^2}\theta(1 - x), \tag{4.17}$$

where

$$\boxed{\eta := \frac{1}{Z(k)}k\frac{d}{dk}Z(k), \qquad \eta_Y := \frac{1}{Y(k)}k\frac{d}{dk}Y(k).} \tag{4.18}$$
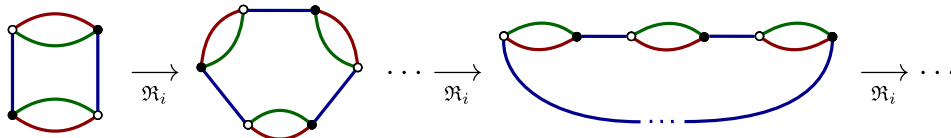
B. Melonic equations in the nonbranching sector

In this section, we will focus on a restricted sector of the theory, the nonbranching melonic sector. We will finally derive the flow equations in this approximation. This sector is stable (at leading order) along the RG and has shown its interest in the past [97,100,125–127]. Note that in this section and in the following, $\Omega = 1$ everywhere.

1. Nonbranching melons

As we recalled in the first part, the most divergent diagrams are said *melonics*. Strictly, melons are connected graphs and are then bubbles as well. For d-colored graphs, melons can be defined recursively as follows:

Definition 5. Any melonic bubble b_κ of valence κ may be deduced from the elementary melon b_1:

$$b_1 := \qquad\qquad , \tag{4.19}$$

replacing successively $\kappa - 1$ colored edges (including maybe color "0") by $(d - 1)$-dipole, the $(d - 1)$-dipole insertion operator $\mathfrak{R}_i$ being defined as

$$\tag{4.20}$$

In formula: $b_\kappa := (\prod_{\alpha=1}^{\kappa-1} \mathfrak{R}_{i_\alpha})b_1$.

For instance, the first bubble on Fig. 1 is a melon. For our nonperturbative investigations, we especially focus on a subsector of the melons, said *nonbranching*.

Definition 6. A nonbranching melonic bubble of valence κ, $b_\kappa^{(\ell)}$ is labeled with a single index $\ell \in [\![1, 5]\!]$ and defined such that:

$$b_\kappa^{(\ell)} := (\mathfrak{R}_\ell)^{\kappa-1}b_1. \tag{4.21}$$

Figure 6 provides the generic structure of melonic nonbranching bubbles in rank 3. Note that the definition holds for diagrams involving square nodes. Another important concept is that of the boundary diagram. It concerns Feynman diagrams, such as the one shown in the Fig. 2. We have the following definition:

Definition 7. Let G be a regular $(d + 1)$-colored Feynman diagram with $2N$ external dotted edges. They are hooked to $2N$ black and white nodes, say externals, and the boundary diagram ∂G of G is the regular d-colored graph, discarding edges with color 0 and such that:

FIG. 6.   Structure of the nonbranching melons, from the smallest one b_2.
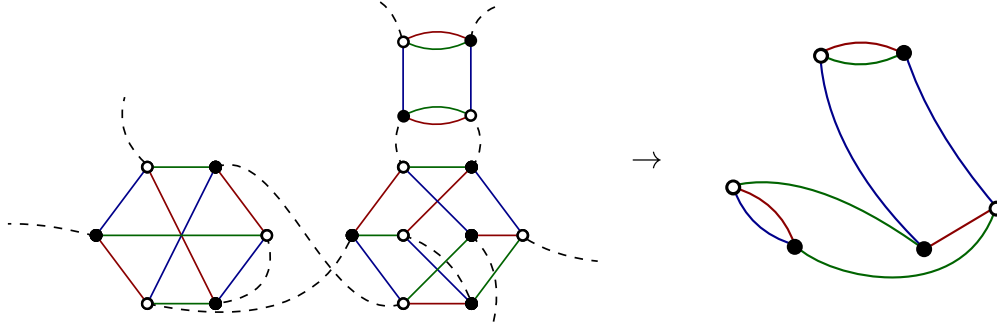
FIG. 7.   Illustration of the mapping $G \to \partial G$ for a six-point Feynman diagram in rank 3.

(1) Nodes of ∂G are external nodes of G
(2) Edges with color $\neq 0$ linking two external nodes are conserved.
(3) Any open cycle made of colors 0 and i between two external nodes n and $\bar{n}$ is replaced by a link of color i in ∂G.

Figure 7 illustrates the mapping for a Feynman diagram in rank 3. Note that the boundary diagram is melonic, but branched in that example.

In the rest of this paper, we will work in the subspace of the theory space, generated by the nonbranched melons. Thus, all 1PI functions will be assumed to admit a Feynman series whose boundary diagrams are nonbranched melons, and we will index each effective vertex by a bubble of this type. Because nonbranching bubbles are labeled with a single color, the corresponding $2n$-point vertex functions decompose along d components,

$$\Gamma_k^{(2n)} = \sum_{\ell=1}^{d} \Gamma_k^{(2n),(\ell)}, \qquad (4.22)$$

each component $\Gamma_k^{(2n),(\ell)}$ being assumed to be labeled with nonbranching melons of valence $2n$. We will now move on to the derivation of the flow equations in the nonbranching sector. We only derive flow equations for two- and four-point functions with zero external momenta and use melonic equations to close the hierarchy, expressing six-point functions in terms of four- and two-point ones.

2. Flow equations

Flow equations for different couplings can be obtained from the flow equation (3.4), taking successive derivative with respect to classical fields $M, \bar{M}, \sigma, \bar{\sigma}$. We introduce the notations $\Xi = \{M, \sigma\}$, $\bar{\Xi} = \{\bar{M}, \bar{\sigma}\}$, and

$$\Gamma_{k, \bar{\Xi}^{a_1} \cdots \bar{\Xi}^{a_P} \cdots \Xi^{b_1} \Xi^{b_P}}^{(2P)} = \frac{\delta^{2P} \Gamma_k}{\delta \bar{\Xi}_{\boldsymbol{p}_1}^{a_1}(\hat{\omega}_1) \cdots \delta \bar{\Xi}_{\boldsymbol{p}_P}^{a_P}(\hat{\omega}_P) \cdots \delta \Xi_{\boldsymbol{p}_P'}^{b_P}(\hat{\omega}_P')}, \qquad (4.23)$$

for $a_i, b_i = 0, 1$, $\Xi^0 = M$, $\Xi^1 = \sigma$. From truncation (4.1), we have

$$\Gamma_{k, \bar{\sigma}\sigma}^{(2)} = Y(k) \delta_{\boldsymbol{p}_1 \boldsymbol{p}_2} \delta(\hat{\omega}_1 - \hat{\omega}_2), \qquad (4.24)$$

and

$$\Gamma_{k, \bar{\sigma} M \bar{M} M}^{(4),(\ell)} = \frac{i}{\pi} \pi_k^{(2)}(p_{1\ell}^2, p_{3\ell}^2)(\mathcal{W}_{\boldsymbol{p}_1 \boldsymbol{p}_2 \boldsymbol{p}_3 \boldsymbol{p}_4}^{(\ell)} + \boldsymbol{p}_2 \leftrightarrow \boldsymbol{p}_4)$$
$$\times \delta(\hat{\omega}_1 - \hat{\omega}_2 + \hat{\omega}_3 - \hat{\omega}_4), \qquad (4.25)$$

where the function $\pi_k^{(2)}(p_{1\ell}^2, p_{3\ell}^2)$ (depending on the square of external momenta) gives the momentum dependence of the vertex, with normalization condition:

$$\pi_k^{(2)}(0,0) =: \lambda(k), \qquad (4.26)$$

defining the effective quartic coupling at scale k. Note that we disregarded any dependence of $\pi_k^{(2)}$ on the frequency. Our truncation is then ultralocal for the time parameter. We moreover introduce the notation:

$$\Gamma_{k, \bar{\Xi}^{a_1} \Xi^{a_2}}^{(2)} =: \gamma_{k, \bar{\Xi}^{a_1} \Xi^{a_2}}^{(2)}(\boldsymbol{p}_1, \hat{\omega}_1) \delta_{\boldsymbol{p}_1 \boldsymbol{p}_2} \delta(\hat{\omega}_1 - \hat{\omega}_2), \qquad (4.27)$$

and we have

$$\gamma_{k, \bar{\sigma} M}^{(2)}(\boldsymbol{p} = \boldsymbol{0}, \hat{\omega}_1 = 0) = im^2(k), \qquad (4.28)$$

and

$$\frac{d}{d\hat{\omega}_1}\gamma^{(2)}_{k,\bar{\sigma}M}(\boldsymbol{p}=\boldsymbol{0},\hat{\omega}_1=0):=Y(k),$$

$$\frac{d}{dp_i^2}\gamma^{(2)}_{k,\bar{\sigma}M}(\boldsymbol{p}=\boldsymbol{0},\hat{\omega}_1=0):=iZ(k), \qquad (4.29)$$

the last equation being valid for all $i = 1, \ldots, d$, agrees with the isotropic assumption. The flow equation for $\gamma^{(2)}_{k,\bar{\sigma}M}$ can be deduced from (3.4), taking derivatives with respect to $\bar{\sigma}$ and M. We obtain

$$\dot{\gamma}^{(2)}_{k,\bar{\sigma}M}(\boldsymbol{p}_1,\hat{\omega}_1)\delta_{\boldsymbol{p}_1\boldsymbol{p}_2}\delta(\hat{\omega}_1-\hat{\omega}_2) = -\text{Tr}\dot{\boldsymbol{R}}_k\boldsymbol{G}_k\Gamma^{(4)}_{k\bar{\sigma}M\bullet\bullet}\boldsymbol{G}_k, \quad (4.30)$$

where we omitted momenta and frequencies to simplify the expression and the trace Tr runs both over momenta, frequencies, and fields. The dots in the four-point functions $\Gamma^{(4)}_{k\bar{\sigma}M\bullet\bullet}$ designates allowed fields in the trace, and we introduced the notation

$$\dot{X} := k\frac{dX}{dk}. \qquad (4.31)$$

Equation (4.30) can be pictured as in Fig. 8, where dotted edges with gray circles materialize propagators, cross-circle
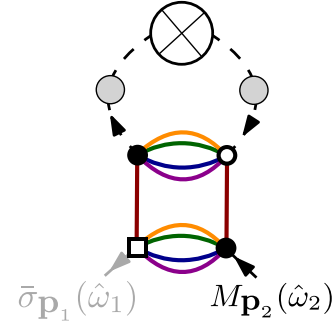
FIG. 8. Representation of the single-loop flow equation for $\gamma^{(2)}_{k,\bar{\sigma}M}$.

materializes regulator contribution $\dot{\boldsymbol{R}}_k$, and we pictured the four-point function in order to make the index structure explicit. On the figure, arrows are oriented from barred to nonbarred fields, and gray half edges materialize response fields. Because $G_{k\bar{\chi}\chi} = 0$ and $R_{k\bar{M}M} = 0$ [see (3.11)], and that from truncation (4.1) the only nonvanishing field configuration for bullets in $\Gamma^{(4)}_{k\bar{\sigma}M\bullet\bullet}$ is $\Gamma^{(4)}_{k\bar{\sigma}M\bar{M}M}$, there are only two contributions allowed for internal fields. Hence, we get

$$(4.32)$$

The two last contributions create only one face, accordingly to definition II A and are therefore less relevant than the two first ones, which are melonics following definition 5. Because we focus in this paper on the ultraviolet (UV) regime,
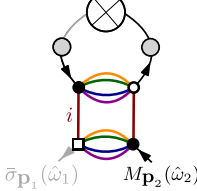
$$\Lambda \gg k \gg 1, \qquad (4.33)$$

for some UV cutoff Λ, and the two last configurations in (4.32) can then be discarded at the leading order. Note that we do not include some numerical factors counting the number of corresponding configurations. For instance, the

first configurations have to be multiplied by a factor 2, counting the two allowed configurations for the internal (black or gray) solid edges:

$$(4.34)$$

the arrows being oriented from "barred" to "nonbarred" fields. Diagrams of Eq. (4.32) can be easily translated in a formula; for instance (we count the diagram twice),

$$
= -2\delta_{\boldsymbol{p}_1\boldsymbol{p}_2}\delta(\hat{\omega}_1 - \hat{\omega}_2)\frac{\pi_k^{(2)}(p_{11}^2, p_{11}^2)}{\pi} \tag{4.35}
$$

$$
\times \sum_{\boldsymbol{p}} \delta_{p_1, p_{11}} \int d\hat{\omega} G_{k,\bar{\sigma}M}(\boldsymbol{p}^2, \hat{\omega}) G_{k,\bar{M}M}(\boldsymbol{p}^2, \hat{\omega}) \dot{R}_k^{(1)}(\boldsymbol{p}, \hat{\omega}) .
$$

In that equation, the components $G_{k,\bar{M}M}$ and $G_{k,\bar{\sigma}M}$ of the two-point function can be computed explicitly as

$$
G_{k,\bar{\sigma}M}(\boldsymbol{p}^2, \hat{\omega}) = -\frac{1}{k^2}\frac{i}{Z(k)}\frac{1}{\hat{f}(x, -y)} , \tag{4.36}
$$

and

$$
G_{k,\bar{M}M}(\boldsymbol{p}^2, \hat{\omega}) = \frac{1}{k^4}\frac{Y(k)}{Z^2(k)}\frac{1 + \hat{\tau}(y)r(x)}{\hat{f}(x, y)\hat{f}(x, -y)} , \tag{4.37}
$$
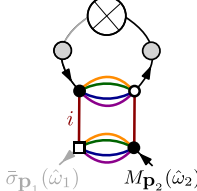
where $r(x) := \alpha(1 - x)\theta(1 - x)$, and for the truncation that we consider,

$$
\hat{f}(x, y) = iy + x + \bar{m}^2 + \hat{\rho}(-y)r(x), \tag{4.38}
$$

the dimensionless and renormalized mass and vertex function $\bar{m}^2$ and $\bar{\pi}_k^{(2)}$ being defined as [see (4.2)]

$$
m^2 =: Z(k)k^2\bar{m}^2, \qquad \pi_k^{(2)} = Z^2(k)\bar{\pi}_k^{(2)}. \tag{4.39}
$$

Using these definitions, a straightforward calculation leads to the expression,
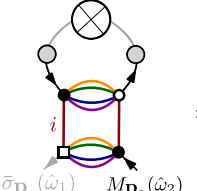
$$
= i\bar{\pi}_k^{(2)}(p_{11}^2, p_{11}^2)\delta_{\boldsymbol{p}_1\boldsymbol{p}_2}\delta(\hat{\omega}_1 - \hat{\omega}_2)Z(k)k^2 L_{21}(x_1) ,
$$

where $x_1 := p_1/k$, and assuming k large enough sums can be replaced by integrals. Hence, we define

$$
L_{21}(x_1) := \frac{2}{\pi}\int_{\mathbb{R}^d} d\mathbf{x}'dy\delta(x_1' - x_1)\mu_1(x', y)\frac{1 + \hat{\tau}(y)r(x')}{\hat{f}(x', y)\hat{f}^2(x', -y)} , \tag{4.40}
$$

having introduced the notation $\mathbf{x} \in \mathbb{R}^d$, with components x_i and square length $x \equiv \sum_i x_i^2$. In the same way, we get the second diagram:

$$
= i\bar{\pi}_k^{(2)}(p_{11}^2, p_{11}^2)\delta_{\boldsymbol{p}_1\boldsymbol{p}_2}\delta(\hat{\omega}_1 - \hat{\omega}_2)Z(k)k^2(-L_{22}(x_1)) , \tag{4.41}
$$

with

$$L_{22}(x_1) = \frac{2}{\pi} \int_{\mathbb{R}^d} d\mathbf{x}' dy \delta(x_1' - x_1) \frac{\mu_2(x', y)}{\hat{f}(x', y)\hat{f}(x', -y)}. \quad (4.42)$$

The flow equation for mass can be obtained by setting $p_1 = 0$. From the normalization condition (4.26), we get

$$\boxed{\beta_{m^2} = -(2 + \eta)m^2 - d\bar{\lambda}(L_{21}(0) - L_{22}(0))}, \quad (4.43)$$

using the conventional notation in field theory $\beta_X := \dot{X}$. In the symmetric phase moreover, where, in particular, $\Gamma_k^{(3)} = 0$, the anomalous dimension η_Y vanishes identically, as it can be easily checked from definitions (4.18) and (4.29):

$$\boxed{\eta_Y = 0 \quad \text{(in the symmetric phase)}}. \quad (4.44)$$

Let us detail the derivation of the flow equation for η. We will not be able to complete the derivation in this section, the end of the derivation being given in Sec. V.

From definition (4.29), we have the self-consistency equation:

$$\boxed{\eta = -\bar{\lambda}'(L_{21}(0) - L_{22}(0)) - \bar{\lambda}\frac{d}{dx_1^2}(L_{21}(x_1) - L_{22}(x_1))\Big|_{x_1=0}}, \quad (4.45)$$

where we defined

$$\frac{d}{dp_1^2}\pi_k^{(2)}(p_1^2, p_1^2)\Big|_{p_1=0} =: Z^2(k)k^{-2}\bar{\lambda}'. \quad (4.46)$$
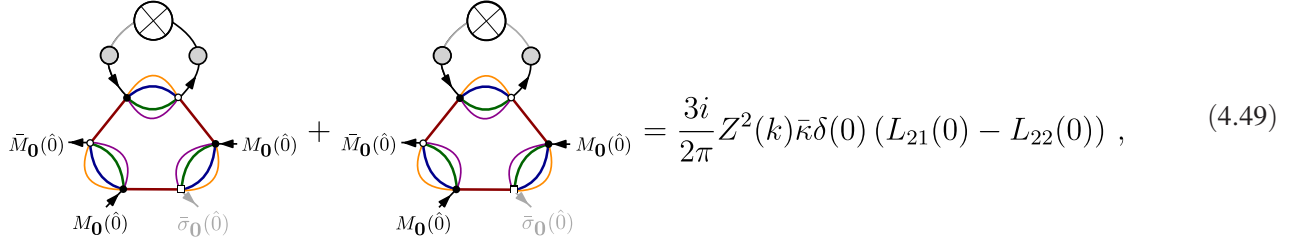
The equation for the four-point coupling λ can be deduced from the renormalization condition (4.25), setting external momenta and frequencies to zero. Deriving Eq. (3.4) one time for $\bar{\sigma}$, one time for $\bar{M}$ and two times concerning M and setting external momenta and frequencies to zero, we get, using the same graphical representation as before,

This equation requires defining the six-point functions, as we defined the four-point ones [Eq. (4.25)]. We need only the zero momenta function, which reads as follows:

$$\Gamma_{k,\bar{\sigma}M\bar{M}M\bar{M}M}^{(6),(\ell)}\Big|_0 = \frac{9i}{\pi^2}\kappa\delta(\hat{\omega}_1 - \hat{\omega}_2 + \hat{\omega}_3 - \hat{\omega}_4 + \hat{\omega}_5 - \hat{\omega}_6), \quad (4.48)$$

where κ denotes the sixtic coupling constant. For the two first diagrams, we get

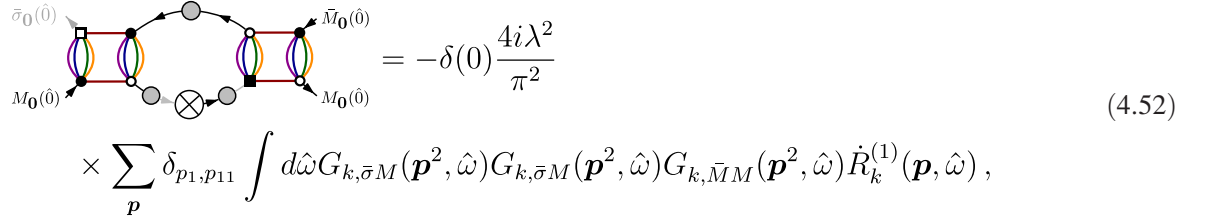$$= \frac{3i}{2\pi} Z^2(k) \bar{\kappa} \delta(0) \left(L_{21}(0) - L_{22}(0) \right), \tag{4.49}$$

where, from (3.34),

$$\kappa =: k^{-2} Z^3(k) \bar{\kappa}. \tag{4.50}$$

Indeed, the maximally divergent two-point diagram that we can build from a melonic six-point interaction has a divergent degree (see proposition 1):
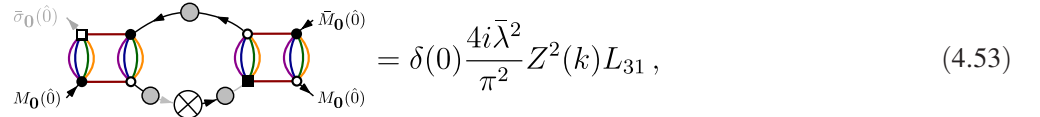
$$\omega(r) = -2L + F = -2 \times 2 + 2 \times (d-1) = 4, \tag{4.51}$$

then $\dim(b) = -2$. The computation of diagrams involving four-point vertices requires being more careful. Let us compute the first one. Explicitly, we have

$$= -\delta(0) \frac{4i\lambda^2}{\pi^2}$$

$$\times \sum_p \delta_{p_1, p_{11}} \int d\hat{\omega} \, G_{k,\bar{\sigma}M}(\boldsymbol{p}^2, \hat{\omega}) G_{k,\bar{\sigma}M}(\boldsymbol{p}^2, \hat{\omega}) G_{k,\bar{M}M}(\boldsymbol{p}^2, \hat{\omega}) \dot{R}_k^{(1)}(\boldsymbol{p}, \hat{\omega}), \tag{4.52}$$

which, after some algebra, can be rewritten as follows:

$$= \delta(0) \frac{4i\bar{\lambda}^2}{\pi^2} Z^2(k) L_{31}, \tag{4.53}$$

with

$$L_{31} = \int_{\mathbb{R}^4} d\mathbf{x} dy \frac{\mu_1(x,y)}{f^2(x,y)} \frac{1 + \tau(y) r(x)}{f(x,y) f(x,-y)}. \tag{4.54}$$

Each diagram can be computed in the same way. One can check, for instance, that the contribution of the first diagram equals one of the fifth diagrams, and after a tedious computation, we get for $\beta_\lambda := \dot{\bar{\lambda}}$

$$\boxed{\begin{aligned} \beta_\lambda = & -2\eta\bar{\lambda} - \tfrac{3}{2}\bar{\kappa}(L_{21}(0) - L_{22}(0)) \\ & + \tfrac{16\bar{\lambda}^2}{\pi} \left(L_{31} + \tfrac{1}{2} L_{32} - L_{33} \right) \end{aligned}}, \tag{4.55}$$

where

$$L_{32} := \int_{\mathbb{R}^4} d\mathbf{x} dy \mu_1(x,y) \frac{1 + \tau(y) r(x)}{f^2(x,y) f^2(x,-y)}, \tag{4.56}$$

$$L_{33} := \int_{\mathbb{R}^4} d\mathbf{x} dy \frac{\mu_2(x,y)}{f^2(x,y) f(x,-y)}. \tag{4.57}$$

Note that to derive these equations, we used the relation:

$$\boxed{G_{k,\bar{\sigma}M}(\hat{\omega}) = G_{k,\bar{M}\sigma}(-\hat{\omega})}, \tag{4.58}$$

which are also true for the bare propagators given by Eq. (2.46).

3. Structure equations

The flow equation (4.55) for the quartic coupling λ involves the sixtic coupling κ. Hence, in principle, we are obliged to consider the flow equation for κ, which involves the octic couplings and so on. The infinite hierarchical structure does not stop, even if:

(1) We stop it abruptly, imposing $\Gamma_k^{(2n)} = 0$ up to some n (crude truncation).

(2) We are able to express $\Gamma_k^{(2n)}$, up to a given n, in terms of $\Gamma_k^{(2(n-1))}$, $\Gamma_k^{(2(n-2))}$ and so on.

The first option has been widely considered for TGFTs [53,55,56,59,60,128], but some instability effects and incompatibilities with symmetry constraints have been noticed in our previous works [62,65,66], and the reliability of its predictions is still debated. The second option is more difficult to implement in general. It happens that we can close the hierarchy in this way by exploiting some constraints coming from the symmetries of the theory and which imply exact relations between effective vertices, such as the Ward identities (see, for instance, [118]). In this paper, we follow the strategy developed in our previous work [97], where authors present a method exploiting the tree structure of leading-order graphs, as melonic graphs, to get nontrivial relations between nonbranching observable. Because melonic diagrams dominate the RG flow in the deep UV, this strategy is expected to outperform the standard vertex expansion. Indeed, this method, called EVE, allows one to close the hierarchy and capture the full momenta dependence of effective vertices. We will now detail it here.

If we consider the quartic model given by (2.25), there are two kinds of quartic vertices, corresponding to vertices of type a and type $\bar{a}$. Hence, a general Feynman graph for the model takes the form given by Fig. 9 (on left), involving type a and type $\bar{a}$ vertices. Note that we have no dotted edges liking square nodes because $G_{k\bar{\chi}\chi} = 0$. We denote as $\mathcal{G}$ the set of Feynman graphs corresponding to this model. We moreover define $\mathcal{F}$ as the surjective map $\mathcal{F}:\mathcal{G}\to\bar{\mathc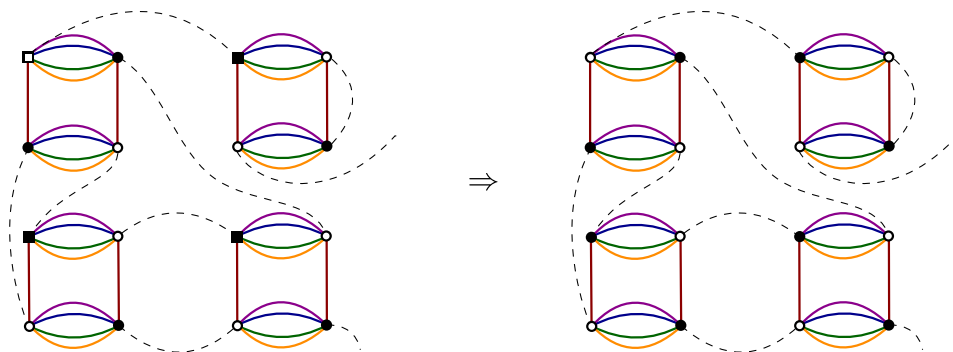al{G}}$, which send any Feynman graph G to a Feynman graph $\bar{G}\in\bar{\mathcal{G}}$ of the equilibrium theory (2.14). We denote as $\bar{\mathcal{G}}$ the set of Feynman graphs for the equilibrium theory. To be more precise, $\mathcal{F}$ acts on a given graph G by replacing all square nodes with disk nodes, without changing their color. A white square becomes a white disk and a black square becomes a black disk, as illustrated on 9. Moreover, propagators (2.46) and (2.47) for the dynamical theory are replaced by the propagator (2.19) of the equilibrium theory, a rank 5 Abelian GFT for U(1) structure group. Obviously, the inverse map $\mathcal{F}^{-1}$ is not one to one in general: $\mathcal{F}^{-1}(\bar{G}) = (G_1, G_2 \cdots, G_K)$, and we denote as K the *multiplicity of the graph* $\bar{G}$. In our previous works, EVE has been considered for the field theory corresponding to the equilibrium state (2.13) in [65,66,97]. The authors showed that melonic nonbranched six-point function $\Gamma_k^{(6),(\ell)}$, corresponding to sixtic melonic boundaries with color ℓ [accordingly with the definition (4.22)], can be expressed in terms of the four-point and two-point functions, and for zero external momenta (which is what we need to close the hierarchy), this relation reads

$$\Gamma_{k,\mathrm{eq}}^{(6),(\ell)}|_0 = (3!)^2 \times \mathcal{A}_{\bar{G}_0}, \qquad (4.59)$$

where $(3!)^2$ counts the number of different configurations for external momenta, and the graph $\bar{G}_0$ is pictured in Fig. 10. Note that $\bar{G}_0$ is not truly a Feynman graph but an *effective graph*, where external four-points vertices are effective four-point functions materialized by their boundary graphs and resuming an arbitrary number of graphs and where the interior two-point functions have been resumed as well [see Eq. (2.19)]:

$$\underline{\mathbf{q}} - \bigcirc - \underline{\mathbf{p}} = \frac{\delta_{\mathbf{pq}}}{\mathbf{p}^2 + m^2 - \Sigma_R(\mathbf{p})}, \qquad (4.60)$$

where $\mathbf{p} \in \mathbb{Z}^5$ and Σ_R means that divergences of the self-energy have been canceled by counterterms Z_∞ and Z_m, accordingly with the renormalization condition (3.30). If

FIG. 9. A typical Feynman graph G (on left) and the corresponding normal graph $\bar{G} = \mathcal{F}(G)$ (on right).
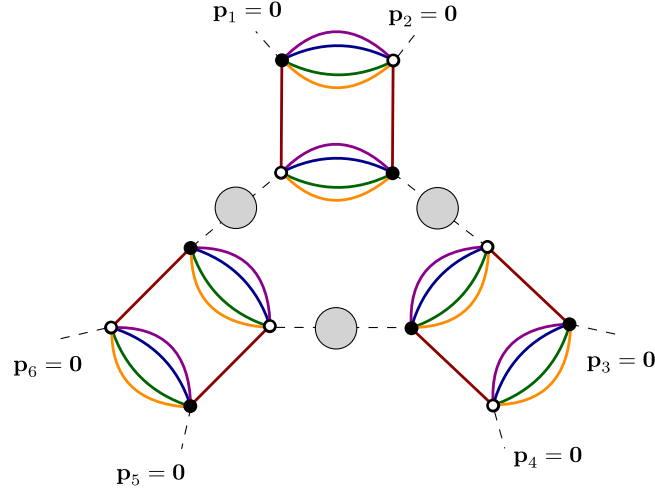
FIG. 10. The effective six-point graph $\bar{G}_0$. The external four-point vertex are indeed effective four-point functions, which we denote by their boundary graph.

we apply the inverse map $\mathcal{F}^{-1}$ to $\bar{G}_0$, we obtain a family of graphs $(G_1, ..., G_K)$ but having different boundaries (see definition 7). Hence, if we restrict ourselves to the graphs having the same boundary ∂G_0 of $\Gamma^{(6),(\ell)}_{k,\sigma\bar{M}M\bar{M}M\bar{M}}|_0$, we focus on the set $S = \{\mathcal{F}^{-1}[\bar{G}_0] | \partial G_i = \partial G_0 \ \forall \ G_i \in \mathcal{F}^{-1}[\bar{G}_0]\}$, where explicitly:

$$\partial G_0 := \quad , \qquad (4.61)$$

and the zero momenta effective vertex function $\Gamma^{(6),(\ell)}_{k,\bar{\sigma}M\bar{M}M\bar{M}M}|_0$ decomposes as

$$\Gamma^{(6),(\ell)}_{k,\sigma\bar{M}M\bar{M}M\bar{M}}|_0 = 12 \times \sum_{G \in S} \mathcal{A}_G, \qquad (4.62)$$

where we used the same notation $\mathcal{A}$ to denote the amplitude of the stochastic model, where $12 = 3! \times 2!$ counts the number of external momenta arrangements as before. It is easy to see that $|S| = 2$, and graphically:

$$\Gamma^{(6),(\ell)}_{k,\sigma\bar{M}M\bar{M}M\bar{M}}|_0 = 12 \times \left(\quad + \quad \right), \qquad (4.63)$$

disregarding external momenta and frequencies for simplicity. Note, moreover, that, as before, external four-point vertices are effective four-point functions materialized by their boundaries. Explicitly, we get

$$\Gamma^{(6),(\ell)}_{k,\sigma\bar{M}M\bar{M}M\bar{M}}|_0 = 12 Z^3(k) k^{-2} i \left(\frac{\bar{\lambda}}{\pi}\right)^3 \times (AI_1 + BI_2)\delta(0), \qquad (4.64)$$

where A and B are numerical constants that we can determine by perturbation theory. It is easy to check that

the loop integrals I_1 and I_2 are equals, and, using the integral approximation introduced before,

$$I_1 := \int_{\mathbb{R}^4} d\mathbf{x} \int dy \frac{1 + \tau(y)r(x)}{f^3(x,y)f(x,-y)}. \qquad (4.65)$$

The perturbation theory leads to $A = B = 1$, and we get from (4.48) and (4.50),

$$\boxed{\bar{\kappa} = \frac{4\bar{\lambda}^3}{3\pi} \int_{\mathbb{R}^4} d\mathbf{x} \int dy \frac{1 + \tau(y)r(x)}{f^3(x,y)f(x,-y)}.} \qquad (4.66)$$

We are now in a position to derive the last piece of the puzzle, namely, the derivative of the effective vertex at zero external momenta (4.46), required to compute the anomalous dimension.

Remark 5. It can be noticed that we used truncation to define the loop integral (4.65). The truncation is in principle expected to be valid only in a small region around k, namely on the support of $\dot{R}_k$. In [97], we showed that using truncation outside this support for divergent integral leads to dramatically wrong conclusions. In the same reference and [65], we showed that it can be a good approximation for convergent integral and, in particular, that this does not introduce Ward identity violations. We use this approximation scheme to compute our convergent integrals in this paper, as I_1 is.

To conclude, not that in our truncation, the integral in (4.65) can be computed analytically. For instance, without coarse graining in frequency ($\hat{\beta} = 0$) and setting $\alpha = 1$, we have

$$\bar{\kappa}|_{\hat{\beta}=0} = \frac{\pi^4 \bar{\lambda}^3 (\bar{m}^2(\bar{m}^2+3)+3)}{6(1+\bar{m}^2)^3}. \tag{4.67}$$

In the opposite limit, for $\alpha = 0$ but $\hat{\beta} = 1$, we get

$$\bar{\kappa}|_{\alpha=0} = \frac{\pi^4 \bar{\lambda}^3}{6\bar{m}^2}. \tag{4.68}$$

Both have an obvious infrared singularity for $\bar{m}^2 = 0$. Finally, for $\alpha = \hat{\beta} = 1$, we get

$$\begin{aligned} \bar{\kappa}|_{\alpha=1,\hat{\beta}=1} = \frac{\pi^4 \lambda^3}{6(1+\bar{m}^2)^3} &(\bar{m}^2(\bar{m}^2+7) \\ &+ 2(\bar{m}^2+1)(2\bar{m}^2+3)\log(1+\bar{m}^2) \\ &- 2(1+\bar{m}^2)(2\bar{m}^2+3)\log(2+\bar{m}^2)+7). \end{aligned} \tag{4.69}$$

V. ANOMALOUS DIMENSION AND WT IDENTITIES

The aim of this section is to use Ward-Takahashi (WT) identities to compute the last ingredients in the expression of anomalous dimension λ', defined in (4.46). Since the interactions are invariants by construction under unitary transformations of the type (2.10), there must exist nontrivial WT identities between effective vertex functions. These identities provide nontrivial relations that constrain the RG flow and allow us to compute the derivative of the effective vertices for their external momenta, which is exactly what we need to compute the anomalous dimension. These WT identities have been extensively discussed in the literature in the last years with this aim; see, for

instance [97], where authors investigate the equilibrium model (2.13).

A. WT identities for unitary symmetry

Working in the Peter-Weyl basis, the unitary transformations (2.10) act formally on fields components as

$$T_{\boldsymbol{p}} \to T'_{\boldsymbol{p}} = \sum_{q_i \in \mathbb{Z}} U_{p_i q_i} T_{\boldsymbol{q}}\Big|_{q_j = p_j \ \forall \ j \neq i}, \tag{5.1}$$

where

$$\sum_{q \in \mathbb{Z}} U^\dagger_{pq} U_{qp'} = \sum_{q \in \mathbb{Z}} U_{pq} U^\dagger_{qp'} = \delta_{pp'}. \tag{5.2}$$

The interaction part of the Hamiltonian $\mathcal{H}$ is invariant under such a transformation. Indeed, invariance is only broken by the Laplacian term in the kinetic action. Let us consider now the classical action S given by (2.38) and the generating functional $Z[J, \bar{J}, \jmath, \bar{\jmath}]$, equation (2.37). The interacting part S_{int} of the classical action is invariant if we transform both fields φ and χ:

$$T_{\boldsymbol{p}} \to T'_{\boldsymbol{p}} = \sum_{\boldsymbol{q} \in \mathbb{Z}^d} \left[\prod_{i=1}^d U^{(i)}_{p_i q_i} \right] T_{\boldsymbol{q}},$$

$$\chi_{\boldsymbol{p}} \to \chi'_{\boldsymbol{p}} = \sum_{\boldsymbol{q} \in \mathbb{Z}^d} \left[\prod_{i=1}^d U^{(i)}_{p_i q_i} \right] \chi_{\boldsymbol{q}}, \tag{5.3}$$

where $\{U^{(i)}\}$ are *d-independent* unitary transformations. We consider infinitesimal transformations,

$$U = I + \epsilon + \mathcal{O}(\epsilon^2), \tag{5.4}$$

where I is the identity matrix (with elements δ_{pq}), and $\epsilon = -\epsilon^\dagger$ is along the trivial representation of the Lie algebra of the unitary group. We furthermore define the operator $\hat{\epsilon}_i$, acting on the ith component of fields as:

$$\hat{\epsilon}_i[T]_{\boldsymbol{p}} := \sum_{q_i} \epsilon_{p_i q_i} T_{\boldsymbol{q}}\big|_{q_j = p_j, j \neq i}. \tag{5.5}$$

The global reparametrization invariance of the path integral defining the generating functional $Z[J, \bar{J}, \jmath, \bar{\jmath}]$ means that:

$$\hat{\epsilon}_i[Z[J, \bar{J}, \jmath, \bar{\jmath}]] = 0, \tag{5.6}$$

for all $i \in [\![1, d]\!]$. We can expand this relation to first order in ϵ:

$$\begin{aligned} 0 \equiv \int d\boldsymbol{q} d\chi & [\hat{\epsilon}_i[S[\boldsymbol{q}, \chi]] + \hat{\epsilon}_i[\Delta S_k[\boldsymbol{q}, \chi]] \\ & - \hat{\epsilon}_i[\boldsymbol{J} \cdot \boldsymbol{q} + \jmath \cdot \chi]] e^{-S[\boldsymbol{q}\chi] - \Delta S_k[\boldsymbol{q}\chi] + \boldsymbol{J} \cdot \boldsymbol{q} + \jmath \cdot \chi}. \end{aligned} \tag{5.7}$$

We will compute each term of the variation separately, starting with the source terms:

Computation of $\hat{\epsilon}_i[\boldsymbol{J}\cdot\boldsymbol{q} + J\cdot\boldsymbol{\chi}]$. The operator $\hat{\epsilon}_i$ acts linearly on each field, and after some arrangements we get

$$
\hat{\epsilon}_i[\boldsymbol{J}\cdot\boldsymbol{q} + J\cdot\boldsymbol{\chi}]
$$

$$
= \int d\omega \sum_{\boldsymbol{p},\boldsymbol{p}'} \prod_{j\neq i} \delta_{p_j p'_j} [\bar{J}_{\boldsymbol{p}}(\omega) T_{\boldsymbol{p}'}(\omega) - \bar{T}_{\boldsymbol{p}}(\omega) J_{\boldsymbol{p}'}(\omega)
$$

$$
+ \bar{J}_{\boldsymbol{p}}(\omega)\chi_{\boldsymbol{p}'}(\omega) - \bar{\chi}_{\boldsymbol{p}}(\omega) J_{\boldsymbol{p}'}(\omega)]\epsilon_{p_i p'_i}. \tag{5.8}
$$

Computation of $\hat{\epsilon}_i[S[\boldsymbol{q},\boldsymbol{\chi}]]$. The variation splits in two contributions, for kinetic part and interactions:

$$
\hat{\epsilon}_i[S[\boldsymbol{q},\boldsymbol{\chi}]] = \hat{\epsilon}_i[S_{\mathrm{kin}}[\boldsymbol{q},\boldsymbol{\chi}]] + \hat{\epsilon}_i[S_{\mathrm{int}}[\boldsymbol{q},\boldsymbol{\chi}]]. \tag{5.9}
$$

The second contribution to interaction vanishes by construction. The kinetic action for the response field $\sum_{\boldsymbol{p}} \bar{\chi}_{\boldsymbol{p}}\chi_{\boldsymbol{p}}$ is invariant as well, and the corresponding variation vanishes. This is also the case for contributions like $\hat{\omega}\sum_{\boldsymbol{p}} \bar{T}_{\boldsymbol{p}}\chi_{\boldsymbol{p}}$ and $m^2\sum_{\boldsymbol{p}} \bar{T}_{\boldsymbol{p}}\chi_{\boldsymbol{p}}$. Finally, only the Laplacian contributes nontrivially to the variation, and we get

$$
\hat{\epsilon}_i[S[\boldsymbol{q},\boldsymbol{\chi}]] = iZ_\infty \int d\omega \sum_{\boldsymbol{p},\boldsymbol{p}'} \prod_{j\neq i} \delta_{p_j p'_j} [p_i^2 - p_i'^2](\bar{\chi}_{\boldsymbol{p}}(\omega) T_{\boldsymbol{p}'}(\omega)
$$

$$
+ \bar{T}_{\boldsymbol{p}}(\omega)\chi_{\boldsymbol{p}'}(\omega))\epsilon_{p_i p'_i}. \tag{5.10}
$$

Computation of $\hat{\epsilon}_i[\Delta S_k[\boldsymbol{q},\boldsymbol{\chi}]]$. The computation of the variation of the regulator follows the same strategy as for the kinetic action:

$$
\hat{\epsilon}_i[\Delta S_k[\boldsymbol{q},\boldsymbol{\chi}]] = \int d\omega \sum_{\boldsymbol{p},\boldsymbol{p}'} \prod_{j\neq i} \delta_{p_j p'_j} (i[R_k^{(1)}(\boldsymbol{p},\omega) - R_k^{(1)}(\boldsymbol{p}',\omega)]\bar{\chi}_{\boldsymbol{p}}(\omega) T_{\boldsymbol{p}'}(\omega) + i[R_k^{(1)}(\boldsymbol{p},-\omega) - R_k^{(1)}(\boldsymbol{p}',-\omega)]\bar{T}_{\boldsymbol{p}}(\omega)\chi_{\boldsymbol{p}'}(\omega)
$$

$$
+ [R_k^{(2)}(\boldsymbol{p},\omega) - R_k^{(2)}(\boldsymbol{p}',\omega)]\bar{\chi}_{\boldsymbol{p}}(\omega)\chi_{\boldsymbol{p}'}(\omega))\epsilon_{p_i p'_i}. \tag{5.11}
$$

Taking into account all these contributions, the variation (5.7) implies the relation:

$$
0 = \int d\omega \sum_{\boldsymbol{p},\boldsymbol{p}'} \prod_{j\neq i} \delta_{p_j p'_j} \Bigg[(iZ_\infty[p_i^2 - p_i'^2] + i[R_k^{(1)}(\boldsymbol{p},\omega) - R_k^{(1)}(\boldsymbol{p}',\omega)])
$$

$$
\times \frac{\partial}{\partial J_{\boldsymbol{p}}(\omega)} \frac{\partial}{\partial \bar{J}_{\boldsymbol{p}'}(\omega)} + (iZ_\infty[p_i^2 - p_i'^2] + i[R_k^{(1)}(\boldsymbol{p},-\omega) - R_k^{(1)}(\boldsymbol{p}',-\omega)])
$$

$$
\times \frac{\partial}{\partial \bar{J}_{\boldsymbol{p}'}(\omega)} \frac{\partial}{\partial J_{\boldsymbol{p}}(\omega)} + [R_k^{(2)}(\boldsymbol{p},\omega) - R_k^{(2)}(\boldsymbol{p}',\omega)] \frac{\partial}{\partial J_{\boldsymbol{p}}(\omega)} \frac{\partial}{\partial \bar{J}_{\boldsymbol{p}'}(\omega)}
$$

$$
- \left(\bar{J}_{\boldsymbol{p}}(\omega) \frac{\partial}{\partial \bar{J}_{\boldsymbol{p}'}(\omega)} - J_{\boldsymbol{p}'}(\omega) \frac{\partial}{\partial J_{\boldsymbol{p}}(\omega)} + \bar{J}_{\boldsymbol{p}}(\omega) \frac{\partial}{\partial \bar{J}_{\boldsymbol{p}'}(\omega)} - J_{\boldsymbol{p}'}(\omega) \frac{\partial}{\partial J_{\boldsymbol{p}}(\omega)} \right) \Bigg] e^{W_k[J,\bar{J},J,\bar{J}]}, \tag{5.12}
$$

where we introduced the free energy:

$$
W_k[J,\bar{J},J,\bar{J}] := \ln Z_k[J,\bar{J},J,\bar{J}]. \tag{5.13}
$$

We also introduce the following notation:

$$
G_{p_1\cdots p_n,\bar{p}_1\cdots\bar{p}_{\bar{n}};p_I\cdots p_M,\bar{p}_1\cdots\bar{p}_{\bar{M}}}^{(n+\bar{n};M+\bar{M})} := \prod_{i=1}^{n} \frac{\partial}{\partial \bar{J}_{p_i}} \prod_{\bar{i}=1}^{\bar{n}} \frac{\partial}{\partial J_{\bar{p}_{\bar{i}}}} \prod_{I=1}^{M} \frac{\partial}{\partial \bar{J}_{p_I}} \prod_{\bar{I}=1}^{\bar{M}} \frac{\partial}{\partial J_{\bar{p}_{\bar{I}}}} W_k, \tag{5.14}
$$

where the notation p_i means $p_i = (\boldsymbol{p}_i, \hat{\omega}_i)$. We furthermore introduce the following notations for classical fields:

$$
M_p := \frac{\partial W_k}{\partial \bar{J}_p}, \qquad \bar{M}_p := \frac{\partial W_k}{\partial J_p}, \qquad \sigma_p := \frac{\partial W_k}{\partial \bar{J}_p}, \qquad \bar{\sigma}_p := \frac{\partial W_k}{\partial J_p}. \tag{5.15}
$$

The equation (5.16) then simplifies, and we deduce the following statement:

Proposition 3. Observable of the equilibrium dynamical model satisfy the following Ward-Takahashi identity:

$$0 = \int d\omega \sum_{\boldsymbol{p},\boldsymbol{p}'} \prod_{j \neq i} \delta_{p_j p'_j} [(iZ_\infty [p_i^2 - p_i'^2] + i[R_k^{(1)}(\boldsymbol{p},\omega) - R_k^{(1)}(\boldsymbol{p}',\omega)])(G_{k,\bar{\sigma}M}^{(1;\bar{1})}(\boldsymbol{p}',\omega;\boldsymbol{p},\omega) + \bar{\sigma}_{\boldsymbol{p}}(\omega)M_{\boldsymbol{p}'}(\omega))$$

$$+ (iZ_\infty [p_i^2 - p_i'^2] + i[R_k^{(1)}(\boldsymbol{p},-\omega) - R_k^{(1)}(\boldsymbol{p}',-\omega)])(G_{k,\bar{M}\sigma}^{(\bar{1};1)}(\boldsymbol{p},\omega;\boldsymbol{p}',\omega) + \sigma_{\boldsymbol{p}'}(\omega)\bar{M}_{\boldsymbol{p}}(\omega))$$

$$+ [R_k^{(2)}(\boldsymbol{p},\omega) - R_k^{(2)}(\boldsymbol{p}',\omega)](G_{k,\bar{\sigma}\sigma}^{(0;1+\bar{1})}(\boldsymbol{p}',\omega;\boldsymbol{p},\omega) + \sigma_{\boldsymbol{p}'}(\omega)\bar{\sigma}_{\boldsymbol{p}}(\omega))$$

$$- \bar{J}_{\boldsymbol{p}}(\omega)M_{\boldsymbol{p}'}(\omega) + J_{\boldsymbol{p}'}(\omega)\bar{M}_{\boldsymbol{p}}(\omega) - \bar{j}_{\boldsymbol{p}}(\omega)\sigma_{\boldsymbol{p}'}(\omega) + j_{\boldsymbol{p}'}(\omega)\bar{\sigma}_{\boldsymbol{p}}(\omega)]\delta_{p_i p}\delta_{p'_i p'}. \tag{5.16}$$

We will exploit these identities in the melonic approximation, focusing on the nonbranching sector of the theory, to compute λ'. A technical complement is given in Appendix C.

B. Computation of λ' defined in (4.46)

We now move to the last Ward identity that we need to achieve our RG program. Applying the fourth derivative $\partial^4 / \partial M_q(\omega_1)\partial\bar{\sigma}_{\bar{q}}(\bar{\omega}_1)\partial M_{q'}(\omega'_1)\partial\bar{M}_{\bar{q}'}(\bar{\omega}'_1)$. As the previous Ward identities provided a relation between the difference of two-point functions at different momenta and the four-point function, the Ward identities that we will derive in this section will provide nontrivial relations between four- and six-point functions and the difference between four-point kernels $\pi_k^{(2)}(p_1^2, p_2^2)$ with different momenta. As for previous relations, we have to note that Ward identities enjoy the same structure as flow equations considered in the previous section and indeed play a symmetric role: Ward identities say how we escape to the purely local sector, i.e., how to move inside the theory space as momentum change, and RG equations say how the theory moves as the cutoff changes. Obviously, the Ward generators do not commute with the flow because flow equations describe the flow of derivative coupling as well (as the anomalous dimension, for instance).

Using the same graphical representation as before, we obtain the equality:

$$(5.17)$$

where permutations of external fields $M_{q'}(\omega_1')$ and $M_q(\omega_1)$ are assumed when they are required. Moreover, we assumed $p' \neq q'$ to cancel the last term involving two four-point diagrams, proportional to $\delta_{p'q'}$. This relation can be translated as a differential equation for $\pi_k^{(2)}$ as follows. We set $p_j = p_j' = q_j = \bar{q}_j = 0 \; \forall \; j \neq i$, $p_i = p_i' + 1$, $q' = \bar{q}' = \mathbf{0}$, $p_i = \bar{q}_i$, and $p_i' = q_i$. With this configuration for the external momenta, the two last parentheses involve the difference:

$$\pi_k^{(2)}(0, p_i^2) - \pi_k^{(2)}(0, (p_i')^2) = \pi_k^{(2)}(0, p_i^2) - \pi_k^{(2)}(0, (p_i - 1)^2), \quad (5.18)$$

which can be approached in the deep UV regime ($\Lambda \gg 1$) by a derivative [see the discussion before equation (C20) in Appendix C]. Hence, setting $p_i = 0$, we have

$$\left[\pi_k^{(2)}(0, p_i^2) - \pi_k^{(2)}(0, (p_i - 1)^2) \right]\bigg|_{p_i=0}$$

$$\approx \frac{d}{dp_i^2} \pi_k^{(2)}(0, p_i^2)\bigg|_{p_i=0} \delta p^2, \quad (5.19)$$

which can be rewritten as

$$\frac{d}{dp_i^2} \pi_k^{(2)}(0, p_i^2)\bigg|_{p_i=0} = \frac{1}{2} \frac{d}{dp_i^2} \pi_k^{(2)}(p_i^2, p_i^2)\bigg|_{p_i=0}, \quad (5.20)$$

assuming $\pi_k^{(2)}$ to be a symmetric function, and the Ward identity reads explicitly,

$$-\frac{1}{2} \frac{i}{\pi} \frac{d}{dp_i^2} \pi_k^{(2)}(p_i^2, p_i^2)\bigg|_{p_i=0}$$

$$= -\frac{12i\kappa}{2^2\pi^2} \mathcal{L}_{k,1} - 4i\left(\frac{\lambda}{\pi}\right)^2 (\mathcal{L}_{k,2}^{(1)} + \mathcal{L}_{k,2}^{(2)}), \quad (5.21)$$

where we defined

$$\mathcal{L}_{k,1} := \int d\omega \sum_{\mathbf{p}\in\mathbb{Z}^4} \left[2\left(iZ_\infty + i\frac{d}{dp_1^2} R_k^{(1)}(\mathbf{p}, \omega) \right) G_{k,\bar{M}M}(\mathbf{p}, \omega) G_{k,\bar{\sigma}M}(\mathbf{p}, \omega) - \frac{d}{dp_1^2} R_k^{(2)}(\mathbf{p}, \omega) G_{k,\bar{\sigma}M}(\mathbf{p}, -\omega) G_{k,\bar{\sigma}M}(\mathbf{p}, \omega) \right]\bigg|_{p_i=0}, \quad (5.22)$$

$$\mathcal{L}_{k,2}^{(1)} := -i \int d\omega \sum_{\mathbf{p}\in\mathbb{Z}^4} \left(iZ_\infty + i\frac{d}{dp_1^2} R_k^{(1)}(\mathbf{p}, \omega) \right) G_{k,\bar{M}M}(\mathbf{p}, \omega) G_{k,\bar{\sigma}M}(\mathbf{p}, \omega) (2G_{k,\bar{\sigma}M}(\mathbf{p}, \omega) + G_{k,\bar{\sigma}M}(\mathbf{p}, -\omega))\bigg|_{p_i=0}, \quad (5.23)$$

and

$$\mathcal{L}_{k,2}^{(2)} := -i \int d\omega \sum_{\mathbf{p}\in\mathbb{Z}^4} \frac{d}{dp_1^2} R_k^{(2)}(\mathbf{p}, \omega) G_{k,\bar{\sigma}M}(\mathbf{p}, -\omega) G_{k,\bar{\sigma}M}^2(\mathbf{p}, \omega)\bigg|_{p_i=0}. \quad (5.24)$$

Using dimensionless quantities and the definition (4.46),

$$\boxed{\bar{\lambda}' = \frac{6\bar{\kappa}}{\pi} \bar{\mathcal{L}}_{k,1} + 8\bar{\lambda}^2 (\bar{\mathcal{L}}_{k,2}^{(1)} + \bar{\mathcal{L}}_{k,2}^{(2)}),} \quad (5.25)$$

where $\bar{\kappa}$ is given by equation (4.66) and, explicitly,

$$\bar{\mathcal{L}}_{k,1} := 2 \int dy \int_{\mathbb{R}^4} dx \left[(Z_\infty Z^{-1}(k) - \alpha\hat{\rho}(y)\theta(1-x)) \frac{1 + \hat{\tau}(y)r(x)}{\hat{f}(x,y)\hat{f}^2(x,-y)} - \frac{1}{2}\alpha\hat{\tau}(y) \frac{\theta(1-x)}{\hat{f}(x,y)\hat{f}(x,-y)} \right], \quad (5.26)$$

$$\bar{\mathcal{L}}_{k,2}^{(1)} := -\int dy \int_{\mathbb{R}^4} dx \left[(Z_\infty Z^{-1}(k) - \alpha\hat{\rho}(y)\theta(1-x)) \frac{1 + \hat{\tau}(y)r(x)}{\hat{f}(x,y)\hat{f}^2(x,-y)} \left(\frac{2}{\hat{f}(x,-y)} + \frac{1}{\hat{f}(x,y)} \right) \right], \quad (5.27)$$
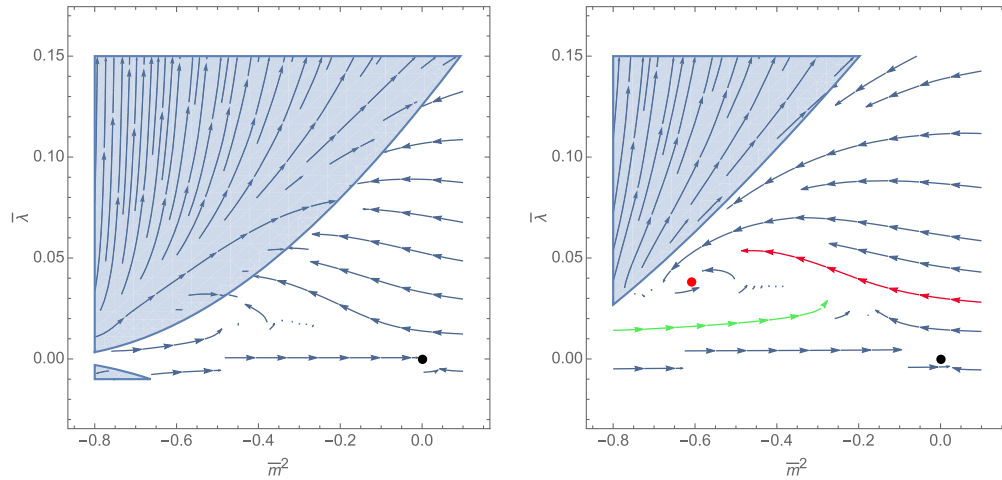
and

FIG. 11.   Numerical picture of the RG flow in the vicinity of the Gaussian fixed point (black dot) for $\alpha = 1$ (on left) and $\alpha = 4$ (on right). Arrows are oriented toward UV scales. The blue region seems to blind the fixed point for the diagram on the left.

$$\bar{\mathcal{L}}_{k,2}^{(2)} := -\alpha \int dy \int_{\mathbb{R}^4} d\boldsymbol{x}\, \hat{\tau}(y) \frac{\theta(1-x)}{\hat{f}(x,y)\hat{f}^2(x,-y)}. \quad (5.28)$$

The previous expression can be simplified again. Indeed, as discussed in Appendix C, Eq. (C.25) allows one to replace $\bar{\mathcal{L}}_{k,1}$ by $\bar{\mathcal{L}}_{k,1} \approx -\pi/2\bar{\lambda}$. Moreover, repeating the argument given in our previous work [97], the sums involved in $\bar{\mathcal{L}}_{k,2}^{(1)}$ and $\bar{\mathcal{L}}_{k,2}^{(2)}$ being superficially convergent, the terms involving Z_∞ have to be canceled in the continuum limit. Indeed, because we focus on the UV regime but so far to the IR scale, $Z_\infty/Z(k) \to 0$ as $1/\ln(\Lambda)$. Finally, using (4.66),

$$\boxed{\begin{aligned} \bar{\lambda}' = \frac{2\bar{\lambda}^2}{3}\int_{\mathbb{R}^4} d\mathbf{x} \int dy \frac{1+\tau(y)r(x)}{f^3(x,y)f(x,-y)} \\ + 8\bar{\lambda}^2(\bar{\mathcal{L}}_{k,2}^{(1)}|_{Z_\infty=0} + \bar{\mathcal{L}}_{k,2}^{(2)}|_{Z_\infty=0}) \end{aligned}} \quad (5.29)$$

We have then computed the last piece of the flow equation for the anomalous dimension, Eq. (4.45), and we move on to the numerical investigations.

VI. NUMERICAL RESULTS AND DISCUSSION

In this section, we provide some numerical results about the flow equations described in the previous section. For the first time, we focus on the limit $\hat{\beta} \to 0$ (i.e., no coarse graining in frequency space), and we provide a description of the global phase space structure, investigate the existence of nontrivial fixed points, and address the optimization issue regarding the computation of critical exponents. A second time, we remove the condition $\hat{\beta} = 0$ and consider a coarse graining both in frequency and moment.[8]

---

[8] An extended discussion about the physical meaning of such a procedure in that context is given in the conclusion.

A. Phase portrait, properties, and optimization for $\hat{\beta} = 0$

In that first section, we set $\hat{\beta} = 0$. In this limit, integrations over y in flow equations are performed from $-\infty$ to $+\infty$ without a cutoff function. First of all, we are interested to look for fixed point solutions and their vicinity. The Gaussian point $\bar{\lambda} = \bar{m}^2 = 0$ is a fixed point, and the β functions read, at first orders:

$$\begin{aligned} \beta_\lambda &= a_0(\alpha)\bar{\lambda}^2 + \mathcal{O}(\bar{m}^2\bar{\lambda}^2), \\ \beta_m &= -2\bar{m}^2 + b_0(\alpha)\bar{\lambda} + \mathcal{O}(\bar{m}^2\bar{\lambda}^2). \end{aligned} \quad (6.1)$$

It can be checked for a reasonable range of values for α that $a_0(\alpha) > 0$, meaning that the theory is *not asymptotically free*. In other words, the theory is not perturbative in the deep UV regime: The coupling constant grows toward UV scales. This contrasts with the standard result about the perturbative regime of the field theory defined by the equilibrium state (2.13), which is asymptotically free ($a_0 < 0$), see [65] and Appendix A 2. For $\alpha = 1$, we have, for instance,

$$a_0(1) \approx 32.90, \qquad b_0(1) = -16.45. \quad (6.2)$$

Note that $b_0(1) = -a_0(1)/2$ is true only for $\alpha = 1$. The fact that b_0 is negative suggests the existence of a large river or "mainstream" effect, dragging the flow. This is illustrated on Fig. 11 for $\alpha = 1$ (on left) and for $\alpha = 4$ (on right), the blue region on the figures corresponding to the phase space domain where the denominator of η is negative. Note that the existence of the fixed point and its properties are highly sensitive to the choice for α as soon as $\alpha \lesssim 3$. Furthermore, for some small values for α, the anomalous dimension η at the fixed point is below the regulator bounds: $\eta > \eta_c = -2$; see Fig. 12. Then at the boundary, the denominator vanishes, and the flow is ill defined. This singularity
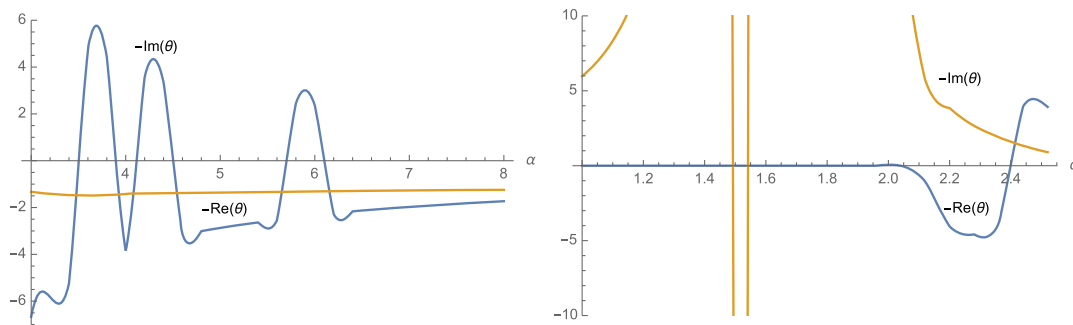
FIG. 12. Dependency of the real and imaginary components for critical exponent on the parameter α. On the left for $\alpha \geq 3$ and on the right for $\alpha < 3$.
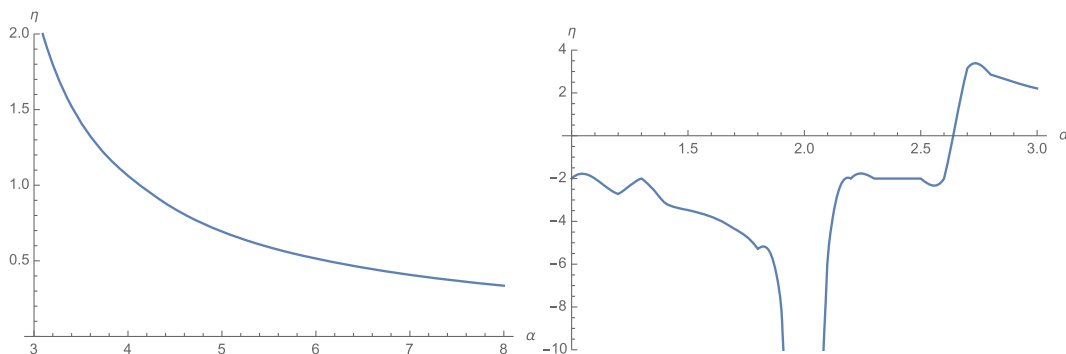

FIG. 13. Dependency of the anomalous dimension on the parameter α for the fixed point solution.

moreover is expected to be a pathology of the symmetric phase expansion (i.e., expansion around zero vacuum), and only the region where the denominator is positive, connected with the Gaussian fixed point $\bar{\lambda} = \bar{m}^2 = 0$ is physical. In both cases, we show the existence of a purely attractive UV fixed point, with complex critical exponents $\theta, \theta = \theta_1 \pm i\theta_2, \theta_1 > 0$.[9] Trajectories are then separated by the critical line joining the interacting fixed point and the Gaussian fixed point. Some trajectories come from positive mass (red curve for example) and someone's come from negative mass (green curve). This is reminiscent of the physics of second-order phase transition, controlled by a nontrivial fixed point [37] in the deep IR. The parametrization for the regulator reveals a strong dependency for $\alpha \lesssim 3$, but increasing α reveals a region where stability is improved. Because the theory is not asymptotically free, the existence of this fixed point ensures the *safety* of the theory in the deep UV. For $\alpha = 4$, we get

$$\theta = 1.57 \pm 4.11i, \qquad (6.3)$$

and for the anomalous dimension, $\eta \approx 1.06$. Figures 12 and 13 show the dependency on α of critical exponent and anomalous dimension at the fixed point. Figure 12 shows that the real part $\theta_1 = \Re(\theta)$ depends weakly on the parameter α as soon as $\alpha > 3$. Furthermore, the imaginary part $\theta_2 = \Im(\theta)$ has some stationary points, for $\alpha \approx 3.7, 4.3,$ and 5.9. These points, on the other hand, correspond to nothing from the point of view of the anomalous dimension, which shows no stationary points. For, $\alpha > 6.4$, however, θ_2 is almost stationary. In this range of values, moreover, the anomalous dimension remains small enough, which is expected to be a good indicator for the convergence of the derivative expansion [129], even if the resulting value for η is large regarding the values considered in the literature, for the Ising model, for instance.[10] Figure 14 shows the behavior of the flow for $\alpha = 7$, the arrow being oriented toward IR scales. The anomalous dimension has value $\eta^* = 0.4$, and the critical exponents are

$$\theta^* = 1.28 \pm 1.98i. \qquad (6.4)$$

---

[9]We define the critical exponent as the opposite of the eigenvalues of the stability matrix M with entries $M_{ij} := \partial_i \beta_j$, i.e., with the opposite sign regarding the ordinary definition.

[10]A relation between the convergence of the derivative expansion and the minimal sensitivity to the choice of the regulator is stressed in [124].
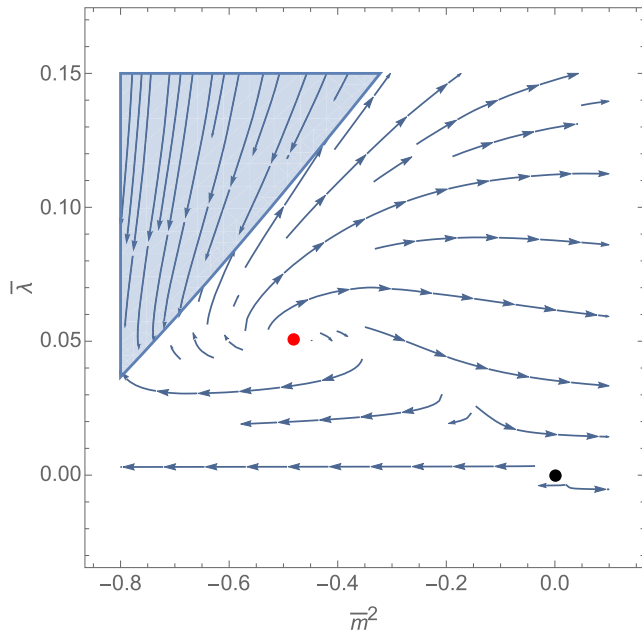
FIG. 14.   Numerical plot of the RG flow for $\alpha = 7$. On this figure, the arrows are oriented from UV to IR scales.

B. Fixed-point analysis for $\hat{\beta} \neq 0$

In this section, we consider coarse graining in both frequency and momentum, with $\hat{\beta} \neq 0$. Once again, we confirm the existence of a UV attractor separating the phase space into two regions, an ergodic phase with positive mass, and an expected nonergodic phase, with negative mass in the IR. The fact that this transition is controlled by an interactive fixed point makes this phase transition a second-order transition [130]. If the β parameter seems to aggravate the dependence on the regulator of the results for a large range of values, and to reduce considerably the portion of the phase space connected to the Gaussian point,

it appears that in a regime where $\hat{\beta}$ is small enough, $\hat{\beta} < 0.5$, a valley of stability exists for the critical exponents and the anomalous dimension, contrary to what it was for the $\hat{\beta} = 0$ case.

These conclusions are summarized in Figs. 15 and 16. These figures represent the dependence of the anomalous dimension and the critical exponents on the parameters α and $\hat{\beta}$. We notice the existence of a global minimum sensitivity point for $\hat{\beta} \approx 0.28$ and $\alpha \approx 3.2$, where the sensitivity of the regulator is minimal. Figure 17 shows the behavior of the RG flow in the vicinity of the interacting fixed point at the minimal sensitivity point, and the resulting critical exponents are complex,

$$\theta \approx 4.45 + 5.46i, \qquad (6.5)$$

with small enough anomalous dimension $\eta \approx -0.05$. Note that, although the predictions are in qualitative agreement with the previous section, the values obtained for the critical exponents are very different from what we obtained for $\hat{\beta} = 0$. Because we were able to find a global stability point for critical exponents and anomalous dimensions, we expect the result of this section to be more reliable than the result of the previous one, but in absence of additional theoretical expectations, we cannot conclude about the absolute reliability of a method with respect to the other one.

VII. CONCLUDING REMARKS

In this paper, we introduced the basics of a stochastic formalism for GFTs in equilibrium dynamics. In that regime, we were able to construct a nonperturbative RG formalism that takes into account time-reversal symmetry and causality of solutions of the stochastic equation (2.4). We focused on a model that describes an Abelian stochastic
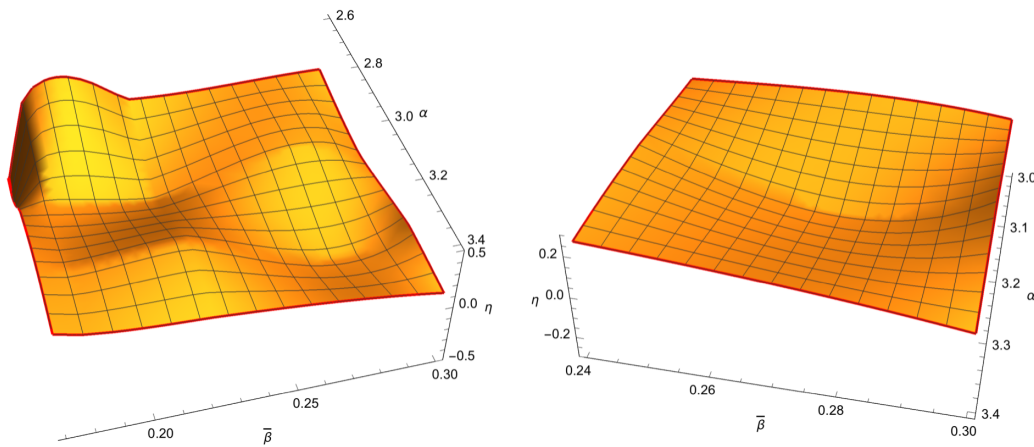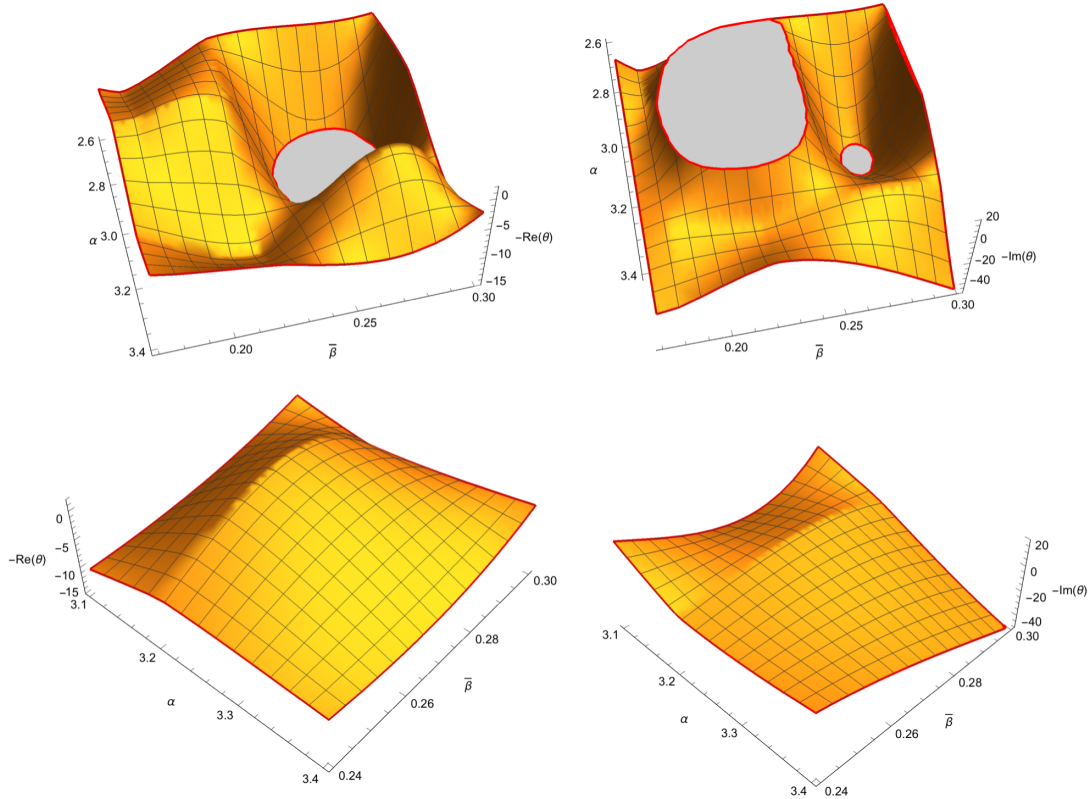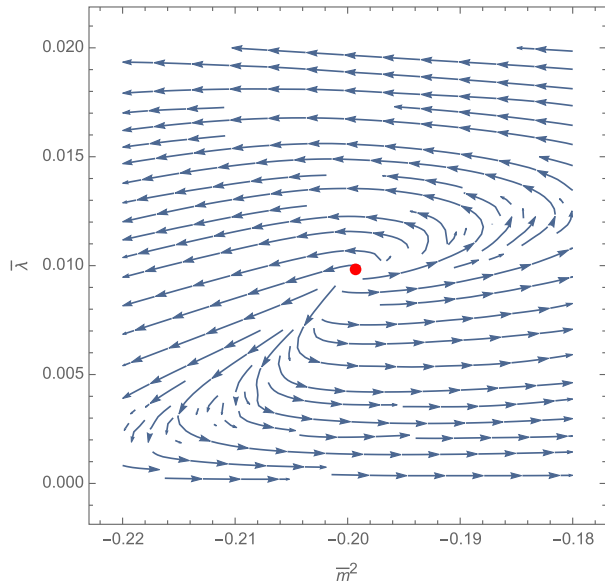

FIG. 15.   Dependency of the anomalous dimension at the fixed point with respect to α and $\hat{\beta}$.

FIG. 16. Dependency of the real and imaginary parts of the critical exponent θ.

FIG. 17. Behavior of the RG flow in the vicinity of the UV attractor for α and $\hat{\beta}$ in the minimal sensitivity domain.

complex field with rank 5 and group structure U(1), whose equilibrium state is a just renormalizable GFT for a pure gravity model. For this model, restricting ourselves to the melonic nonbranching sector of the theory in the symmetric phase, we were able to construct an exact RG solution of the flow equation, closing the infinite hierarchy of the equation around just renormalizable interactions. This strategy, mixing melonic equations and WT identities, allows one to express vertex functions $\Gamma_k^{(2n)}$ for $n \geq 3$ in terms of $\Gamma_k^{(4)}$ and $\Gamma_k^{(2)}$, keeping by this way the full momenta dependence of the vertex, and to compute the derivative of the vertex for an external moment that plays an important role in the derivation of the anomalous dimension. Hence, the resulting equations describe the full nonbranching sector and can be easily investigated numerically.

Our numerical investigations have revealed the existence of a nontrivial fixed point, possessing the characteristics of an ultraviolet attractor, in a physically relevant regime where the dependence on the parameters defining the controller is minimal. The choice of this parameterization considerably restricts the space of physical controllers, and this optimization would deserve to be further investigated. On this point, our results also show that coarse graining in both frequency and momentum (i.e., using the degrees of freedom of the background scalar field as an external notion of scale) seems to improve the stability (and thus, the reliability) of the results. Thus, we predict the existence of a second-order phase transition associated with an ergodicity break in the IR, controlled by a nontrivial UV fixed point. The scenario is reminiscent of the asymptotic safety

scenario encountered, for instance, for $f(R)$-gravity models [130–133], and provides a strong evidence in favor of UV completion of our model [37]. Note that our construction focus on the deep UV regime and UV completion issue, and due to the compactness of the structure group $U(1) \sim S_1$, symmetry restoration is expected in the deep IR due to the survival of zero modes. A way to solve this limitation should be to construct a kind of thermodynamic limit, sending the radius of the compact space S_1 to infinity, or to consider a noncompact group; see, for instance, [30,56,134–136] and references therein. Finally, the reader could be confused about the fact that the continuum limits $\Lambda \to \infty$ seem to be in contradiction with the observation that the theory is not asymptotically free, and three remarks about these observations are in order. (1) The flow equations receive contributions only for a small window of momenta around the IR cutoff k, and the Wetterich equation is then well-defined in the limit $k \ll \Lambda$. (2) The counterterms for the theory are designed such that the equilibrium distribution, which defines an asymptotically free theory (see Appendix A 2), is perturbatively renormalizable. (3) Despite the fact that the out-of-equilibrium theory is not asymptotically free, it seems to be protected from Landau Pole and triviality by the existence of a UV attractive fixed point for the complete cyclic melonic sector. This fixed point is reminiscent of an asymptotic safety scenario ensuring UV completeness of the theory, and one expects that it guarantees that the theory is consistent for all momenta scales (it is at least a necessary condition; see, for instance, [37].

Although we focused on a toy model, disregarding some physical inputs in TGFTs, especially following the group structure that is not Abelian for realistic quantum gravity models, and in regard to some gauge symmetry like Gauss or Plebanski constraints, we expect that the general framework detailed in this paper could be suitable to investigate stochastic aspects of the best candidates for quantum gravity. Finally, even if the "time" has been interpreted as a relational time, as the configurations of some matter fields, other matter fields could be added to the group fields, such that equilibrium states describe quantum gravity interacting with matter rather than a pure gravity regime. Another way of investigation concerns another current discrete approach to quantum gravity, for instance, RTM. One can imagine a RTM described a dynamical tensorial variable $T_{i_1,\ldots,i_d}(t)$, by the same kind of equation like (2.4). Such an equation will describe a stochastic tensor, and one may imagine many ways to approach its dynamics. A renormalization group study, similar to what we did in this paper, is, for instance, expected, with the difference that RTM does not enjoy an intrinsic scaling law as for TGFTs. Hence, more sophisticated approaches are required to construct

reliable truncations, which we will discuss in a forthcoming work.

APPENDIX A: EQUILIBRIUM STATE'S RG

In this section, we review shortly the main results about RG for the equilibrium state (2.13), which describes a pure gravity TGFT, for a complex group field with rank d. We focus on $d = 5$, for an Abelian model with group structure $U(1)$ and quartic melonic interactions (2.25). This model has been largely investigated in the literature; see [65,97,99,114,137] and references therein. In this section, we sketch the main lines of the reference [65] that the reader may consult for more details. In Sec. A 1, we provide a derivation of the relation between counterterms for the wave function and coupling and a formal expression for them. Note that for this derivation, we make use of the standard Schwinger-Dyson equation, considered in full detail in [126,127], in contrast with the discussion given in [65] based on the existence of a finite radius of convergence for the renormalized series (see also [100]). Note that in this section, we define equilibrium state as $\rho \sim e^{-\mathcal{H}}$, without the factor 2 that can be canceled by a global redefinition of fields.

1. Melonic Schwinger-Dyson equation and counterterms

Schwinger-Dyson equations in quantum field theory are relations between observable, generally taking the form of self-consistency equations for 1PI functions. For the TFGT that we considered in this paper, two of them are especially relevant in the melonic sector, for two- and four-point functions and have the structure pictured in Fig. 18 (see [127] for more details). Note that we focus on two- and four-point functions because the quartic model is just renormalizable, and both these relations are sufficient to constrain the counterterms.

Note that, in the second figure, we assumed that the 1PI four-point function has the connected quartic melonic for boundary, and $\pi_{\text{melo}}^{(\ell)}$ is defined by

$$\Gamma_{\bar{M}M\bar{M}M}^{(4),(\ell)} = 2\pi_{\text{melo}}^{(\ell)}(p_{1\ell}^2, p_{3\ell}^2)(\mathcal{W}_{p_1 p_2 p_3 p_4}^{(\ell)} + p_2 \leftrightarrow p_4). \tag{A1}$$

Moreover, Σ_{melo} designates the self-energy, related to the full two-point function G_{melo} and the bare propagator C by the Dyson equation:
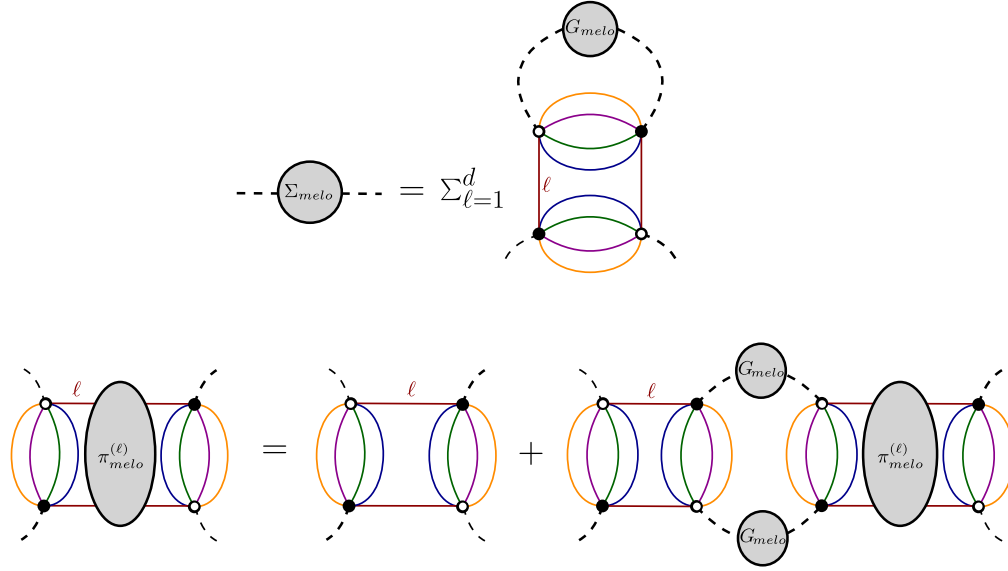
FIG. 18. Closed relations between the two- and four-point functions obtained from the Schwinger-Dyson equations in the melonic sector, as the "melo" index recalls.

$$G_{\text{melo}} = \frac{1}{C^{-1} - \Sigma_{\text{melo}}}, \quad (A2)$$

where following the definitions of Sec. III C 1,

$$C^{-1}(\boldsymbol{p}) = Z_{-\infty}\boldsymbol{p}^2 + m^2. \quad (A3)$$

Translated in equations, the first closed relations pictured in Fig. 18 reads,

$$\Sigma_{\text{melo}}(\boldsymbol{p}) = -2Z_\lambda \lambda_r \sum_{\ell=1}^{d} \sum_{\boldsymbol{q} \in \mathbb{Z}^d} \delta_{p_\ell q_\ell} \frac{1}{Z_\infty \boldsymbol{q}^2 + m^2 - \Sigma_{\text{melo}}(\boldsymbol{q})}. \quad (A4)$$

This relation means that $\Sigma_{\text{melo}}(\boldsymbol{p}) =: \sum_\ell \sigma(p_\ell^2)$, with

$$\sigma(p^2) = -2Z_\lambda \lambda_r \sum_{\boldsymbol{q} \in \mathbb{Z}^d} \delta_{pq_1} \frac{1}{Z_\infty \boldsymbol{q}^2 + m^2 - \Sigma_{\text{melo}}(\boldsymbol{q})}. \quad (A5)$$

Accordingly with the renormalization condition (3.30), Z_{infty} and Z_m are such that (see [97] and references therein)

$$Z_\infty - \sigma'(0) = 1, \qquad Z_m m_r^2 - d \times \sigma(0) = m_r^2. \quad (A6)$$

Hence,

$$\frac{1}{Z_\infty \boldsymbol{q}^2 + m^2 - \Sigma_{\text{melo}}(\boldsymbol{q})} = \frac{1}{\boldsymbol{q}^2 + m_r^2 + \sum_{\ell=1}^{d} \sigma_r(q_\ell^2)}, \quad (A7)$$

where $\sigma_r(q_\ell^2) = \mathcal{O}(q_\ell^4)$, with zero and first derivative equal to zero. Differentiating relation (A5) with respect to p^2, and setting $p = 0$, we get

$$-\sigma'(0) \equiv 1 - Z_\infty = -2Z_\lambda \lambda_r A_\infty, \quad (A8)$$

where A_∞ has been defined in (3.33). Now, let us consider the second relation, pictured in Fig. 18. In the equation, this relation reads, setting all the external momenta to zero,

$$4\pi_{\text{melo}}^{(\ell)}(0,0) = 4Z_\lambda \lambda_r - 8Z_\lambda \lambda_r \pi_{\text{melo}}^{(\ell)}(0,0) A_\infty. \quad (A9)$$

If we use the standard renormalization condition (see [37,123]),

$$\pi_{\text{melo}}^{(\ell)}(0,0) =: \lambda_r, \quad (A10)$$

and the previous relation simplifies as

$$\boxed{Z_\lambda^{-1} = 1 - 2\lambda_r A_\infty}. \quad (A11)$$

Moreover, from (A8),

$$Z_\lambda^{-1} - \frac{Z_\infty}{Z_\lambda} = -2Z_\lambda \lambda_r A_\infty, \quad (A12)$$

and using (A11), we obtain, finally,

$$\boxed{Z_\infty = Z_\lambda}. \quad (A13)$$

2. Nonperturbative RG in the nonbranching sector

In this section, we summarize some aspects of the nonperturbative RG in the symmetric phase for the melonic nonbranching sector using EVE. All details can be found in [65], as recalled at the beginning of this section. The derivation of the equation follows essentially the same strategy as explained in Sec. IV B 2. Hence, in the deep UV regime $1 \ll k \ll \Lambda$, and using the Litim regulator,

$$r_k(\boldsymbol{p}) = Z(k)(k^2 - \boldsymbol{p}^2)\theta(k^2 - \boldsymbol{p}^2), \qquad (A14)$$

the resulting β functions read,

$$\begin{cases} \beta_m = -(2+\eta)\bar{m}^2 - 10\bar{\lambda}\frac{\pi^2}{(1+\bar{m}^2)^2}\left(1+\frac{\eta}{6}\right), \\ \beta_\lambda = -2\eta\bar{\lambda} + 4\bar{\lambda}^2\frac{\pi^2}{(1+\bar{m}^2)^3}\left(1+\frac{\eta}{6}\right)\left[1 - 6\pi^2\bar{\lambda}\left(\frac{1}{(1+\bar{m}^2)^2} + \left(1+\frac{1}{1+\bar{m}^2}\right)\right)\right], \end{cases} \qquad (A15)$$

where the anomalous dimension η is given by

$$\eta = 4\bar{\lambda}\pi^2 \frac{(1+\bar{m}^2)^2 - \bar{\lambda}\pi^2(2+\bar{m}^2)}{(1+\bar{m}^2)^2\Omega(\bar{\lambda},\bar{m}^2) + 2\frac{(2+\bar{m}^2)}{3}\bar{\lambda}^2\pi^4}, \qquad (A16)$$

and

$$\Omega(\bar{m}^2, \bar{\lambda}) \coloneqq (\bar{m}^2+1)^2 - \pi^2\bar{\lambda}. \qquad (A17)$$

To obtain these equations, we closed the hierarchy using the same method as discussed in the Sec. IV B 3, by expressing $\Gamma_k^{(6)}$ in the expression of β_λ in terms of $\bar{\lambda}$ and $\bar{m}^2$. Moreover, we used the Ward identities to compute the derivative of the four-point vertex $\Gamma_k^{(4)}$ with respect to external momenta, which plays a role in the computation of the anomalous dimension η. This additional contribution, of order $\bar{\lambda}^2$, is not a small correction for a pure local potential approximation disregarding such a contribution. Indeed, taking into account this term pushes forward the singularity of the denominator of η down the singularity $\bar{m}^2 = -1$, coming from our restriction to the symmetric phase, and thus maximally extends the investigated portion of the full phase space. In the computation of loops involved both in the expression for $\Gamma_k^{(6)}$ and the derivative of $\Gamma_k^{(4)}$, we used the derivative expansion for two-point function, the same approximation used for the computation of flow equations. In [65] and reference therein, it has been pointed out that such an approximation makes sense for the computation of superficially convergent integrals and remains in agreement with Ward identities. Hence, the RG flow described by Eq. (A15) satisfies the Ward identities. Moreover, the computer program Mathematica is not able to find any physically relevant fixed point for that system, and the Gaussian fixed point is the only UV-relevant fixed point, at least in this regime.

The quartic model (considered as an initial condition for the RG flow) is endowed with an additional amazing specificity. Indeed, the Ward identities impose a constraint between four- and two-point functions that can be translated locally along the RG flow as a nontrivial relation between β functions for relevant couplings:

$$\boxed{\beta_\lambda + \eta\bar{\lambda}\frac{\Omega(\bar{m}^2,\bar{\lambda})}{(1+\bar{m}^2)^2} - \frac{2\pi^2\bar{\lambda}^2}{(1+\bar{m}^2)^3}\beta_m = 0}. \qquad (A18)$$

The flow equation for $\bar{m}^2$ given by (A15) is exact in the melonic sector, as we restrict ourselves to the connected interactions. Hence, Eq. (A18) defines the function β_λ. On the other hand, the flow equation for λ involves $\Gamma_k^{(6)}$. Therefore, equalizing the two expressions for β_λ provides a nontrivial expression for $\Gamma_k^{(6)}$ (with zero external momenta). Note that this contribution may involve, in principle, nonconnected contributions, but we discard them from our analysis. Hence, we can use the resulting expression for $\Gamma_k^{(6)}$ in the Ward identity expressing the derivative of four-point functions for external momenta, as discussed in section V B. Finally, this expression allows computing the anomalous dimension:

$$\eta = \frac{4\pi^2\bar{\lambda}\left(\frac{\pi^2\bar{\lambda}}{5(1+\bar{m}^2)^3} + 1\right)}{(1+\bar{m}^2)^2 - \Omega_1(\bar{m}^2,\bar{\lambda})}, \qquad (A19)$$

where

$$\Omega_1(\bar{m}^2,\bar{\lambda}) \coloneqq \frac{6\pi^2\bar{\lambda}}{5} - \frac{4\pi^4\bar{\lambda}^2}{(1+\bar{m}^2)^3} - \frac{12\pi^2\bar{\lambda}\bar{m}^2}{5(1+\bar{m}^2)} - \frac{4\pi^2\bar{\lambda}}{5(1+\bar{m}^2)}. \qquad (A20)$$

This strategy is expected to provide a nontrivial improvement for the previous system (A15) because no additional approximations are required to compute loops involved in the structure equations, as we had to do in Sec. IV B 3. However, the conclusions are essentially the same: The theory is asymptotically free in the UV, and no physically relevant additional fixed point in found.[11] Near the Gaussian fixed point,

$$\boxed{\eta \approx 4\pi^2\bar{\lambda}, \qquad \beta_\lambda \approx -\eta\bar{\lambda}}. \qquad (A21)$$

---

[11]Indeed, the constraint (A18) imposes $\eta = 0$ for any nontrivial fixed point, but the solution (A19) shows that $\bar{\lambda} = 0$ is the only non-negative solution for $\bar{m}^2 > -1$.

APPENDIX B: PROOF OF RELATION (3.20)

From time reversal symmetry, ΔS_k transforms as

$$
\begin{aligned}
\Delta S_k[\boldsymbol{q},\boldsymbol{\chi}] \to \sum_{\boldsymbol{p}\in\mathbb{Z}^d} \int dt dt' \Big(& \bar{\chi}_{\boldsymbol{p}}(t)R_k^{(2)}(\boldsymbol{p},t'-t)\chi_{\boldsymbol{p}}(t') + i\bar{\chi}_{\boldsymbol{p}}(t)R_k^{(1)}(\boldsymbol{p},t'-t)T_{\boldsymbol{p}}(t') - i\bar{T}_{\boldsymbol{p}}(t')R_k^{(1)}(\boldsymbol{p},t'-t)\chi_{\boldsymbol{p}}(t) \\
& - \frac{2}{\Omega}\dot{\bar{T}}_{\boldsymbol{p}}(t)R_k^{(1)}(\boldsymbol{p},t'-t)T_{\boldsymbol{p}}(t') - \frac{2}{\Omega}\bar{T}_{\boldsymbol{p}}(t')R_k^{(1)}(\boldsymbol{p},t'-t)\dot{T}_{\boldsymbol{p}}(t) + \frac{2i}{\Omega}R_k^{(2)}(\boldsymbol{p},t'-t)(\dot{\bar{T}}_{\boldsymbol{p}}(t)\chi_{\boldsymbol{p}}(t') - \bar{\chi}_{\boldsymbol{p}}(t)\dot{T}_{\boldsymbol{p}}(t')) \\
& + \frac{4}{\Omega^2}\dot{\bar{T}}_{\boldsymbol{p}}(t)R_k^{(2)}(\boldsymbol{p},t'-t)\dot{T}_{\boldsymbol{p}}(t') \Big).
\end{aligned}
\tag{B1}
$$

Because $R_k^{(2)}$ is symmetric in its arguments, we have again

$$
\begin{aligned}
\Delta S_k[\boldsymbol{q},\boldsymbol{\chi}] \to \sum_{\boldsymbol{p}\in\mathbb{Z}^d} \int dt dt' \Big(& \bar{\chi}_{\boldsymbol{p}}(t)R_k^{(2)}(\boldsymbol{p},t'-t)\chi_{\boldsymbol{p}}(t') + i\bar{\chi}_{\boldsymbol{p}}(t)R_k^{(1)}(\boldsymbol{p},t'-t)T_{\boldsymbol{p}}(t') - i\bar{T}_{\boldsymbol{p}}(t')R_k^{(1)}(\boldsymbol{p},t'-t)\chi_{\boldsymbol{p}}(t) \\
& - \frac{2}{\Omega}\dot{\bar{T}}_{\boldsymbol{p}}(t)R_k^{(1)}(\boldsymbol{p},t'-t)T_{\boldsymbol{p}}(t') - \frac{2}{\Omega}\bar{T}_{\boldsymbol{p}}(t')R_k^{(1)}(\boldsymbol{p},t'-t)\dot{T}_{\boldsymbol{p}}(t) + \frac{2i}{\Omega}R_k^{(2)}(\boldsymbol{p},t'-t)(\dot{\bar{T}}_{\boldsymbol{p}}(t)\chi_{\boldsymbol{p}}(t') - \bar{\chi}_{\boldsymbol{p}}(t)\dot{T}_{\boldsymbol{p}}(t')) \\
& + \frac{2}{\Omega^2}\dot{\bar{T}}_{\boldsymbol{p}}(t)(R_k^{(2)}(\boldsymbol{p},t'-t) + R_k^{(2)}(\boldsymbol{p},t-t'))\dot{T}_{\boldsymbol{p}}(t') \Big).
\end{aligned}
\tag{B2}
$$

Integrating by part, we find that the invariance condition of ΔS_k by time reversal is written, up to a total derivative:

$$
\begin{aligned}
0 \equiv \sum_{\boldsymbol{p}\in\mathbb{Z}^d} \int dt dt' \Big(& i\bar{\chi}_{\boldsymbol{p}}(t)\Big(R_k^{(1)}(\boldsymbol{p},t'-t) - R_k^{(1)}(\boldsymbol{p},t-t') + \frac{2}{\Omega}\dot{R}_k^{(2)}(\boldsymbol{p},t-t')\Big)T_{\boldsymbol{p}}(t') \\
& - i\bar{T}_{\boldsymbol{p}}(t')\Big(R_k^{(1)}(\boldsymbol{p},t'-t) - R_k^{(1)}(\boldsymbol{p},t-t') + \frac{2}{\Omega}\dot{R}_k^{(2)}(\boldsymbol{p},t'-t)\Big)\chi_{\boldsymbol{p}}(t) \\
& - \frac{2}{\Omega}\dot{\bar{T}}_{\boldsymbol{p}}(t)\Big(R_k^{(1)}(\boldsymbol{p},t'-t) - \frac{1}{\Omega}\dot{R}_k^{(2)}(\boldsymbol{p},t'-t)\Big)T_{\boldsymbol{p}}(t') - \frac{2}{\Omega}\bar{T}_{\boldsymbol{p}}(t')\Big(R_k^{(1)}(\boldsymbol{p},t'-t) - \frac{1}{\Omega}\dot{R}_k^{(2)}(\boldsymbol{p},t'-t)\Big)\dot{T}_{\boldsymbol{p}}(t) \Big).
\end{aligned}
\tag{B3}
$$

Finally, exploiting the fact that $R_k^{(2)}$ is a symmetric function, the two last terms can be rewritten as follows:

$$
\begin{aligned}
0 \equiv \sum_{\boldsymbol{p}\in\mathbb{Z}^d} \int dt dt' \Big(& i\bar{\chi}_{\boldsymbol{p}}(t)\Big(R_k^{(1)}(\boldsymbol{p},t'-t) - R_k^{(1)}(\boldsymbol{p},t-t') + \frac{2}{\Omega}\dot{R}_k^{(2)}(\boldsymbol{p},t-t')\Big)T_{\boldsymbol{p}}(t') \\
& - i\bar{T}_{\boldsymbol{p}}(t')\Big(R_k^{(1)}(\boldsymbol{p},t'-t) - R_k^{(1)}(\boldsymbol{p},t-t') - \frac{2}{\Omega}\dot{R}_k^{(2)}(\boldsymbol{p},t'-t)\Big)\chi_{\boldsymbol{p}}(t) \\
& - \frac{2}{\Omega}\dot{\bar{T}}_{\boldsymbol{p}}(t)\Big(R_k^{(1)}(\boldsymbol{p},t'-t) - R_k^{(1)}(\boldsymbol{p},t-t') - \frac{2}{\Omega}\dot{R}_k^{(2)}(\boldsymbol{p},t'-t)\Big)T_{\boldsymbol{p}}(t') \Big).
\end{aligned}
\tag{B4}
$$

These relations show that a sufficient condition to avoid breaking the time reflection symmetry along the RG flow is to impose (3.20).

APPENDIX C: MELONICS WT IDENTICIES FOR TWO- AND FOUR-POINT VERTICES

We give in this appendix a technical complement on Ward identities, focusing on the relation between four-point and two-point functions. Relations between 1PI functions can be obtained by taking successive derivatives for the sources but vanishing them at the end of the computation.

Alternatively, one can derive with respect to the classical fields, and this is what we do in the following sections.

Another proof of heteroclicity. Let us start by considering the second functional derivative on both sides of the equation (5.16) with respect to the classical fields $M_{\boldsymbol{p}}(\omega)$ and $\bar{M}_{\boldsymbol{p}}(\omega)$. We apply the operator $\partial^2/\partial M_{\boldsymbol{q}}(\omega_1)\partial \bar{M}_{\bar{\boldsymbol{q}}}(\bar{\omega}_1)$ on Eq. (5.16), and because of definition (3.2), we have

$$\frac{\partial M_{\boldsymbol{p}}(\omega)}{\partial J_{\boldsymbol{p}'}(\omega')} = \frac{\partial^2 W_k}{\partial \bar{J}_{\boldsymbol{p}}(\omega)\partial J_{\boldsymbol{p}'}(\omega')}, \qquad (C1)$$

and

$$\frac{\partial \Gamma_k}{\partial M_{\boldsymbol{p}}(\omega)} = \bar{J}_{\boldsymbol{p}}(\omega) - iR_k^{(1)}(\boldsymbol{p},\omega)\bar{\sigma}_{\boldsymbol{p}}(\omega), \qquad (C2)$$

$$\frac{\partial \Gamma_k}{\partial \sigma_{\boldsymbol{p}}(\omega)} = \bar{J}_{\boldsymbol{p}}(\omega) - [\bar{\sigma}_{\boldsymbol{p}}(\omega)R_k^{(2)}(\boldsymbol{p},\omega) + iR_k^{(1)}(\boldsymbol{p},-\omega)\bar{M}_{\boldsymbol{p}}(\omega)]. \qquad (C3)$$

We introduce the notations:

$$\delta p^2 := p^2 - (p')^2,$$

$$R_k^{(I)}(\boldsymbol{p},\omega) - R_k^{(I)}(\boldsymbol{p}',\omega) := \delta R_k^{(I)}(\boldsymbol{p},\omega), \qquad (C4)$$

and we get

$$0 = \int d\omega \sum_{\boldsymbol{p},} \sum_{\boldsymbol{p}'} \prod_{j \neq i} \delta_{p_j p'_j} \left[(iZ_\infty \delta p^2 + i\delta R_k^{(1)}(\boldsymbol{p},\omega)) \frac{\partial^2 G_{k,\bar{\sigma}M}^{(1;\bar{1})}(\boldsymbol{p}',\omega;\boldsymbol{p},\omega)}{\partial M_{\boldsymbol{q}}(\omega_1)\partial \bar{M}_{\bar{\boldsymbol{q}}}(\bar{\omega}_1)} + (iZ_\infty \delta p^2 + i\delta R_k^{(1)}(\boldsymbol{p},-\omega)) \frac{\partial^2 G_{k,\bar{M}\sigma}^{(\bar{1};1)}(\boldsymbol{p},\omega;\boldsymbol{p}',\omega)}{\partial M_{\boldsymbol{q}}(\omega_1)\partial \bar{M}_{\bar{\boldsymbol{q}}}(\bar{\omega}_1)} \right.$$

$$\left. + \delta R_k^{(2)}(\boldsymbol{p},\omega) \times \frac{\partial^2 G_{k,\bar{\sigma}\sigma}^{(0;1+\bar{1})}(\boldsymbol{p}',\omega;\boldsymbol{p},\omega)}{\partial M_{\boldsymbol{q}}(\omega_1)\partial \bar{M}_{\bar{\boldsymbol{q}}}(\bar{\omega}_1)} - \frac{\partial \bar{J}_{\boldsymbol{p}}(\omega)}{\partial \bar{M}_{\bar{\boldsymbol{q}}}(\bar{\omega}_1)} \delta_{p'q}\delta(\omega - \omega_1) + \frac{\partial J_{\boldsymbol{p}'}(\omega)}{\partial M_{\boldsymbol{q}}(\omega_1)} \delta_{p\bar{q}}\delta(\omega - \bar{\omega}_1) \right] \delta_{p_i p} \delta_{p'_i p'}. \qquad (C5)$$

Derivatives to sources can be easily computed, leading to

$$\frac{\partial \bar{J}_{\boldsymbol{p}}(\omega)}{\partial \bar{M}_{\bar{\boldsymbol{q}}}(\bar{\omega}_1)} = \frac{\partial^2 \Gamma_k}{\partial \bar{M}_{\bar{\boldsymbol{q}}}(\bar{\omega}_1)\partial M_{\boldsymbol{p}}(\omega)},$$

$$\frac{\partial J_{\boldsymbol{p}'}(\omega)}{\partial M_{\boldsymbol{q}}(\omega_1)} = \frac{\partial^2 \Gamma_k}{\partial M_{\boldsymbol{q}}(\omega_1)\partial \bar{M}_{\boldsymbol{p}'}(\omega)}. \qquad (C6)$$

In the same way,

$$\frac{\partial \bar{J}_{\boldsymbol{p}}(\omega)}{\partial \bar{M}_{\bar{\boldsymbol{q}}}(\bar{\omega}_1)} = \frac{\partial^2 \Gamma_k}{\partial \bar{M}_{\bar{\boldsymbol{q}}}(\bar{\omega}_1)\partial \sigma_{\boldsymbol{p}}(\omega)} + iR_k^{(1)}(\bar{\boldsymbol{q}},-\omega)\delta_{p\bar{q}}\delta(\omega - \bar{\omega}_1),$$

$$(C7)$$

and

$$\frac{\partial J_{\boldsymbol{p}'}(\omega)}{\partial M_{\boldsymbol{q}}(\omega_1)} = \frac{\partial^2 \Gamma_k}{\partial M_{\boldsymbol{q}}(\omega_1)\partial \bar{\sigma}_{\boldsymbol{p}'}(\omega)} + iR_k^{(1)}(\boldsymbol{q},\omega)\delta_{p'q}\delta(\omega - \omega_1).$$

$$(C8)$$

The derivatives of the two-point functions can be rewritten as follows. Note that because $\partial \bar{J}_{\boldsymbol{p}}(\omega)/\partial \bar{M}_{\bar{\boldsymbol{q}}}(\bar{\omega}) = 0$, we must have [using the short notation $p \equiv (\boldsymbol{p},\omega)$],

$$\sum_{p_1} \frac{\partial J_{p_1}}{\partial M_q} \frac{\partial \sigma_p}{\partial J_{p_1}} = \sum_{p_1} \frac{\partial J_{p_1}}{\partial M_q} \langle \bar{\chi}_{p_1} \chi_p \rangle = 0, \qquad (C9)$$

because $G_{k,\bar{\chi}\chi} = 0$ [Eq. (2.48)]. We made use of (C9) to obtain (C5). The functional derivatives can be easily computed following the method described in the previous section to obtain the flow equations. Because we focus on the symmetric phase and assume that effective vertices must have only one component along the response field and that $G_{k,\bar{\sigma}\sigma} = 0$, we have

$$\frac{\partial^2 G_{k,\bar{\sigma}M}^{(1;\bar{1})}(\boldsymbol{p}',\omega;\boldsymbol{p},\omega)}{\partial M_{\boldsymbol{q}}(\omega_1)\partial \bar{M}_{\bar{\boldsymbol{q}}}(\bar{\omega}_1)} = -\sum_{p_1,p'_1} G_{k,\bar{\sigma}M}(p',p'_1)\Gamma_{k,M\bar{M}M\bar{\sigma}}^{(4)}(q,q',p'_1,p_1)G_{k,\bar{\sigma}M}(p_1,p). \qquad (C10)$$

In the same way,

$$\frac{\partial^2 G_{k,\bar{M}\sigma}^{(\bar{1};1)}(\boldsymbol{p},\omega;\boldsymbol{p}',\omega)}{\partial M_{\boldsymbol{q}}(\omega_1)\partial \bar{M}_{\bar{\boldsymbol{q}}}(\bar{\omega}_1)} = -\sum_{p_1,p'_1} G_{k,\bar{M}\sigma}(p,p_1)\Gamma_{k,M\bar{M}\sigma\bar{M}}^{(4)}(q,q',p'_1,p_1)G_{k,\bar{M}\sigma}(p'_1,p'), \qquad (C11)$$

and

$$\frac{\partial^2 G_{k,\bar{\sigma}\sigma}^{(0;1+\bar{1})}(\boldsymbol{p}',\omega;\boldsymbol{p},\omega)}{\partial M_{\boldsymbol{q}}(\omega_1)\partial \bar{M}_{\bar{\boldsymbol{q}}}(\bar{\omega}_1)} = -\sum_{p_1,p_1'} G_{k,\bar{\sigma}M}(p,p_1)\Gamma_{k,M\tilde{M}M\tilde{M}}^{(4)}(q,q',p_1',p_1)G_{k,\bar{M}\sigma}(p_1',p'). \tag{C12}$$

Following the definition (4.25), we introduce $\Gamma_{k,M\tilde{M}M\tilde{M}}^{(4)} =: \sum_\ell \Gamma_{k,M\tilde{M}M\tilde{M}}^{(4),(\ell)}$, and the decomposition:

$$\Gamma_{k,M\tilde{M}M\tilde{M}}^{(4),(\ell)}(p_1,p_2,p_3,p_4) =: \frac{i}{\pi}\varpi_k^{(2)}(p_{1\ell}^2,p_{3\ell}^2)(\mathcal{W}_{p_1,p_2,p_3,p_4}^{(\ell)} + p_2 \leftrightarrow p_4)\delta(\hat{\omega}_1 - \hat{\omega}_2 + \hat{\omega}_3 - \hat{\omega}_4), \tag{C13}$$

such that Ward identity (C5) reads as follows:

$$\tag{C14}$$

where we introduced the kernels [following the convention of (3.11)]:

$$\Delta_k(\boldsymbol{p},\omega) \equiv \begin{pmatrix} 0 & iZ_\infty\delta p^2 + i\delta R_k^{(1)}(\boldsymbol{p},\omega) \\ iZ_\infty\delta p^2 + i\delta R_k^{(1)}(\boldsymbol{p},-\omega) & 0 \end{pmatrix}\delta_{p_i p}\delta_{p_i'p'} =: \Delta_k'(\boldsymbol{p},\omega)\delta p^2, \tag{C15}$$

and

$$\delta_k(\boldsymbol{p},\omega) \equiv \delta R_k^{(2)}(\boldsymbol{p},\omega)\delta p^2 \delta_{p_i p}\delta_{p_i'p'} =: \delta_k'(\boldsymbol{p},\omega)\delta p^2. \tag{C16}$$
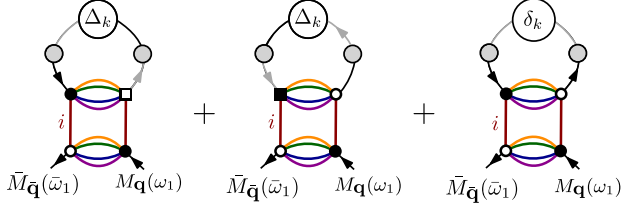
Equation (C14) involves two kinds of diagrams. The first ones, corresponding to the first, third, and fifth contributions to the left-hand side of (C14) create $(d-2)$ or $(d-1)$ faces, respectively, for $\ell \neq i$ and $\ell = i$.

   (i) For $\ell \neq i$, the contribution vanishes because Kronecker deltas in $\mathcal{W}_{p_1\bar{p}_2 p_3 \bar{p}_4}^{(\ell)}$ impose $p = p'$.

   (ii) For $\ell = i$, the contribution does not vanish and is melonic following definition 2: $F = d - 1(=4)$, $L = V = 1$, and $\rho = 0$.

The second kind of diagram corresponds to the second, fourth, and sixth contributions to the right-hand side of (C14). They create no more than 0 or 1 face, respectively, for $\ell \neq i$ and $\ell = i$.

   (i) For $\ell \neq i$, the contribution vanishes because Kronecker deltas impose $p = p'$.

   (ii) For $\ell = i$, the contribution does not vanish, but it is not melonic ($\rho = 3$).

We restrict ourselves to the melonic sector, which, as recalled in Sec. II is the most divergent one, and thus, the most relevant for RG. From these observations, the leading-order (melonics) contribution to identities (C14) reads as
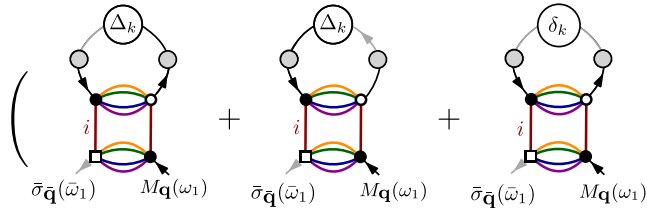
$$- \sum_{p,p'} \prod_{j \neq i} \delta_{p_j p'_j} \left[\frac{\partial \bar{J}_p(\omega_1)}{\partial \bar{M}_{\bar{q}}(\bar{\omega}_1)} \delta_{p'q} \right.$$

$$\left. - \frac{\partial J_{p'}(\bar{\omega}_1)}{\partial M_q(\omega_1)} \delta_{p\bar{q}} \right] \delta_{p_i p} \delta_{p'_i p'} = 0 \quad \text{(Melonic order)}, \tag{C17}$$

There are many options to interpret this equation. We know, from condition (2.48), that the two last terms must vanish exactly. Hence, we have essentially two kinds of integrals. The two first contributions involve loop integrals $\int d\omega G^2_{k,\bar{\sigma}M}(\omega)$ and $\int d\omega G^2_{k,\bar{M}\sigma}(\omega)$. If we assume causality, these integrals have to vanish for the same reason as we discussed in Remark 3 [Eq. (3.29)]. Moreover, terms like $\int d\omega \delta R^{(1)}_k(\omega) G^2_{k,\bar{\sigma}M}(\omega)$ vanish for the same reason as the left-hand side of equation (3.27) vanishes. With this argument, the last integral, which reads $\int d\omega \delta R^{(2)}_k(\omega) G_{k,\bar{\sigma}M}(\omega) G_{k,\bar{M}\sigma}(\omega)$, does not vanish, and the Ward identity imposes $\varpi^{(2)}_k = 0$, meaning that $\Gamma^{(2+\bar{2},)}_k = 0$. This is expected because of the discussion of Sec. III B, where causality was assumed as well, but the fact that this condition comes from a constraint imposed by an internal symmetry is a nontrivial result. The origin of this phenomenon can be traced from the arguments discussed in [65],

where authors pointed out a parallel between renormalization group equations and Ward identities. Indeed, if the flow equations dictate how the interactions change with the scale, the Ward identities dictate how the interactions deviate from ultralocality (i.e., from exact unit invariance). Thus, if in Sec. III B, we were able to demonstrate the absence of response field independent interaction terms by an argument from the renormalization group, Ward's identities show that a local theory whose initial conditions correspond to the model (2.38) cannot deviate from locality by response field independent contributions.

Relation between $Z(k)$ and $\lambda(k)$. In the same vein, but applying the operator $\partial^2 / \partial M_q(\omega_1) \partial \bar{\sigma}_{\bar{q}}(\bar{\omega}_1)$ on the Ward identity (5.16), we obtain a relation between $\Gamma^{(4)}_{k,\sigma \bar{M}M\bar{M}}$ and $\Gamma^{(2)}_{k,\bar{\sigma}M}$. Using the same graphical representation as previously, we get (we introduce all the Kronecker and Dirac δ to be more clear)

$$\left(\cdots \right) \delta_{p'q_i} \delta_{p\bar{q}_i} \prod_{j \neq i} \delta_{q_j \bar{q}_j} \delta(\omega_1 - \bar{\omega}_1) \tag{C18}$$

$$- \sum_{p,p'} \prod_{j \neq i} \delta_{p_j p'_j} \Delta_k(p, \omega_1) \delta_{p\bar{q}} \delta_{qp'} \delta(\omega_1 - \bar{\omega}_1) + \sum_{p,p'} \prod_{j \neq i} \delta_{p_j p'_j} \left[\gamma^{(2)}_{k,\bar{\sigma}M}(p, \omega_1) - \gamma^{(2)}_{k,\bar{\sigma}M}(p', \omega_1) \right]$$

$$\times \delta_{p'q} \delta_{p\bar{q}} \delta_{p_i p} \delta_{p'_i p'} \delta(\omega_1 - \bar{\omega}_1) + \sum_{p,p'} \prod_{j \neq i} \delta_{p_j p'_j} \delta_{p\bar{q}} \delta_{qp'} i \delta R^{(1)}_k(p, \omega_1) \delta(\omega_1 - \bar{\omega}_1) = 0,$$
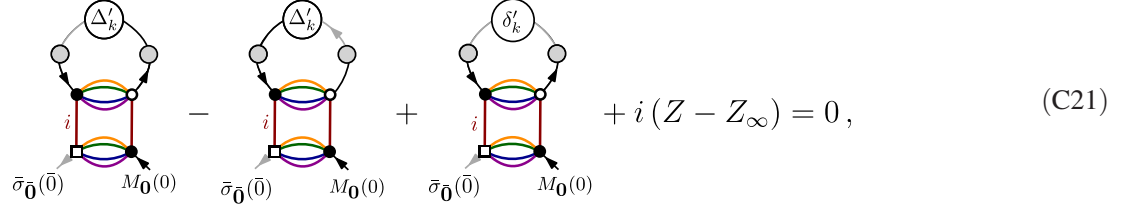
where we dropped out the nonmelonic contributions and assumed them to be in the symmetric phase, using definition (4.27). Because of the definition of Δ_k, the second and fourth contributions simplify. We set $q_\perp = q'_\perp$, $p' = q_i$, $p = \bar{q}_i$, and $p = p' + 1$. In the deep UV regime, it is suitable to use a continuous approximation to compute finite differences. We introduce the nearly continuous variable $x := p/\Lambda$, where Λ denotes some UV cutoff, such that, for any function $f(p^2)$ that can be expressed in terms of dimensionless quantities as $f(p^2) = \Lambda^r \tilde{f}(x^2)$, and $(x' = x + 1/\Lambda)$:

$$f((p')^2) - f(p^2) = \Lambda^r(\tilde{f}((x')^2) - \tilde{f}(x^2)) = \Lambda^{r-2}\left(\frac{d\tilde{f}}{dx^2} + \mathcal{O}(1/\Lambda^2)\right). \tag{C19}$$

Hence, from the definition (4.29), we have

$$[\gamma^{(2)}_{k,\bar{\sigma}M}(\boldsymbol{p},0) - \gamma^{(2)}_{k,\bar{\sigma}M}(\boldsymbol{p}',0)]|_{p_i=0} \approx iZ\delta p^2 + \mathcal{O}(\delta p^2), \tag{C20}$$

in agreement with Eq. (4.29), accordingly with our choice $\Omega = 1$. Finally, setting external momenta to zero, the Ward identity reads,

$$+ i(Z - Z_\infty) = 0, \tag{C21}$$

or explicitly,

$$\frac{2\lambda(k)}{\pi} \int d\omega \sum_{\boldsymbol{p}\in\mathbb{Z}^{d-1}} \left[2\left(iZ_\infty + i\frac{d}{dp_1^2}R_k^{(1)}(\boldsymbol{p},\omega)\right)G_{k,\bar{M}M}(\boldsymbol{p},\omega)G_{k,\bar{\sigma}M}(\boldsymbol{p},\omega)\right.$$

$$\left. + \frac{d}{dp_1^2}R_k^{(2)}(\boldsymbol{p},\omega)G_{k,\bar{M}\sigma}(\boldsymbol{p},\omega)G_{k,\bar{\sigma}M}(\boldsymbol{p},\omega)\right]\Bigg|_{p_i=0} = -(Z - Z_\infty). \tag{C22}$$

This equation can be rewritten using dimensionless quantities as follows:

$$\frac{4\bar{\lambda}(k)}{\pi} \int dy \int_{\mathbb{R}^4} dx \left[(1 - \bar{Z}(k)\alpha\hat{\rho}(y)\theta(1-x))\frac{1 + \hat{\tau}(y)r(x)}{\hat{f}(x,y)\hat{f}^2(x,-y)} - \frac{1}{2}\alpha\bar{Z}(k)\hat{\tau}(y)\frac{\theta(1-x)}{\hat{f}(x,y)\hat{f}(x,-y)}\right] = 1 - \bar{Z}(k), \tag{C23}$$

where:

$$\bar{Z}(k) := \frac{Z(k)}{Z_\infty}. \tag{C24}$$

Note that, in these equations, $\hat{f}(x,y)$ is not expected to be of the form given by Eq. (4.38), except maybe for the terms involving the regulator. Indeed, for these terms, the selected windows of momenta are the same as for the flow equations. Hence, assuming the truncation (4.38) for this contribution is not an additional assumption than assuming its validity for the computation of the flow equation themselves. Following the arguments given in [97], $Z_\infty^{-1} \sim \ln(\Lambda)$, and in the continuum limit, the previous Ward identity becomes

$$\frac{4\bar{\lambda}(k)}{\pi} \int dy \int_{\mathbb{R}^4} dx \left[(Z_\infty Z^{-1}(k) - \alpha\hat{\rho}(y)\theta(1-x))\frac{1 + \hat{\tau}(y)r(x)}{\hat{f}(x,y)\hat{f}^2(x,-y)} - \frac{1}{2}\alpha\hat{\tau}(y)\frac{\theta(1-x)}{\hat{f}(x,y)\hat{f}(x,-y)}\right] \approx -1, \tag{C25}$$

[1] L. Freidel, Group field theory: An overview, Int. J. Theor. Phys. **44**, 1769 (2005).

[2] A. Baratin and D. Oriti, Ten questions on group field theory (and their tentative answers), J. Phys. Conf. Ser. **360**, 012002 (2012).

[3] D. Oriti, The microscopic dynamics of quantum space as a group field theory, arXiv:1110.5606.

[4] D. Oriti, The group field theory approach to quantum gravity, arXiv:gr-qc/0607032.

[5] T. Krajewski, Group field theories, arXiv:1210.6257.

[6] A. Perez, The Spin-Foam approach to Quantum Gravity, Living Rev. Relativity **16**, 3 (2013).

[7] A. Ashtekar and E. Bianchi, A short review of loop quantum gravity, Rep. Prog. Phys. **84**, 042001 (2021).

[8] C. Rovelli, *Springer Handbook of Spacetime*, edited by A. Ashtekar and V. Petkov (Springer-Verlag Berlin, Heidelberg, 2014), pp. 751–757.

[9] T. Thiemann, *Modern Canonical Quantum General Relativity*, Cambridge Monographs on Mathematical Physics (Cambridge University Press, Cambridge, England, 2007), ISBN: 978-0-511-75568-2, 978-0-521-84263-1.

[10] L. Smolin, Newtonian gravity in loop quantum gravity, arXiv:1001.3668.

[11] D. Oriti, Group field theory as the 2nd quantization of loop quantum gravity, arXiv:1310.7786.

[12] D. Oriti, J. P. Ryan, and J. Thürigen, Group field theories for all loop quantum gravity, New J. Phys. **17**, 023042 (2015).

[13] B. Eynard, T. Kimura, and S. Ribault, Random matrices, arXiv:1510.04430.

[14] P. Francesco, P. Ginsparg, and J. Zinn-Justin, 2D gravity and random matrices, Phys. Rep. **254**, 1 (1995).

[15] N. Seiberg, Emergent spacetime, *The Quantum Structure of Space and Time (proceeding)* (World Scientific, Singapore, 2007).

[16] R. G. Gurău, *Random Tensors* (Oxford University Press, New York, 2017).

[17] V. Rivasseau, Random tensors and quantum gravity, SIGMA **12**, 069 (2016).

[18] R. Gurau, Invitation to random tensors, SIGMA **12**, 094 (2016).

[19] D. Benedetti, S. Carrozza, R. Gurau, and M. Kolanowski, The $1/N$ expansion of the symmetric traceless and the antisymmetric tensor models in rank three, Commun. Math. Phys. **371**, 55 (2019).

[20] S. Carrozza, Large N limit of irreducible tensor models: $O(N)$ rank-3 tensors with mixed permutation symmetry, J. High Energy Phys. 06 (2018) 039.

[21] S. Carrozza and S. Harribey, Melonic large N limit of 5-index irreducible random tensors, Commun. Math. Phys. **390**, 1219 (2022).

[22] S. Carrozza and A. Tanasa, $O(N)$ random tensor models, Lett. Math. Phys. **106**, 1531 (2016).

[23] V. Bonzom, R. Gurau, and V. Rivasseau, Random tensor models in the large N limit: Uncoloring the colored tensor models, Phys. Rev. D **85**, 084037 (2012).

[24] V. Bonzom, R. Gurau, A. Riello, and V. Rivasseau, Critical behavior of colored tensor models in the large N limit, Nucl. Phys. **B853**, 174 (2011).

[25] V. Bonzom, R. Gurau, J. P. Ryan, and A. Tanasa, The double scaling limit of random tensor models, J. High Energy Phys. 09 (2014) 051.

[26] S. Dartois, R. Gurau, and V. Rivasseau, Double scaling in tensor models with a quartic interaction, J. High Energy Phys. 09 (2013) 088.

[27] A. F. Jercher, D. Oriti, and A. G. A. Pithis, Emergent cosmology from quantum gravity in the Lorentzian Barrett-Crane tensorial group field theory model, J. Cosmol. Astropart. Phys. 01 (2022) 050.

[28] A. Baratin and D. Oriti, Quantum simplicial geometry in the group field theory formalism: Reconsidering the Barrett-Crane model, New J. Phys. **13**, 125011 (2011).

[29] A. Baratin and D. Oriti, Group field theory and simplicial gravity path integrals: A model for Holst-Plebanski gravity, Phys. Rev. D **85**, 044003 (2012).

[30] V. Lahoche and D. Oriti, Renormalization of a tensorial field theory on the homogeneous space SU(2)/U(1), J. Phys. A **50**, 025201 (2017).

[31] S. Carrozza, D. Oriti, and V. Rivasseau, Renormalization of tensorial group field theories: Abelian U(1) models in four dimensions, Commun. Math. Phys. **327**, 603 (2014).

[32] S. Carrozza, D. Oriti, and V. Rivasseau, Renormalization of a SU(2) tensorial group field theory in three dimensions, Commun. Math. Phys. **330**, 581 (2014).

[33] D. Oriti, Disappearance and emergence of space and time in quantum gravity, arXiv:1302.2849.

[34] D. Oriti, The complex timeless emergence of time in quantum gravity, arXiv:2110.08641.

[35] D. Oriti, Levels of spacetime emergence in quantum gravity, arXiv:1807.04875.

[36] D. Oriti, Tensorial group field theory condensate cosmology as an example of spacetime emergence in quantum gravity, arXiv:2112.02585.

[37] J. Zinn-Justin, *From Random Walks to Random Matrices* (Oxford University Press, 2019).

[38] J. Zinn-Justin, *Quantum Field Theory and Critical Phenomena*, International Series of Monographs on Physics Vol. 77 (Oxford University Press, New York, 2021).

[39] B. Dittrich, The continuum limit of loop quantum gravity—a framework for solving the theory, arXiv:1409.1450.

[40] E. Baloitcha, V. Lahoche, and D. Ousmane Samary, Flowing in discrete gravity models and Ward identities: A review, Eur. Phys. J. Plus **136**, 982 (2021).

[41] A. Eichhorn, J. Lumma, A. D. Pereira, and A. Sikandar, Universal critical behavior in tensor models for four-dimensional quantum gravity, J. High Energy Phys. 02 (2020) 110.

[42] A. Eichhorn, J. Lumma, T. Koslowski, and A. D. Pereira, toward background independent quantum gravity with tensor models, Classical Quantum Gravity **36**, 155007 (2019).

[43] A. Eichhorn and T. Koslowski, Toward phase transitions between discrete and continuum quantum spacetime from the renormalization group, Phys. Rev. D **90**, 104039 (2014).

[44] A. Eichhorn and T. Koslowski, Continuum limit in matrix models for quantum gravity from the functional renormalization group, Phys. Rev. D **88**, 084016 (2013).

[45] E. Brézin and J. Zinn-Justin, Renormalization group approach to matrix models, Phys. Lett. B **288**, 54 (1992).

[46] V. Lahoche and D. Ousmane Samary, Reliability of the local truncations for the random tensor models renormalization group flow, Phys. Rev. D **102**, 056002 (2020).

[47] V. Lahoche and D. Ousmane Samary, Revisited functional renormalization group approach for random matrices in the large-N limit, Phys. Rev. D **101**, 106015 (2020).

[48] S. Carrozza, *Tensorial Methods and Renormalization in Group Field Theories* (Springer International Publishing, New York, 2014).

[49] J. Ben Geloun and V. Bonzom, Radiative corrections in the Boulatov-Ooguri tensor model: The 2-point function, Int. J. Theor. Phys. **50**, 2819 (2011).

[50] S. Carrozza, Discrete renormalization group for SU(2) tensorial group field theory, Ann. l'Inst. Henri Poincaré D **2**, 49 (2015).

[51] S. Carrozza, Group field theory in dimension four minus epsilon, Phys. Rev. D **91**, 065023 (2015).

[52] S. Carrozza, Flowing in group field theory space: A review, SIGMA **12**, 070 (2016).

[53] J. B. Geloun, T. A. Koslowski, D. Oriti, and A. D. Pereira, Functional renormalization group analysis of rank-3 tensorial group field theory: The full quartic invariant truncation, Phys. Rev. D **97**, 126018 (2018).

[54] J. B. Geloun and V. Rivasseau, A renormalizable 4-dimensional tensor field theory, arXiv:1111.4997.

[55] J. B. Geloun, R. Martini, and D. Oriti, Functional renormalization group analysis of tensorial group field theories on $\mathbb{R}^d$., Phys. Rev. D **94**, 024017 (2016).

[56] D. Benedetti, J. B. Geloun, and D. Oriti, Functional renormalisation group approach for tensorial group field theory: A rank-3 model, J. High Energy Phys. 03 (2015) 084.

[57] D. Benedetti and V. Lahoche, Functional renormalization group approach for tensorial group field theory: A rank-6 model with closure constraint, Classical Quantum Gravity **33**, 095003 (2016).

[58] V. Lahoche and D. Ousmane Samary, Functional renormalization group for the $U(1) - T_5^6$ tensorial group field theory with closure constraint, Phys. Rev. D **95**, 045013 (2017).

[59] S. Carrozza and V. Lahoche, Asymptotic safety in three-dimensional SU(2) group field theory: Evidence in the local potential approximation, Classical Quantum Gravity **34**, 115004 (2017).

[60] S. Carrozza, V. Lahoche, and D. Oriti, Renormalizable group field theory beyond melonic diagrams: An example in rank four, Phys. Rev. D **96** 066007 (2017).

[61] S. Carrozza, Discrete renormalization group for SU(2) tensorial group field theory, Ann. Inst. Henri Poincaré D Comb. Phys. Interact. **2**, 49 (2015).

[62] V. Lahoche and D. Ousmane Samary, Ward identity violation for melonic T^4-truncation, Nucl. Phys. **B940**, 190 (2019).

[63] V. Lahoche and D. Ousmane Samary, Ward-constrained melonic renormalization group flow for the rank-four ϕ^6 tensorial group field theory, Phys. Rev. D **100**, 086009 (2019).

[64] V. Lahoche and D. Ousmane Samary, Large-d behavior of the Feynman amplitudes for a just renormalizable tensorial group field theory, Phys. Rev. D **103**, 085006 (2021).

[65] V. Lahoche and D. Ousmane Samary, Pedagogical comments about nonperturbative Ward-constrained melonic renormalization group flow, Phys. Rev. D **101**, 024001 (2020).

[66] V. Lahoche, B.-B. B. Natta, and D. Ousmane Samary, No Ward-Takahashi identity violation for Abelian tensorial group field theories with a closure constraint, Phys. Rev. D **104**, 106013 (2021).

[67] V. Lahoche, D. Ousmane Samary, and A. D. Pereira, Renormalization group flow of coupled tensorial group field theories: Toward the Ising model on random lattices, Phys. Rev. D **101**, 064014 (2020).

[68] D. Oriti, D. Pranzetti, and L. Sindoni, Black holes as quantum gravity condensates, Phys. Rev. D **97**, 066017 (2018).

[69] S. Gielen and D. Oriti, Cosmological perturbations from full quantum gravity, Phys. Rev. D **98**, 106019 (2018).

[70] M. de Cesare, D. Oriti, A. G. A. Pithis, and M. Sakellariadou, Dynamics of anisotropies close to a cosmological bounce in quantum gravity, Classical Quantum Gravity **35**, 015014 (2018).

[71] A. Kegeles, D. Oriti, and C. Tomlin, Inequivalent coherent state representations in group field theory, Classical Quantum Gravity **35**, 125011 (2018).

[72] D. Oriti, The universe as a quantum gravity condensate, C.R. Phys. **18**, 235 (2017).

[73] D. Oriti, D. Pranzetti, and L. Sindoni, Horizon Entropy from Quantum Gravity Condensates, Phys. Rev. Lett. **116**, 211301 (2016).

[74] D. Oriti, D. Pranzetti, J. P. Ryan, and L. Sindoni, Generalized quantum gravity condensates for homogeneous geometries and cosmology, Classical Quantum Gravity **32**, 235016 (2015).

[75] S. Gielen and D. Oriti, Quantum cosmology from quantum gravity condensates: Cosmological variables and lattice-refined dynamics, New J. Phys. **16**, 123004 (2014).

[76] S. Gielen, D. Oriti, and L. Sindoni, Homogeneous cosmologies as group field theory condensates, J. High Energy Phys. 06 (2014) 013.

[77] L. Marchetti and D. Oriti, Effective dynamics of scalar cosmological perturbations from quantum gravity, J. Cosmol. Astropart. Phys. 07 (2022) 004.

[78] S. Gielen, L. Marchetti, D. Oriti, and A. Polaczek, Effective cosmology from one-body operators in group field theory, Classical Quantum Gravity **39**, 075002 (2022).

[79] D. Oriti, L. Sindoni, and E. Wilson-Ewing, Bouncing cosmologies from quantum gravity condensates, Classical Quantum Gravity **34**, 04LT01 (2017).

[80] D. Oriti, L. Sindoni, and E. Wilson-Ewing, Emergent Friedmann dynamics with a quantum bounce from quantum gravity condensates, Classical Quantum Gravity **33**, 224001 (2016).

[81] R. Livi and P. Politi, *Nonequilibrium Statistical Physics: A Modern Perspective* (Cambridge University Press, Cambridge, England, 2017).

[82] C. Rovelli, Statistical mechanics of gravity and the thermodynamical origin of time, Classical Quantum Gravity **10,** 1549 (1993).

[83] C. Rovelli, The statistical state of the universe, Classical Quantum Gravity **10,** 1567 (1993).

[84] C. Rovelli and M. Smerlak, Thermal time and the Tolman-Ehrenfest effect: Temperature as the "speed of time", Classical Quantum Gravity **28,** 075007 (2011).

[85] N. C. Menicucci, S. J. Olson, and G. J. Milburn, Clocks and relationalism in the thermal time hypothesis, arXiv:1108.0883.

[86] P. Martinetti and C. Rovelli, Diamonds's temperature: Unruh effect for bounded trajectories and thermal time hypothesis, Classical Quantum Gravity **20,** 4919 (2003).

[87] A. Connes and C. Rovelli, Von Neumann algebra automorphisms and time thermodynamics relation in general covariant quantum theories, Classical Quantum Gravity **11,** 2899 (1994).

[88] I. Kotecha, On generalised statistical equilibrium and discrete quantum gravity, arXiv:2010.15445.

[89] E. Wilson-Ewing, A relational Hamiltonian for group field theory, Phys. Rev. D **99,** 086017 (2019).

[90] Y. Li, D. Oriti, and M. Zhang, Group field theory for quantum gravity minimally coupled to a scalar field, Classical Quantum Gravity **34,** 195001 (2017).

[91] L. Marchetti, D. Oriti, A. G. A. Pithis, and J. Thürigen, Phase transitions in tensorial group field theories: Landau-Ginzburg analysis of models with both local and nonlocal degrees of freedom, J. High Energy Phys. 12 (2021) 201.

[92] T. R. Morris, On truncations of the exact renormalization group, Phys. Lett. B **334,** 355 (1994).

[93] T. R. MORRIS, The exact renormalization group and approximate solutions, Int. J. Mod. Phys. A **09,** 2411 (1994).

[94] J. Berges, N. Tetradis, and C. Wetterich, Non-perturbative renormalization flow in quantum field theory and statistical physics, Phys. Rep. **363,** 223 (2002).

[95] B. Delamotte, An introduction to the nonperturbative renormalization group, in *Renormalization Group and Effective Field Theory Approaches to Many-Body Systems* (Springer, Berlin, Heidelberg, 2012), pp. 49–132.

[96] N. Dupuis, L. Canet, A. Eichhorn, W. Metzner, J. Pawlowski, M. Tissier, and N. Wschebor, The nonperturbative functional renormalization group and its applications, Phys. Rep. **910,** 1 (2021).

[97] V. Lahoche and D. Ousmane Samary, Nonperturbative renormalization group beyond melonic sector: The effective vertex expansion method for group fields theories, Phys. Rev. D **98,** 126010 (2018).

[98] E. Baloitcha, V. Lahoche, and D. Ousmane Samary, Flowing in discrete gravity models and Ward identities: A review, Eur. Phys. J. Plus **136,** 982 (2021).

[99] D. Ousmane Samary and F. Vignes-Tourneret, Just renormalizable TGFT's on $U(1)^d$ with gauge invariance, Commun. Math. Phys. **329,** 545 (2014).

[100] V. Lahoche, D. Oriti, and V. Rivasseau, Renormalization of an abelian tensor group field theory: Solution at leading order, J. High Energy Phys. 04 (2015) 095.

[101] L. Canet, H. Chate, and B. Delamotte, General framework of the non-perturbative renormalization group for non-equilibrium steady states, J. Phys. A **44,** 495001 (2011).

[102] R. Mannella and P. V. McClintock, *The Random and Fluctuating World, Celebrating Two Decades of Fluctuation and Noise Letters*, edited by P. V. E. McClintock and L. B. Kish (World Scientific, 2022), 10.1142/12720.

[103] C. Aron, G. Biroli, and L. F. Cugliandolo, Symmetries of generating functionals of Langevin processes with colored multiplicative noise, J. Stat. Mech. (2010) P11018.

[104] C. Duclut and B. Delamotte, Frequency regulators for the nonperturbative renormalization group: A general study and the model A as a benchmark, Phys. Rev. E **95,** 012107 (2017).

[105] V. Lahoche, D. Ousmane Samary, and M. Ouerfelli, Functional renormalization group for multilinear disordered Langevin dynamics I: Formalism and first numerical investigations at equilibrium, J. Phys. Commun. **6,** 055002 (2022).

[106] F. Synatschke, G. Bergner, H. Gies, and A. Wipf, Flow equation for supersymmetric quantum mechanics, J. High Energy Phys. 03 (2009) 028.

[107] D. Zappala, Improving the renormalization group approach to the quantum mechanical double well potential, Phys. Lett. A **290,** 35 (2001).

[108] T. Prokopec and G. Rigopoulos, Functional renormalization group for stochastic inflation, J. Cosmol. Astropart. Phys. 08 (2018) 013.

[109] A. Wilkins, G. Rigopoulos, and E. Masoero, Functional renormalisation group for Brownian motion I: The effective equations of motion, arXiv:2008.00472.

[110] A. Wilkins, G. Rigopoulos, and E. Masoero, Functional renormalisation group for Brownian motion II: Accelerated dynamics in and out of equilibrium, Phys. Rev. E **106,** 054109 (2022).

[111] S. G. Jakobs, M. Pletyukhov, and H. Schoeller, Nonequilibrium functional renormalization group with frequency-dependent vertex function: A study of the single-impurity Anderson model, Phys. Rev. B **81,** 195109 (2010).

[112] H. Schoeller, A perturbative nonequilibrium renormalization group method for dissipative quantum mechanics, Eur. Phys. J. Spec. Top. **168,** 179 (2009).

[113] K.-I. Aoki and A. Horikoshi, Nonperturbative renormalization group approach for quantum dissipative systems, Phys. Rev. A **66,** 042105 (2002).

[114] D. Ousmane Samary, Beta functions of $U(1)^d$ gauge invariant just renormalizable tensor models, Phys. Rev. D **88,** 105003 (2013).

[115] J. M. Pawlowski, Aspects of the functional renormalisation group, Ann. Phys. (Amsterdam) **322,** 2831 (2007).

[116] J. M. Pawlowski, M. M. Scherer, R. Schmidt, and S. J. Wetzel, Physics and the choice of regulators in functional renormalisation group flows, Ann. Phys. (Amsterdam) **384,** 165 (2017).

[117] L. Canet, B. Delamotte, D. Mouhanna, and J. Vidal, Optimization of the derivative expansion in the nonperturbative renormalization group, Phys. Rev. D **67,** 065004 (2003).

[118] L. Canet, H. Chate, B. Delamotte, and N. Wschebor, Non-perturbative renormalisation group for the Kardar-Parisi-Zhang equation: General framework and first applications, Phys. Rev. E **84,** 061128 (2011).

[119] J. Zinn-Justin, Renormalization of gauge theories, Lect. Notes Phys. **37,** 1 (1975).

[120] H. Gies, Introduction to the functional RG and applications to gauge theories, Lect. Notes Phys. **852,** 287 (2012).

[121] U. M. B. Marconi, A. Puglisi, L. Rondoni, and A. Vulpiani, Fluctuation–dissipation: Response theory in statistical physics, Phys. Rep. **461,** 111 (2008).

[122] R. Kubo, The fluctuation-dissipation theorem, Rep. Prog. Phys. **29,** 255 (1966).

[123] M. E. Peskin, *An Introduction to Quantum Field Theory* (CRC Press, Boca Raton, 2018), 10.1201/9780429503559.

[124] G. De Polsi and N. Wschebor, The regulator dependence in the functional renormalization group: A quantitative explanation Phys. Rev. E **106,** 024111 (2022).

[125] R. Pascalie, C. I. Pérez-Sánchez, A. Tanasa, and R. Wulkenhaar, On the large N limit of Schwinger-Dyson equations of a rank-3 tensor field theory, J. Math. Phys. (N.Y.) **60,** 7 (2019).

[126] D. Ousmane Samary, C. I. Pérez-Sánchez, F. Vignes-Tourneret, and R. Wulkenhaar, Correlation functions of a just renormalizable tensorial group field theory: The melonic approximation, Classical Quantum Gravity **32,** 175012 (2015).

[127] D. Ousmane Samary, Closed equations of the two-point functions for tensorial group field theory, Classical Quantum Gravity **31,** 185005 (2014).

[128] J. B. Geloun, R. Martini, and D. Oriti, Functional renormalization group analysis of a tensorial group field theory on $\mathbb{R}^3$., Europhys. Lett. **112,** 31001 (2015).

[129] I. Balog, H. Chaté, B. Delamotte, M. Marohnic, and N. Wschebor, Convergence of Nonperturbative Approximations to the Renormalization Group, Phys. Rev. Lett. **123,** 240604 (2019).

[130] S. Nagy, Lectures on renormalization and asymptotic safety, Ann. Phys. (Amsterdam) **350,** 310 (2014).

[131] M. Reuter and F. Saueressig, *Quantum Gravity and the Functional Renormalization Group: The Road toward Asymptotic Safety* (Cambridge University Press, Cambridge, England, 2019).

[132] A. Eichhorn, An asymptotically safe guide to quantum gravity and matter, Front. Astron. Space Sci. **5,** 47 (2019).

[133] K. G. Falls, D. F. Litim, and J. Schröder, Aspects of asymptotic safety for quantum gravity, Phys. Rev. D **99,** 126015 (2019).

[134] D. Benedetti, Critical behavior in spherical and hyperbolic spaces, J. Stat. Mech. (2015) P01002.

[135] A. G. Pithis and J. Thürigen, Phase transitions in TGFT: Functional renormalization group in the cyclic-melonic potential approximation and equivalence to O(N) models, J. High Energy Phys. 12 (2020) 159.

[136] A. G. Pithis and J. Thürigen, (No) phase transition in tensorial group field theory, Phys. Lett. B **816,** 136215 (2021).

[137] V. Lahoche and D. Ousmane Samary, Ward identity violation for melonic T^4-truncation, Nucl. Phys. **B940,** 190 (2019).